DLR- DEUTSCHES ZENTRUM FÜR LUFT UND RAUMFAHRT

Forest biomass estimations derived from 3D forest structure in Remote Sensing (LIDAR, Radar)

A thesis submitted to the School of Forest Science and
Resource Management
Sustainable Resource Management Program

By:

Astor Toraño Caicoya
March-2010

Advisor:

Dr. Peter Biber

Lehrstuhl für Walwachstumkunde

Systemwissen für Wald und Menschen

Technische Universität München

Second Advisor:

Prof. Dr. Irena Hajnsek

Institute of Environmental Engineering

ETH Zurich

Acknowledgements

This thesis is the final result of the Master Program "Sustainable Resource Management" at the Forestry Faculty of Technische Universität München in the collaboration with German Aerospace Agency (DLR- Deutsches Zentrum für Luft und Raumfahrt). I would like to express my gratitude especially Prof. Dr. Irena Hajnsek and Dr. Konstantinos Papathanassiou for giving me the possibility to develop this work at the DLR and Florian Kugler for his supervision, experience and advices. I would also like to acknowledge also Dr. Biber and Prof. Dr. Pretzsch for their support.

Many thanks to all the colleagues at the Pol-InSAR group for the great company, for all of those great moments in and out of the DLR with the ones that left (Daniela, Anna and Ernesto) and the ones who are still here.

And last, but definitely not least, to my SRMs friends who have made my experience in Germany unique. Especially to Tyra for the great corrections and English/German help, Saša for her "crazy" contributions, the Pablo for his constant encouragements and Kleo & Susi for two years of great coexistence at the "Pumkin Wg".

Table of contents

List of figures

List of Tables

1 Introduction

1.1 Global biomass stock map

Biomass is of interest for a number of reasons. It is the raw material of food, fiber and fuelwood. It is important for soil, fire, water management. It is related to vegetation structure, which in turn influences biodiversity. It determines the magnitude and rate of autotrophic respiration. And, finally, biomass density determines the amount of carbon emitted to the atmosphere when ecosystems are disturbed (Houghton, et al., 2009). However, even if steadily increasing, our knowledge of the amount of carbon stored in forests is incomplete.

According to Brown (1997) biomass is defined as the total amount of aboveground living organic matter in trees expressed as oven-dry tons per unit area. This biomass accounts for the greatest fraction of the total living biomass in forests and does not pose too many logistical problems in its estimation. From tree allometry it is now known that above-ground biomass (and thus carbon contained in the vegetation) might be predicted by trunk diameter, basal area or height of trees. Biomass estimates and changes in carbon allocation were calculated for various different areas in all major rain forest regions. These estimates are restricted to selected research plots and a spatially complete coverage is still lacking.

To overcome the uncertainty in our knowledge of carbon stored in vegetation and to monitor future changes satellite observation seems to be a practical solution. Although various studies used remote sensing for forest characterization ((Mette, 2007); (Koetz, 2006)) are region-wide coverage is still missing. Therefore, Houghton (2009) laid out the required specifications for a future satellite remote sensing mission to significantly reduce the currently existing uncertainties.

One crucial aspect in the development of remote sensing algorithms for vegetation, however, is the ground-validation of the remote sensing measurements. Nowadays remote sensing accurately measures, for example, the height of the canopy (Mette, 2007). It would therefore be of interest to compare forest inventory data with results from remote sensing at the same scale. This attempt is especially difficult in tropical forest, but so less in intensively measured temperate regions, like Germany.

1.2 Improvement of biomass estimations: forest vertical structure

Through forest allometry, it is known how the above-ground biomass can be calculated with the help of remote sensing systems like the height to biomass allometry, calculated from Pol-InSAR (Radar) in Mette (2007), or in the study of Balzter (2007). However, the applications of these methodologies are optimal just for homogeneous forest conditions: even aged, single species stands; but forests on a global scale present, on the other hand, a much higher diversity. Thus, natural forests in the tropical region and in the temperate zones tend to form mixed stands with complex structures that make the height to biomass allometric relations inaccurate. Even in managed forests, especially in central Europe, forest management increasingly tends to create complex structures to make stands more resistant against the changing climatic conditions.

Characterization of structure in moderate to high biomass forests is a major challenge in remote sensing. While remote sensing has had considerable success in measuring the structural characteristics of vegetation in areas where the canopy cover is relatively sparse there is not much research on dense forest canopies (Lefsky, et al., 1999). Therefore if it is wanted to derive biomass from complex dense ecosystems new approaches need to be developed.

To solve this problem other parameters can be used in addition to the traditional allometry to characterize the forest relations in complex systems. Two main variables appear in literature as the most suitable: forest density and forest structure. Forest density has been extensively used over the years and it is a very well know forest parameter (Reineke, 1933) (Pretzsch, et al., 2005), even though the measurement of forest density parameters with remote sensing systems have appeared to be not able to be resolved. Nevertheless, some remote sensing systems, like LIDAR and radar are capable of resolving forest structural parameters from the vertical backscattering of

the forest components ((Tebaldini, et al., 2008); (Cloude, 2005); (Lefsky, et al., 2002); (Harding, et al., 2001)).

Forest structure, both in horizontal and vertical dimension, is a key factor for the functioning of forest ecosystems. The dispersion and number of tree elements within the three dimensional space directly controls the exchange and fluxes of energy and mass between the vegetation and the rest of the ecosystem (Houghton, et al., 2009). The structure of forests, particularly in the vertical direction, has been used as an indicator of above-ground biomass, ecosystem state and biodiversity. Moreover, the vertical forest structure helps to the quantification of the above-ground biomass, which in turn indicates the above-ground carbon stock of the observed forest and is a determinant to understand the global carbon cycle.

In several studies (Harding, 2001; Blair, 1999) it is shown how vertical structure can improve biomass measurements as well as the intrinsic relation that exists between the biomass evolution over time and the forest vertical structure development. However there is a lack of research in the development of reproducible methods to describe forest vertical structure. Thus, it is necessary to develop a methodology that is capable of describing the biomass vertical forest structure with stable and reproducible parameters that can be applied to different forest environments.

1.3 Remote sensing for "structure to biomass measurements": LIDAR and radar

Of the different remote sensing techniques that are available nowadays two active systems present a higher capacity to characterize forest structure from the rest: LIDAR and radar.

In recent years, the estimation of forest structure heights has been the object of study by radar systems. The exploitation of multi-baseline SAR (Systematic Aperture Radar) data for conducting topographic analysis has been presented as a very useful technique, due to its capacity to resolve multiple targets within the resolution cells ((Tebaldini, et al., 2008), (Reigber, et al., 2000))

Laser altimetry or LIDAR (Light Detection and Ranging) is an alternative remote sensing technology particularly suited to derive information about biophysical parameters such as tree

height, fractional vegetation cover or canopy geometry (Lefsky, et al., 2002). The measurement principle of LIDAR relies on laser pulses propagating vertically through the canopy, while scattering events with the vegetation are recorded as a function of time. The response obtained by LIDAR is consequently dependent on the vertical distribution of canopy elements such as foliage and branches, as well as the underlying terrain (Houghton, et al., 2009) .

However, for the retrieval of forest parameters based on LIDAR or radar data, the interaction of the emitted signal with the complex 3D structure has to be adequately understood and interpreted. It is therefore possible to say that the main challenge of a study on the remote sensing for Earth observations is to establish a solid relationship between the diverse measurements of the backscattered signals and the parameters that are wanted to be estimated (Koetz, 2006).

1.3.1 Remote sensing context: Tandem-L and DESDyni missions

This study is done in the context of the two satellite missions DESDynI and Tandem-L. The characterization of forest structure is one of the main goals of both missions. The purpose of this study is therefore it is intended to provide forest vertical structure parameters to support the development of these missions. In addition, the question of links between the remote sensing systems and the biomass through forest vertical structure is established in the framework of both missions. The two missions are described next:

DESDynI (Deformation, Ecosystem Structure, and Dynamics of Ice) is an L-band InSAR and laser altimeter for studying surface and ice sheet deformation, used for understanding natural hazards, climate and vegetation structure for ecosystem health. DESDynI addresses many of the scientific objectives assigned high priority by the decadal survey. It will measure the height and structure of forests, changes in carbon storage in vegetation, ice sheet deformation and dynamics, and changes in Earth's surface and the movement of magma. These measurements will improve our understanding of the effects of changing climate and land use on species habitats and atmospheric CO_2. DESDynI measurements will also facilitate the monitoring of species habitats, understanding the response of ice sheets to climate change and the impact on sea level, and forecasting the likelihood of earthquakes, volcanic eruptions, and landslides (Freeman, et al., 2008).

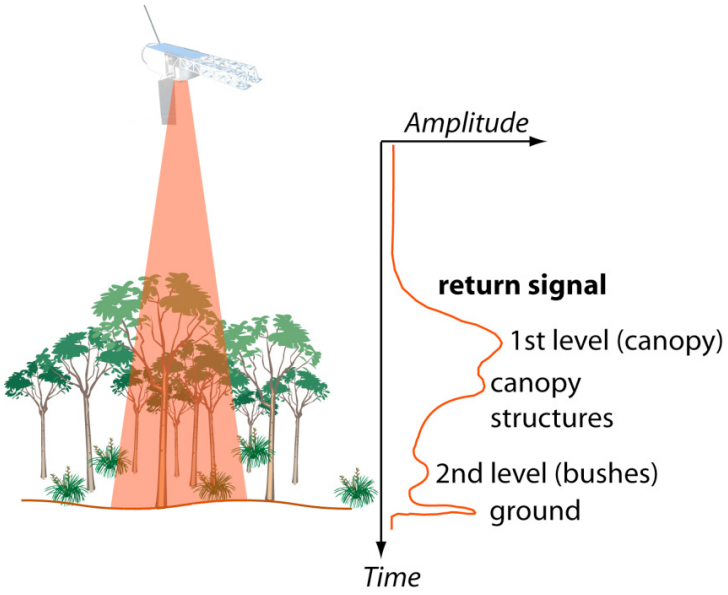

Figure 1 - The return signal waveform from LIDAR contains information on the height and structure of forest canopy. DESDynI's multi-beam LIDAR will sample global forest ecosystems on a grid pattern (Freeman, et al., 2008).

According to Freeman (2008) NASA hosted a workshop in July 2007 to assess the DESDynI mission, articulate the expected scientific return from DESDynI, and recommend next steps for the mission. The primary mission objectives for DESDynI are to:

1. Determine the likelihood of earthquakes, volcanic eruptions, and landslides.
2. Predict the response of ice sheets to climate change and impact on sea level.
3. Characterizing the effects of changing climate and land use on species habitats and carbon budget.

And as an application:

4. Monitor the migration of fluids associated with hydrocarbon production and groundwater resources.

The second mission mentioned is the Tandem-L mission. Tandem-L is a German proposal for an innovative interferometric radar mission to monitor the Earth system and its intricate dynamics. Important mission objectives are global inventories of forest height and above-ground biomass, large-scale measurements of Earth surface deformations due to plate tectonics, erosion

and anthropogenic activities, observations of glacier movements and 3-D structure changes in land and sea ice, and the monitoring of ocean surface currents (Krieger, et al., 2009).

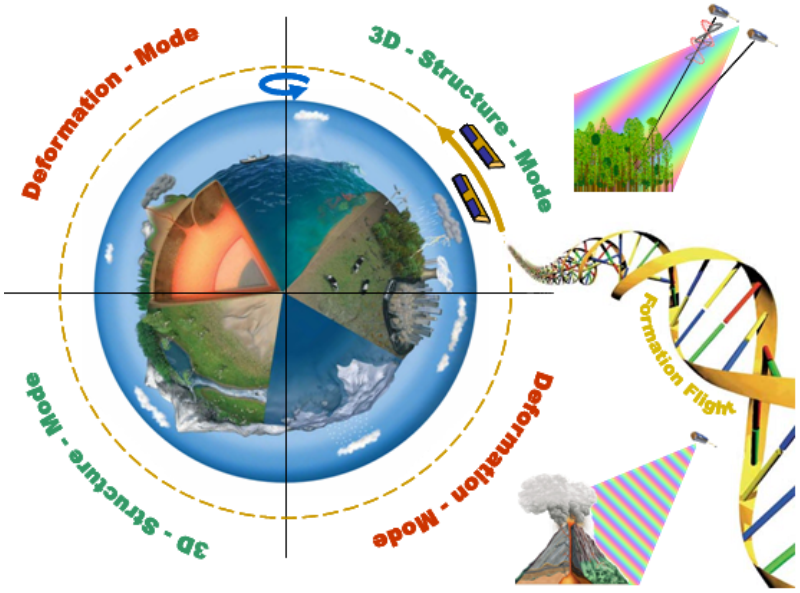

Figure 2 – The Tandem-L mission concept relies on a systematic data acquisition strategy using a pair of L-band SAR satellites flying in close formation. The satellite system is operated in two basic data acquisition modes: 3-D structure mode and deformation mode. New SAR imaging techniques enable frequent coverage with high geometric resolution. (Krieger, et al., 2009).

The Tandem-L mission concept is based on co-flying two fully-polarimetric L-band SAR satellites in a close formation. The synergistic use of two satellites enables highly accurate interferometric measurements to derive contiguous 3-D structure profiles and their spatiotemporal evolution. The advanced imaging capabilities and the systematic data acquisition strategy make Tandem-L a unique observatory to significantly advance our scientific understanding of environmental processes in the bio-, geo-, cryo-, and hydrosphere.

The German Tandem-L mission proposal has in its primary science objectives several commonalities with the DESDynI mission. DLR and NASA/JPL are currently investigating in the scope of a pre-phase. A study of the feasibility of a joint mission that meets or even exceeds the science requirements of both proposals and at the same time provides a significant cost reduction for each partner.

1.4 Goal and objectives

In conclusion the goal of this study is to investigate the potential of forest vertical structure for biomass estimation by remote sensing systems. From this main goal three individual objectives can be defined:

- Description and parameterization of vertical structure.
- Evaluation of the potential of structure parameters in forest biomass estimations.
- Test of the applicability of vertical forest structure parameters for biomass estimation using a remote sensing system.

This study will be divided in two main parts. The first part is the characterization of forest vertical biomass. For this purpose first vertical forest biomass profiles will be created. Their capacity to represent the vertical distribution of the biomass will be tested. Then analyses of possible structure parameters will be analyzed on their capacity to improve biomass estimations to characterize vertical biomass forest structure. The second part will be the application of the developed vertical forest biomass parameters in Remote Sensing systems, which in this case will be an airborne LIDAR system.

2 Materials and methods

2.1 Test site Traunstein

2.1.1 Description

The test site for this study is located in the forest of Traunstein ("Traunsteiner Stadtwald"). The well documented data base together with its diverse conditions are the main reasons for choosing Traunstein as the test site for this case study. Traunstein is generally characterized as having highly diverse structural conditions, i.e. mixed composition of species with different heights, diameters and ages.

For the later analysis not all the districts that belong to the administrative unit of the "Traunsteiner Stadtwald" will be used. It will be focused on the areas with available remote sensing data: the districts IV (Bürgerwald) and VII (Heiligengeistwald). These districts lie east of the city of Traunstein (Figure 3). In the following sections the forest holding "Stadtwld Traunstein" will be characterized based on the Management Plan for the Municipality of Traunstein (Moshammer, 2010).

2.1.2 General Characteristics

The test-site Traunstein is located in the pre-alpine moraine landscape of the southeastern Bavaria, near the city of Traunstein. The topography varies from 600-650 m a.s.l., with only few steep slopes. The climatic conditions with a mean annual temperature of 7.3 °C and precipitation of more than 1600 mm favor mixed mountainous forests. The vegetation period lasts from 150 to 160 days with a mean temperature of 14°C and a minimum precipitation of 800 mm. The potential vegetation community is the Luzulo luzuloidis-Fagetum accompanied by: Adoxo

moschatellinae-Aceretum, Galio rotundifolii-Abietetum, Galio odorati-Fagetum and Vaccinio vitis-idaee-Abietum.

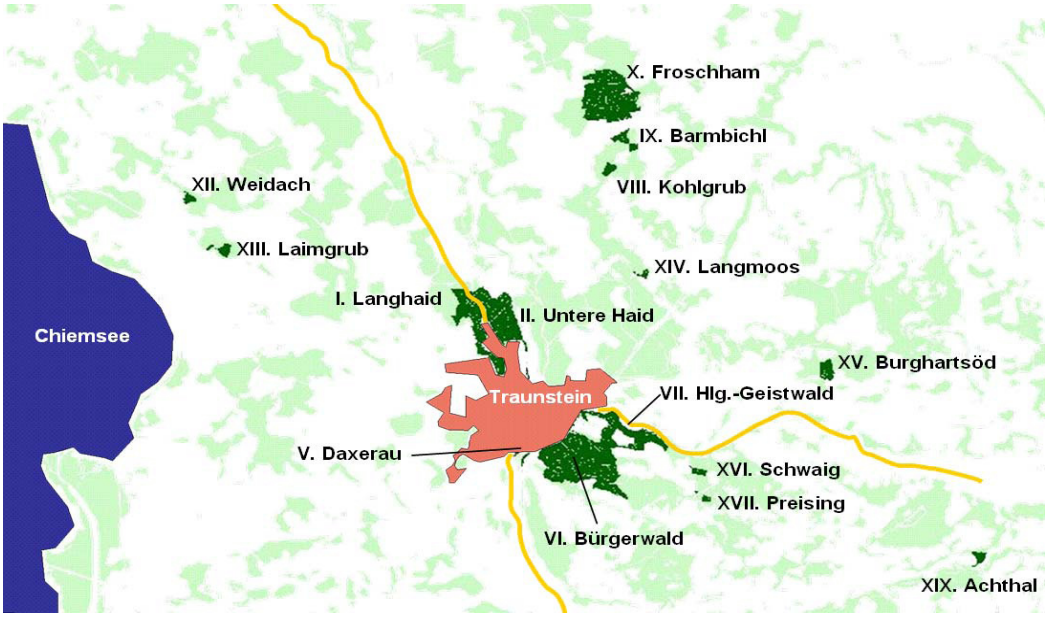

Figure 3- Location of the 15 districts that belong to the "Traunsteiner Wald" (Moshammer, 2010).

In reality the species composition is dominated by spruce (*Picea abies*), beech (*Fagus sylvatica*) and fir (*Abies alba*). The noble broadleaves are mainly represented by Maple (*Acer pseudoplatanus*) with a content of ca. 65% and by ash (*Fraxinus excelsior*) together ocupying 30% of the surface.

Four out of five parts of the area corresponds to a climatic category of moderately fresh to fresh. Thus, most of the present species have a good grow well under these conditions. However, in 5% of the area the water content of the soil belongs to the category moderately dry to moderately fresh. Under these conditions and following the prognosis of climate change the management tends to reduce the presence of big homogeneous areas of spruce or fir. It is therefore intended to increase the areas of mixed forest where broadleaves will help to keep the stability of the stand.

2.1.3 Forest management

In the period from 2000 to 2008 an intensive stock reduction has taken place in Traunstein. Moreover, as mentioned, due to the effects of changing conditions (Climate Change) a different structure is aimed for. Thus, the main management purpose is the establishment of permanent and stable stands avoiding big areas with even aged stands. According to the different management plans from 2000 and the inventory of 2008 the upper age classes have been reduced for all species; coniferous stands (spruce) are more affected, while the mixed stands (with broadleaves) are increased.

Figure 4- Plots distribution for the Stands of Bürgerwald and Heiligengeistwald. Each red point represents an inventory plot. (Aerial photograph Bayerngefliegung)

The prescribed yield of timber according to the management plan (Moshammer, 2010) in 2003 was 7600 Efm year^{-1} (13.2 Efm ha^{-1} year^{-1}). Assuming a growth rate of 12 Efm year^{-1} ha^{-1} the harvested timber absorbs the growth rate and reduces stock.

In the period from 2000 to 2008 34% of the timber harvested corresponds with impacts conditioned harvesting. Two thirds of this amount were the consequence of three important storm phenomena, Lothar in 1999, Kyrill in 2007 and Paula in 2008. The remaining third corresponds to several storms that occurred in the dry year of 2003 in combination with bark beetle attacks.

These phenomena have had a determinant impact on forest management and forest structure; Spruce stands with low stability were chiefly affected.

2.1.4 Summary of the inventory plots characteristics

The two districts considered for the study cover an area of 218 ha. Quantitative information about the forest is provided by means of the forest inventory that was carried out in 2008 based on a 100x100 m. grid. Altogether, 228 inventory points were located within the test area (Figure 4).

The permanent inventory plots were established using three concentric circles. In each of the different circles, trees with specific diameters were measured. The largest circle with a radius of 12.62 m encloses an area of 500m^2 and trees with diameters larger than 30 cm were measured. The second circle has a radius of 6.31 m (125m^2) and trees with diameters larger than 10 cm were measured. The smallest circle has a radius of 3.15m (31 m^2) and all trees within this area were measured.

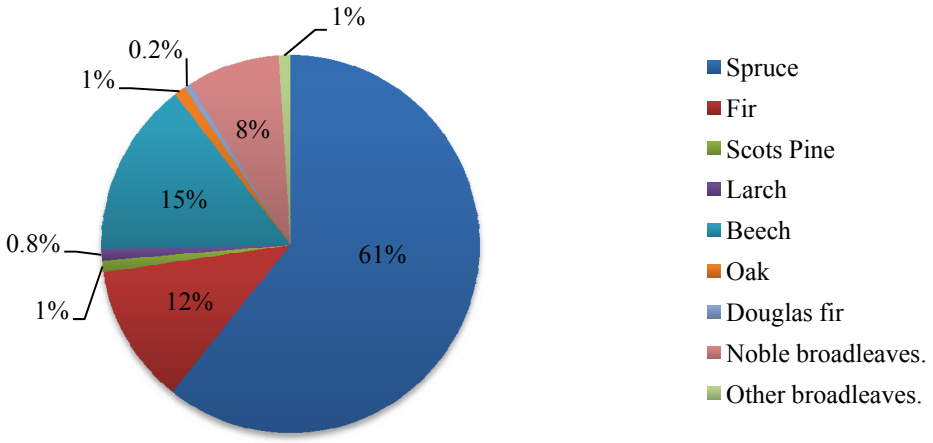

Figure 5- Species relative distribution for inventory in 2008 (Moshammer, 2010).

1.1.1 Stand structure and species composition

Changes in the conditions of Traunstein forest are analyzed in the following. In the inventory of 1998 the volume was 237,780 Efm (425 Efm/ha) while in the 2008 a volume of 174,280 Efm (308Efm/ha) was registered. In other words, in this ten-year period the stock

volume was reduced by 63,500 Efm (117 Efm/ha), i.e. is a 28% of the volume. This illustrates the forest management aim of a strong stock reduction.

With regards to the species composition, the actual proportion of conifer to broadleaves is 60:40.Coniferous trees are dominated by spruce making up 61% of the total followed by fir with a 4%. From the broadleaves, beech is the dominant tree species with an 15% (Figure 5).

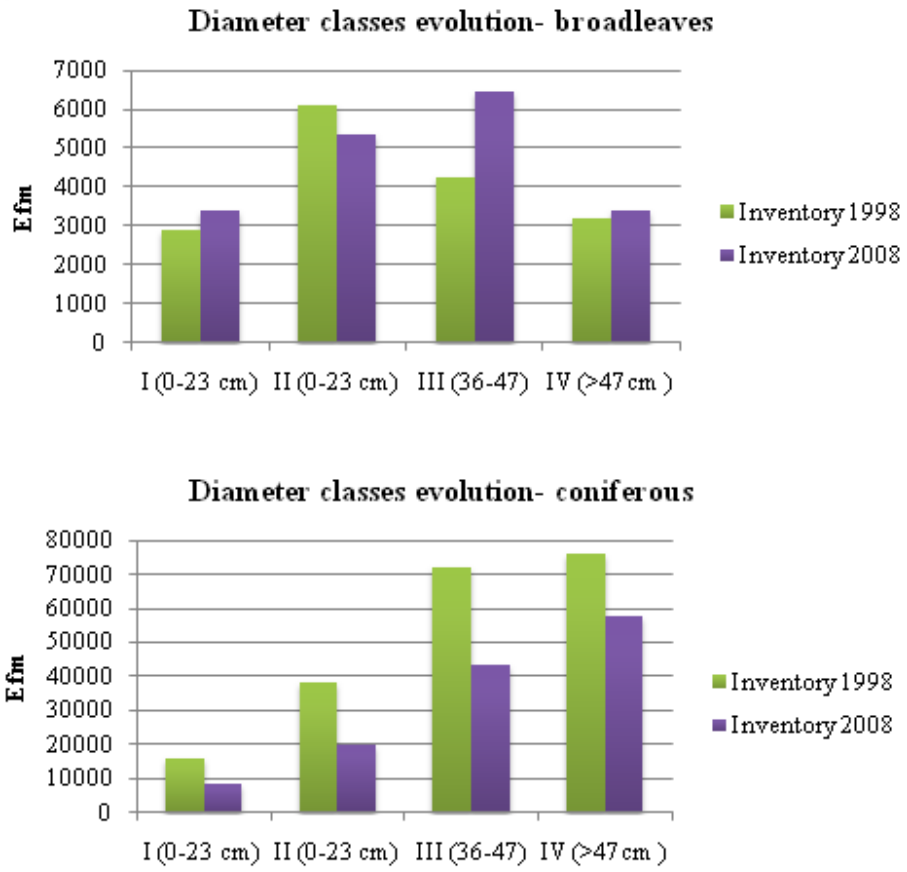

Figure 6- Evolution of the species distribution from the inventory of 1998 to the inventory in 2008 for broadleaves (top) and conifer (bottom)

The evolution of the species distribution from 1998 to 2008 is summarized as follows (Figure 6):

- With a proportion of 75% in 1998 to 61 % in 2008 the Spruce is still the dominant tree species.

- From 2008 to 2009 the fraction of broadleaves species increased at expenses of conifer (mainly spruce). The mixed areas of fir, beech and noble broadleaves have also increased.
- Scotts pine, larch, douglas fir and oak with the rest of the broadleaves represent together only 4% of the total inventory.

Figure 6 shows distributions of inventory data in diameter classes. While in 1998 broadleaved trees were concentrated in the lower diameter classes, in 2008 they were more equally distributed in all classes. Distribution of coniferous trees over diameter classes did not change between the two inventories. But total amount of coniferous trees was reduced in all diameter classes.

2.2 Theory of allometry

Allometry is the science concerning the relations between size dimensions of living systems. Forest allometry refers to the size dimensions of forests. Nowadays size relations are understood as the result of phylo- and ontogenetic evolution that have optimized and still optimize functional advantages and obligations: "Organic proportionalities often reflect consequences of natural selection operating on the relation between form and function" (Niklas, 1994). In this sense, the study of allometry is motivated by the attempt to understand the adaptations of the living organisms to their environment.

Besides the physiological and evolutionary implications, allometric relations are quite practical when estimating a size dimension from another that is much easier to measure (Mette, 2007). Theory of allometry is applicable when estimations of forest biomass can be used from first order measurable parameters like forest height or forest vertical structure.

2.2.1 Forest parameters

In the most general formulation, forests are defined as plant formations that are constituted mainly from trees and cover with sufficient extent for the development of a characteristic forest climate (Burschel, et al., 1997). The first criterion "tree" refers to woody

upright, perennial plants with branching at the tip, reaching at maturity at least 5-7 m. The second criterion "characteristic forest climate" depends on height, density and extension of the forest.

The FAO (2001 a/b, Annex 7.1) sets the limits of these parameters as follows:

> 5m tree height at maturity (3m cold or dry zones)
> 10% canopy cover (open 10-40%, closed > 40%)
> 0.5 ha extension.

The criteria applied for the discrimination between forest and non-forest areas have important consequences. Statistics about forest cover, biomass, etc. change with the definition of forest, and are often connected to legal questions concerning management, protection, subsidies, Kyoto etc. (Mette, 2007).

2.2.1.1 First order parameters

The main parameters that characterize a tree in a dendrometric scene sense are:

- Tree species: relates to wood density and tree shape.
- Tree dbh (m): diameter at breast height (1.3m) above-ground.
- Tree height (m): vertical distance between ground and tree tip.
- Tree volume (m^3) or biomass (Mg): most integrative structural parameter.

While volume is more of a forestry standard, biomass is the ecological standard. Biomass can be calculated from volume through multiplication with species-specific wood density weight ρ (g cm^{-3}):

$$Biomass = Volume \cdot \rho \qquad (2.2.1)$$

Volume and biomass are typically defined as stem volume or biomass, usable wood volume or biomass, or total wood volume or biomass, although biomass can also include non-woody parts of the tree.

The stem volume can be calculated from tree height h, diameter dbh and the shape factor f_z; tree biomass b_{stem} is obtained after the multiplication with the woody density ρ (eq. (2.2.2)) .

In this way, biomass is considered as a first order parameter as it has been obtained by the multiplication of directly measured parameters.

$$b_{stem} = h \cdot \pi\left({}^{1}/_{2}\, dbh\right)^{2} \cdot f_z \cdot \rho \tag{2.2.2}$$

The shape factor accounts for the stem shape, for the height of the reference diameter and for the definition of volume. It typically assumes values around 0.5.

Finally the forest biomass is calculated as the sum of the individual stem biomasses related to an area unit (typically ha). If the tree dimensions are more or less similar, i.e. in an even aged forest, then the biomass can be calculated using mean height h_{mid} and mean dbh dbh_{mid}, denoted by *mid*, and multiplied by the tree number per hectare *N*:

$$B_{forest} = \sum_{i=0}^{n} b_{stem} \tag{2.2.3}$$

$$B_{forest} = h_{mid} \cdot N \cdot \pi(\frac{1}{2} \quad dbh_{mid})2 \cdot f_z \cdot \rho_{mid} \tag{2.2.4}$$

2.2.1.2 Biomass as a second order parameter

Biomass is usually treated as a first order parameter calculated from variables like diameter, height and wood density. However, for this study it must be considered as a second order parameter as it is necessary to account for all parts of the tree (stem, branches, and leaves) that are especially important for carbon stock estimations. Direct measurements of all of these contributions are very elaborate and not practical in large-scale inventories. Therefore most approaches are restricted to measure dbh or height to derive branch and leaf biomass with regressions (allometric relations).

Most investigations on forest volume or biomass estimates are based on dbh and height, but only few studies have harvested the whole tree for direct measurements. Thus, the generalized regressions that can extrapolate the tree dbh or volume measurements to the other

biomass components are often uncertain. In reference to Brown and Lugo (1992, see Brown 1997), these regression factors are termed biomass expansion factors (BEF).

The FAO uses two standards, the VOB10, the volume over bark of all trees above 10 cm dbh, and the above-ground biomass, which includes the woody part (stem, bark, branches, twigs) of trees, alive or dead, shrubs and bushes (FAO, 2001). The VOB10 rather addresses the forestry community and represents what was actually measured; the above-ground biomass addresses more the ecology and global community, and was derived from the dbh or volume using more or less generalized regressions (Mette, 2007).

2.2.2 The allometric equation

The allometric relations are based on the development of specific equations that involve first order parameters and empirically calculated coefficients. The allometric equation is defined as the power function of the mathematical solution of a relative growth equation (Mette, 2007).

The following are some common expressions used especially in the forestry theory,:

$$y = a \cdot x^c \tag{2.2.5}$$

This equation can also be formulated logarithmically:

$$lny = lna + c \cdot lnx \tag{2.2.6}$$

where x represents a measured parameter (first order) and a and c are the coefficients. The allometric factor is denoted by a, the allometric exponent c.

In literature the logarithmic expression is more frequently applied; due to its linearity it is an easily visible indicator of an allometric and study objects that may vary over several orders of magnitude. However, for limited size ranges with linear intervals the logarithmic representation emphasizes low values.

2.2.2.1 Allometric reference functions

For a set of allometric relations with a similar allometric exponent ‘c’, the ratio of the allometric factors ‘a’ is a directly scale of the functions to each other. Often, it makes sense to

choose one equation as the "allometric reference function" f_{ref} with a certain c_{ref} and a_{ref}. If for an allometric function f_1 the exponent c_{ref} is enforced, then the ratio of the allometric factors a_1/a_{ref} shall be defined as the "allometric level l_a".

$$f_{ref} = a_{ref} \cdot x^{c(ref)} \tag{2.2.7}$$

$$f_1 = a_1 \cdot x^{c(ref)} \tag{2.2.8}$$

$$l_a = {}^{a_1}/_{a_{ref}} \tag{2.2.9}$$

The allometric reference equation and the allometric level that are the basis for the concept of the height-biomass allometry, as explained in (Mette, 2007), are introduced in the next chapter.

2.2.2.2 Introduction to the Stand Density Index

A well known example of an allometric equation in forestry is the Stand Density Index SDI which relates the mid dbh and the tree number *N* over an allometric exponent of -1.605, i.e. the Reineke exponent. This allometric exponent explains a self-thinning rule assuming the same allometric relationship between size and density for a wide spectrum of species under these self-thinning conditions (Reineke, 1933).

$$SDI = N \cdot \left({}^{25.4}/_{dbh_{mid}}\right)^{-1.605} \tag{2.2.10}$$

The SDI was postulated for woody plants and it is an early empirically based species invariant scaling law with a considerable importance in forest practice and forest science (Pretzsch, 2006).

2.2.3 Eco-Physiological implications

The physiological relevance of the allometric functions lies in the interpretation that any organ of the organism receives a part of the total growth energy that is proportional to the relative size. The allometric exponent 'c' is a measure for the organism's internal distribution strategy.

Often it is proposed that volume or biomass related allometric functions scale with exponents of thirds due to the 3-dimensional volume unit (m^3) (Bertalanffy, 1942).

Traditional allometry concerns itself to the relations of parameters of organs during growth. The connection between allometry and growth can be studied in the theory of "dynamic morphology" (Bertalanffy, 1942) which states that any organic system is essentially a hierarchy of processes in a dynamic balance between assembly, or anabolism, and breakdown or catabolism.

Classical allometry is based on animal communities but it has also been equally applied to plants and plant communities, especially trees and forests (Mette, 2007). Some of the main characteristics of plant communities that distinguish them from animals and define the theoretical base for the forest allometric relations can be summarized as follows:

1. Plants can grow, in theory, indefinitely.
2. Woody plants consist to a great part of dead biomass, in essence vascular xylem tissue. A transport system that exceeds diffusion by several orders of magnitude can only be built through the death of these (dead) cells. The transport system enables plants to grow in height and gain in competition for light. Moreover, the characteristic strong cell's wall is required to support the negative pressure trough the water conduction and the mechanical structural integrity.
3. Plants are highly flexible in shape, in comparison with animals.

These three points are of major importance to define the relations within the trees and they define the principles of forest structure. Especially the capacity of these xylem cells to support the tree weight and the mechanical efforts. In fact, even if in theory, tree growth is not restricted the capacity of the individual to support the gravity forces and the disturbances will define its shape and size.

2.2.4 Height to biomass allometry

The allometry between height and biomass is a relatively old concept in forestry and the close relation between height and stem volume has been extensively described in Pretzsch

(2001). In the following, the study of Mette (2007) will be explained, using the allometric relations for a Spruce stand in the test site of Traunstein.

The height to biomass allometry as investigated by Mette (2007) has been based on German standard forestry tables. Since allometry is based on yield tables these relations are forest type-specific and it is therefore needed to discuss how strong the height-biomass allometry depends on the forest type. The study of Mette (2007) is based on an even-aged spruce stand. Thus, the parameters used for the height to biomass allometry are derived for these specific conditions. The parameters that determine this relation are stand conditions and age, forest management and forest species. The consideration of these three parameters is fundamental to understand the strength and limitations of the height-biomass allometry under such particular stand conditions:

1) An age and stand condition independent height-biomass relation can be derived for Norway spruce: in the general on yield tables it can be seen that different stand conditions lead to different growth rates. Hence, when estimating stem biomass from stand age, information about the stand conditions is very important.

On the other hand, when estimating stem biomass from tree height, the influences of stand conditions is almost negligible: a specific height corresponds to a specific biomass, no matter whether it is at a young age in a fast growing forest (under favorable conditions) or at an old age by a slow growing forest (under adverse stand conditions). Hence, an allometric height-biomass relation for Norway spruce can be established here and is independent of stand conditions and age (Mette, et al., 2003).

2) The variability of the height-biomass relation for Norway spruce: The forest yield tables used in the allometric relation (Mette, 2007), were only registered for managed forest systems, where the growth rate is maximized through a moderate to strong thinning of weaker trees. The yield tables used, especially with regard to of the type of management (thinning), can be considered as assumptions in the allometry. Therefore, allometric relations will always possess a certain variability due to missing information about forest management and structure.

3) The effect of species: Depending on the species the allometric exponent varies. Thus, height-biomass relation between different species can vary within a limited range of +/- 15% for the main species that are present at the test site Traunstein (Mette, et al., 2003), see also Figure 7. The range, which in this case is rather limited, can be wider depending on the conditions and variety (mixture) of species at the site.

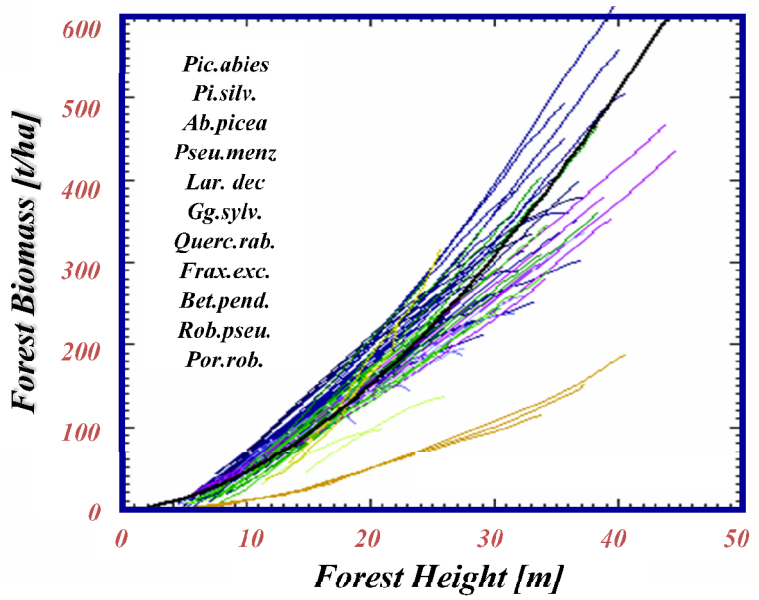

Figure 7- Regression curves for the collection of yield tables used by Mette (2007). The curve used for the allometric equation is represented in black

In the case of a spruce stand at the test site of Traunstein the allometric equation has an allometric factor of 0.68 and an allometric exponent of 1.76:

$$Biomass_{stand} = 0.68 \cdot (tree\ height_{stand})^{1.76} \qquad (2.2.11)$$

For mixed species conditions, however, this formula can change due to the different allometric levels and allometric exponents. In Figure 7 a set of height to biomass regressions for different species extracted from the forest yield tables is displayed, which were used in Mette (2007) to derive the general height to biomass allometric relation:

$$Biomass_{stand} = 0.66 \cdot (tree\ height_{stand})^{1.50} \qquad (2.2.12)$$

2.2.5 Allometric improvements: density and structure

As noted in the previous chapter the height to biomass allometry has several limitations. It has its maximum potential applied to even aged single species stands but it does not show the same degree of adjustment under mixed conditions (mixed forest species) or with a higher structural diversity. Therefore, some additional second parameters, which can describe more complex forest systems, are needed to improve the height to biomass allometry for these conditions. These density and structure, are later discussed.

2.2.5.1 Density and self-thinning: usage of the SDI

Although the principle of allometry was derived from individual-based considerations, it can be applied meaningfully to plant communities under self-thinning conditions (Yoda, K.; Kira, T.; Ogawa, H; Hozummi, K., 1963). As plants grow in size their demands on resources and growing space increase. If resources are no longer adequate for all stand components, self-thinning will be initiated and the number of plants per unit area (density N) will decrease. The size density allometry of plants under self-thinning is particularly informative under eco-physiological and production economics aspects because, under self-thinning conditions, size-density allometry reveals the species-specific, critical demand on resources and growing space of average trees at a given mean size (Pretzsch, et al., 2005).

Stand dynamics under self-thinning conditions can give extra information for eco-physiological and production aspects in terms of volume and biomass. Moreover, it reveals species specific critical demands on resources and growing space, establishing a relation between density and tree size.

This simple and general rule allows us to reduce the complexity of the allometric relation; however, it has the risk of neglecting individual species peculiarities, which are essential for assessment and understanding the dynamics of organisms, populations or ecosystems (Pretzsch, 2006). If it is combined with the model equation of the height to biomass allometry (eq.(2.2.5)) the following equation can be derived:

$$B = a_0 \cdot h^{a_1} \cdot SDI^{a_2} \tag{2.2.13}$$

The biomass can then be estimated with the usage of just the height of the stand h (dominant, mean height) and the Stand Density Index calculated with eq. (2.2.13).

2.2.5.2 Structure

Vertical forest structure is of interest to many disciplines and is consistently discussed in the context of ecosystem management. The vertical stratification is defined by the tree crowns is a forest attribute that influences both tree growth and the understory structure. Therefore, it can be a very useful parameter to consider when making management decisions that affect the structure of stands, i.e. volume or biomass oriented studies (Lathan, et al., 1998).

The forest dynamics are the main forming factor of the forest vertical structure. The arrangement and vertical distribution of trees biomass changes during stand development because of many different factors: competition, tree mortality, the initiation of new understory trees, and the growth of previously suppressed trees. In addition, herbivory, spatial heterogeneity, environmental factors, and disturbances contribute to the complex vertical and horizontal structural patterns that develop the forest structure.

On the other hand, structural changes that result in differences in the amount and distribution of biomass in stands affect the stand functions such as photosynthesis and respiration. Moreover the structural patterns of the overstory trees affect the canopy gap structure due to the participation of light and precipitation received by the understory layers. This gap structure is also affected by a variety of factors coming from the spatial position of nearly trees, density and arrangements of branches (Lathan, et al., 1998). Because of all of these interactions forest vertical structure is a dynamic forest characteristic and it is intrinsically related with forest evolution. As a summary, the stock of forest biomass is determined by the trees vertical and horizontal spatial arrangements and it changes over time due to numerous interactions and disturbances.

However, vertical structure and the calculation of biomass out of vertical structure are not so extensively treated in literature. One possible approach that will be used in this study is the creation of forest vertical biomass profiles. In this study vertical biomass profiles are parameterized and the relation between these parameters is investigated.

2.3 Biomass model, from tree to plot level

2.3.1 Individual tree representation

To define the above-ground biomass of a tree it is necessary to first estimate the volume of the two main tree compartments already mentioned, the stem and the crown. Volume estimations are described by the following set of parameters, measured during forest inventory: tree species, diameter at breast height (*dbh*), total height (*h*), the tree position defined by the coordinates (x, y). Additionally, the height of the crown base (*kra*) and crown diameter (*kd*) are calculated from the measured parameters.

Table 1 – Tree volume parameters.

Tree volume parameters	
Inventory information	**Model derived**
tree species	height of the crown base (*kra*)
diameter at breast height (*dbh)*	crown diameter (*kd*)
total height (*h*)	
tree position *(x, y)*	

Every tree is assumed to stand straight up. Species specific crown models are used to represent three dimensional crown shapes. These models assume the crown to be rotation-symmetric in horizontal direction and split vertically between an upper and a lower part. Shape and relative length of upper and lower crown section is species-specific, but the crown is always assumed to be of maximum width (*kd*) at the height where both sections meet each other (Pretzsch, et al., 2002).

2.3.1.1 Stem

In this study two stem volume models were used:

1. Cylinder
2. Cone

Calculations use diameter at breast height *(dbh)*, and tree height as input variables.

Cylinder:

The simplest shape that can be adapted to the stem is a cylinder using the dbh as diameter and the total height of the tree as cylinder height. The cylindrical shape distributes the volume equally along height, as a consequence the volume of the upper parts of the stem are overestimated while the lower parts are underestimated.

Cone:

The next shape considered is a cone (Figure 8). The height of the cone will be the tree height and the basal diameter corresponds with the extrapolated dbh at 1.3 m. from the ground. In this case, the volume per meter decreases with height as a function of the characteristic shpe as described by the perimeter of the cone:

$$y_i = \sqrt{{r_i}^2 + {h_i}^2} \tag{2.3.1}$$

The cone tends to overestimate the volume in the lower parts of the stem and to underestimate the middle parts. Nevertheless, it offers a good representation of the top, especially for coniferous species.

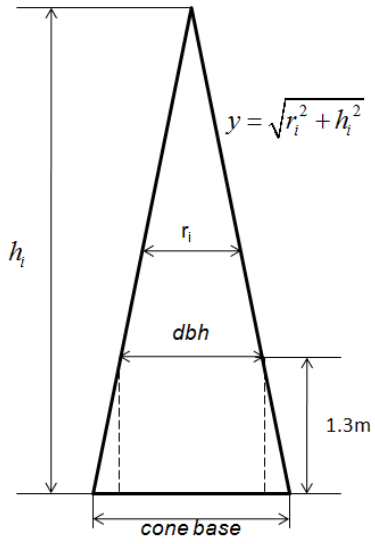

Figure 8 – Stem cone model. The stem is modeled as a cone using basic tree variables (dbh and height).

Another step in complexity would be to integrate the real shape of the tree, usually accounted by the form factor. Because the cone model already yielded results of sufficient quality an extension to real stem shapes was not necessary.

2.3.1.2 Crown

The crown shape model as it is explained below is based on the investigation of Pretzsch (2001). The model allows for calculation of the average, species specific crown shapes. The biometric reproduction of crown perimeter can be carried out for different species using eq. 5.3.2 in a standard calculation procedure describing the change in crown radius with increasing the distance to the tip (E).

For the light crown (r_l) the radius is calculated by:

$$r_l = a \cdot E^b \tag{2.3.2}$$

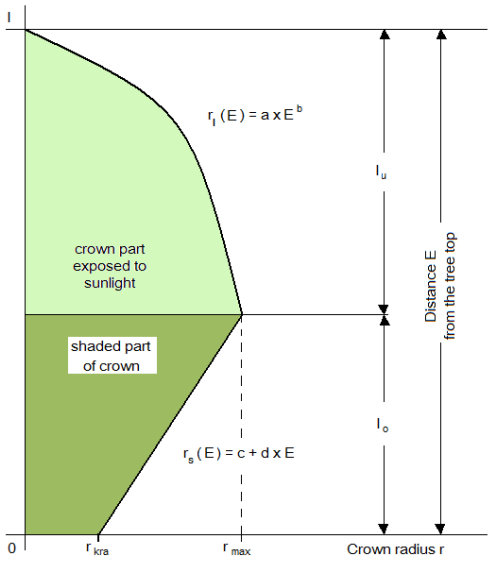

Figure 9 – Schematic representation of the sunlit and shaded crown. (Pretzsch, 2001)

where the parameter 'a' is an individual parameter for each tree and the exponent 'b' is specific for each tree species. The parameter 'b' tends to represent a conic form for the spruce (b=1.0). For the crowns of fir, the Scotts pine and oak 'b' represents a quadratic paraboloid (b=0.5) and

for beech a cubic paraboloid (b=0.33). For a cylindrical shape the value of 'b' should be equal to 0.

The shape of the shaded crown will be analogous according to the tree species equation:

$$r_s = c + E \cdot d \tag{2.3.3}$$

The specifications for each of the species and the coefficients a,b,c,d as well as the specific crown lengths 'l_o' and maximum radius 'r_{kra}' are displayed in Table 2. The input variables, total crown length ($l = l_o + l_u$) and mean crown radius (r_{max}), are needed to determine the parameters a, b, c and d in the crown shape model for the different species. The meaning of the variables is also displayed in the Figure 9. With the input parameters tree height, crown base height, mean crown radius, and with the species-specific crown shape parameter, one can calculate the spatial expansion of the crown, crown volume and crown surface area.

Table 2- Crown shape models for the sunlit and shaded crown for main tree species in Central Europe.

Forest species	**Light crown**			**Shadow crown**		
	a	l_o	b	c	d	r_{kra}
Norway Spruce (Picea abies)	r_{max}/ l_o	l·0.66	1.00	For all species:	For all species:	r_{max} ·0.50
Silver fir (Abies alba)	$r_{max}/(l_o)^{0.5}$	l·0.50	0.50			r_{max} ·0.50
Scotts pine (Pinus sylvestris)	$r_{max}/(l_o)^{0.5}$	l·0.64	0.50			r_{max} ·0.50
Larch (Larix deciduas)	$r_{max}/(l_o)^{0.45}$	l·0.80	0.45	r_{max}-d · l_o	$\frac{r_{kra}-r_{max}}{l-l_o}$	r_{max} ·0.80
E. beech (Fagus sylvatica)	$r_{max}/(l_o)^{0.33}$	l·0.40	0.33			r_{max} ·0.33
Oak (Quercus petrea)	$r_{max}/(l_o)^{0.5}$	l·0.50	0.50			r_{max} ·0.50
Black alder (Alnus glutinosa)	$r_{max}/(l_o)^{0.5}$	l·0.56	0.50			r_{max}

For the estimation of the crown size two parameters are needed: the crown base height kra and the crown radius kd. The model is based on the following equations:

$$\text{kra} = \text{h} \cdot (1 - \text{e}^{-\left(\text{a}_0 + \text{a}_1 \frac{\text{h}}{\text{bhd}} + \text{a}_2 \cdot \text{bhd}\right)}) \tag{2.3.4}$$

$$kd = e^{b_0 + b_1 \cdot ln(bhd) + b_2 \cdot h + (\frac{b}{bhd})} \quad (2.3.5)$$

where h is the tree height in m, bhd the diameter at breast height in cm, $a_0 \cdots a_2$ and $b_0 \cdots b_3$ specific species dependent parameters (Pretzsch, 2001).

In the following, calculation of crown parameters using of crown parameters using Table 2 is demonstrated for the main species, Norway spruce and European beech:

For Norway spruce, the crown shape model assumes that crown width is greatest at 66% of the crown length from the tip (l_o= l x 0.66). This height is used to define the boundary between the sunlit crown, represented as a conical tip for Norway spruce, and the shaded crown, which is approximated by a frustum. A circle represents the crown surface area. At crown base height, the crown radius *kra* is estimated to be the half of the greatest crown radius (r_{kra}= r_{max} x 0.50). For European beech, the model assumes that the greatest crown width occurs at 40% of crown length from the tip of the tree (l_o= l x 0.40). The shape of the sunlit and shaded crowns are represented by a cubic parabola, and frustum respectively. The crown diameter at crown base height is estimated as 33% of the greatest crown width (r_{kra}= r_{max} x 0.50). In the model for Silver fir, the greatest crown diameter is set at a 50% of the crown length (l_o= l x 0.50).

2.3.2 From volume to biomass

Biomass is calculated as a function of the volume models. In this study, some methods pn how to derive biomass from stem and crown compartments are considered. All the possibilities tested are displayed in Figure 10.

2.3.2.1 Stem

The stem biomass is directly obtained from the modeled volume times the dry wood density of each species (Table 3):

$$Biomass = V \cdot \rho \quad (2.3.6)$$

where V is the volume of the stem in m^3 and ρ the density in kg/m^3.

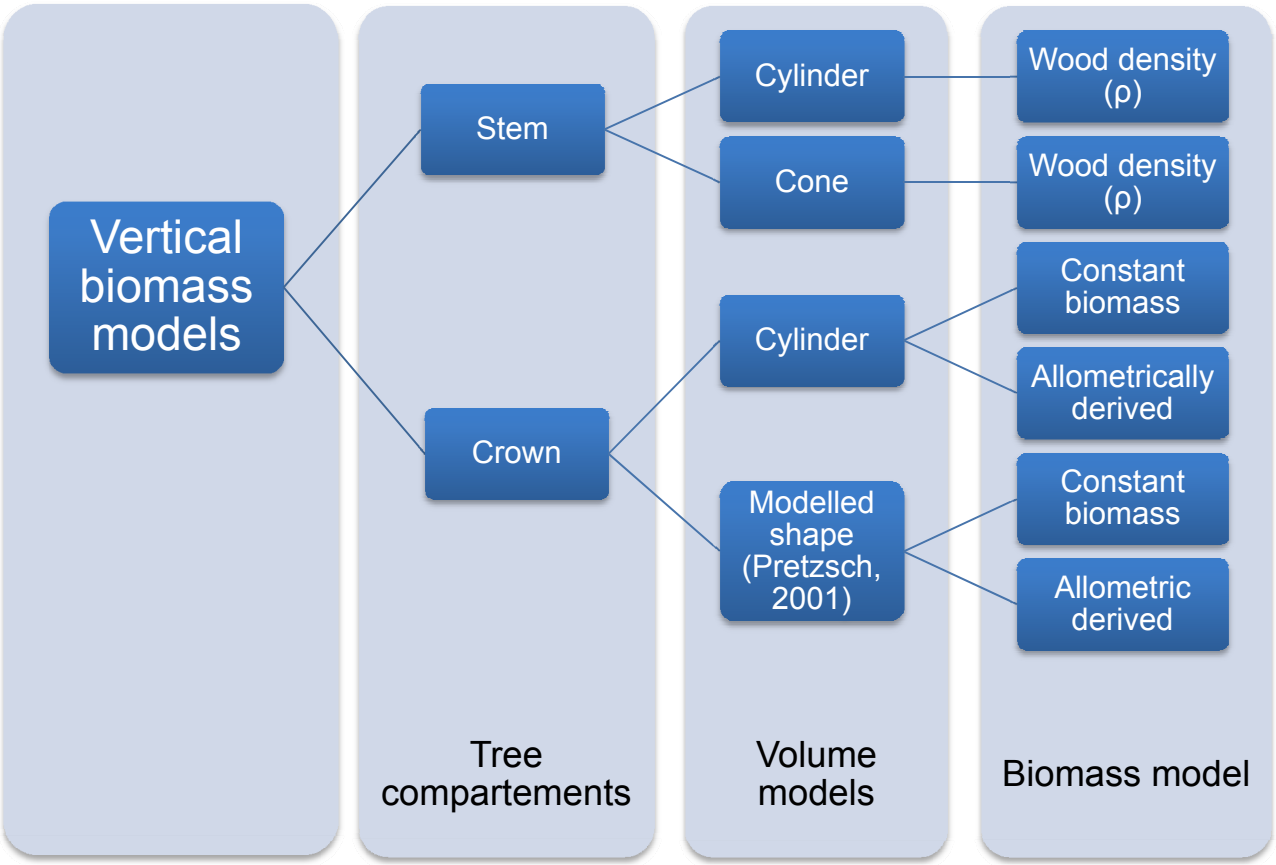

Figure 10 – Vertical biomass models generation, from volume to biomass.

Table 3- Dry wood density of the main forest species in the Traunstein test site according to the Wood Density Databes (2009).

Species	Density (kg/m^3)
Spruce (*Picea abies*)	500
Beech (*Fagus sylvatica*)	650
Fir (*Abies alba*)	480
Oak (*Quercus petrea*)	720
Scots pine (*Pinus sylvestris*)	513
Other species	650

2.3.2.2 Crown

For the estimation of the biomass enclosed by the tree crowns two methods are tested:

- Constant biomass density for all species (0.002 kg/m^3).
- Allometrically derived biomass

A value of 0.002 kg/m^3 was used. This value represents the mean of crown density for the most of the species treated in this study.

For the last point, an extensive database of equations that were developed dependent on species was used (Zianis, et al., 2005). Collected equations include tree biomass estimations and biomass of different tree compartments, including the crown. This publication can be used as guide to the original publications of the shown equations. Equations describe crown biomass as a function of tree height and/or dependent on species (see Table 4).

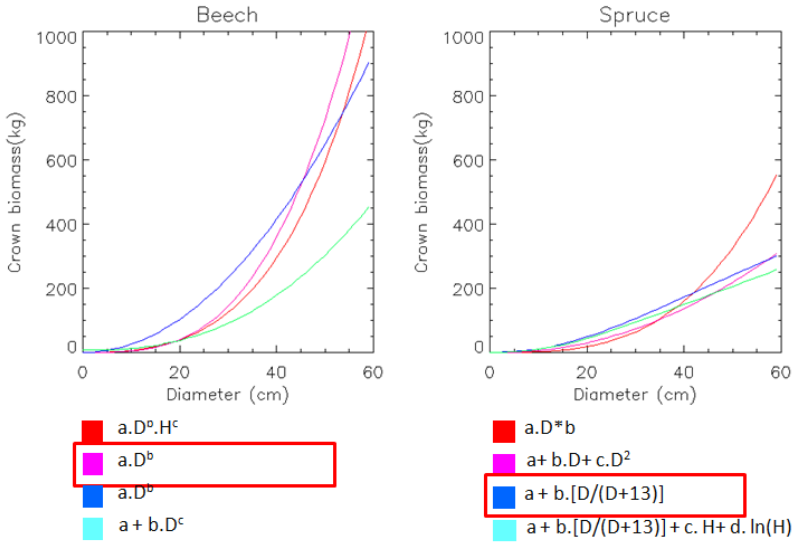

Figure 11 – Representation of the selected allometric equations for beech (right) and spruce (left). Each color represents a different biomass allometric equation (biomass against diameter - dbh). The selected equation is highlighted by a red rectangle.

For each species there are several equations for crown biomass available (Figure 7); one of them was selected according to the following conditions, in order of importance:

1. Similar environmental conditions (relations from different areas).

2. Good adjustments.
3. Wide range of samples.
4. Depending on the variable preferred *dbh.*

Table 4 – Selected crown biomass allometric equations for the main species of Traunstein test site. D is the diameter at breast height (dbh) (Zianis, et al., 2005)

Species	Equation	Parameters		
		a	b	c
Spruce (Picea abies) (Mg)	$a + b.[D/(D+13)]$	-1.2804	8.5242	-
Beech (Fagus sylvatica) (Mg)	$a.D^{b}$	0.0031	3.161	-
Fir (Abies alba) (kg)	$a+ b.D^{c}$	0.0060722	$9.58x10^{-6}$	2.5578
Scotts pine (Pinus sylvestris) (Mg)	$a + b.[D/(D +10)]$	-2.8604	9.1015	-
Sessile oak (Quercus petrea) (kg)	$a. D^2$	$2.1612x10^{-4}$	-	-
Rest = Beech	$a.D^{b}$	0.0031	3.161	-

2.3.3 Plot representation: Forest vertical biomass profiles

All measured trees for an inventory plot can be represented in terms of biomass according to the model described in the previous chapter. Each horizontal cross-section can be connected to a biomass value. For the calculation of biomass profiles each tree was sampled in 1m steps.

Biomass profiles are represented on a two axis basis, where the biomass is in the 'x' axis and the height in the 'y' axis (Figure 12). To calculate a biomass profile along height the biomass for each individual tree is summed in intervals of 1 meter along the height for all the trees that have been measured within the inventory plots. The integral of the area is the total biomass and the highest value the top height..

The calculated biomass consists of the two considered compartments, stem and crown. Biomass distribution along height gives a characteristic profile for each plot, being able to account for the total biomass stock (integral of the profile) and allows classifying a forest in terms of management and structure. An example of a typical biomass profile as found in Traunstein forest is displayed in Figure 12.

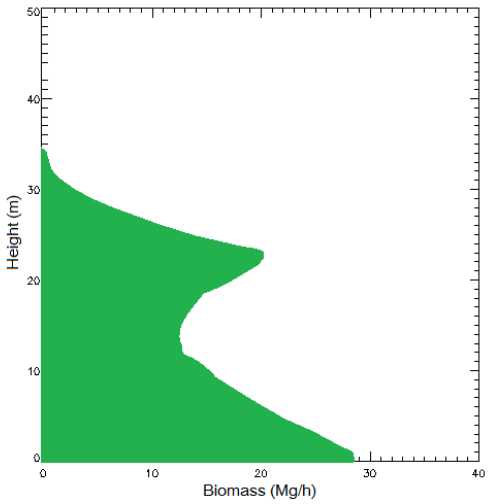

Figure 12 – Biomass profile for a typical plot of Traunstein test site. The shaded/colored area corresponds with the total biomass stock.

2.3.4 Vertical profiles validation

2.3.4.1 Terrestrial LIDAR based comparisons

Terrestrial light detection and ranging (TLIDAR) systems record the 3-D position of objects within the scanner field of view by measuring the time delay between the transmission of a laser pulse and the detection of the return pulse reflected from the target. Terrestrial LIDAR systems provide permanent 3-D records of the vegetation structure and detailed information about forest canopy architecture. They have, therefore, received a lot attention in forest management, ecology as well as remote sensing and urban planning applications (Cote, et al., 2009). The reconstruction of wood and foliage elements can become difficult when the scans cannot penetrate the canopy sufficiently, thus not allowing the regeneration of 3-D tree architecture. TLIDAR scans made in natural forest environments usually require dealing with different levels of obstruction between the various vegetation components (Hopkinson, et al., 2004), which can introduce errors of the measurements in the upper canopy layers.

Having access to detailed 3-D forest architecture information enables new approaches for the validation of space borne measurements and derived products (Cote, et al., 2009). For example, point clouds of forest canopies, taken by TLIDAR, can be used in conjunction with validated vegetation models to evaluate current methodologies.

A TLIDAR profile relates the vertical distribution of intercepted tree compartments and ground. For this study, terrestrial LIDAR profiles for 8 of the inventory plots are available. TLIDAR profiles were used to evaluate biomass profiles.

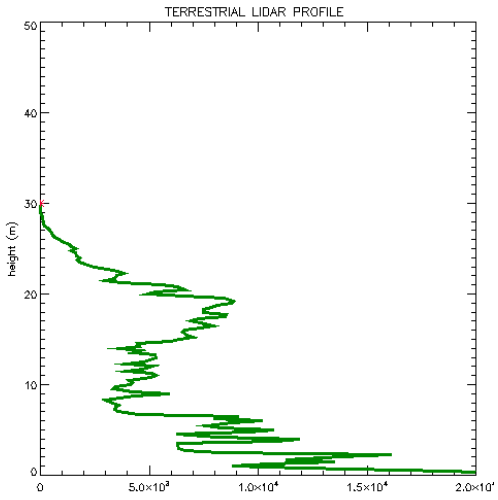

Figure 13 – Characteristic TLIDAR profile obtained from the sum of all the hits that are contained in each 12 cm bins. The x-axis represents the number of LIDAR hits and the y-axis the bin's height.

2.3.4.2 Forest level validation: Allometric relations

The best biomass model is selected and tested in two phases. First the vertical biomass profiles are compared with the TLIDAR profiles, at plot level. Second, at the forest level, height to biomass allometric relations are analyzed for the different models.

TLIDAR profiles help the selection of an appropriate biomass model in a qualitative test. In this test it is possible to see that both types of profiles, vertical biomass profiles and TLIDAR, are able to represent characteristic forest parameters and can be compared between themselves. The TLIDAR are assumed to represent a realistic distribution of biomass along height. The shape of the profiles obtained from different assumptions (cylindrical or conic stem, cylindrical or modeled crown, for different biomass estimation methods) can be directly compared with the TLIDAR profile shapes. The two main compartments considered, crown and stem, can be analyzed individually or combined for total biomass considerations. A representation of this test is displayed in Figure 14.

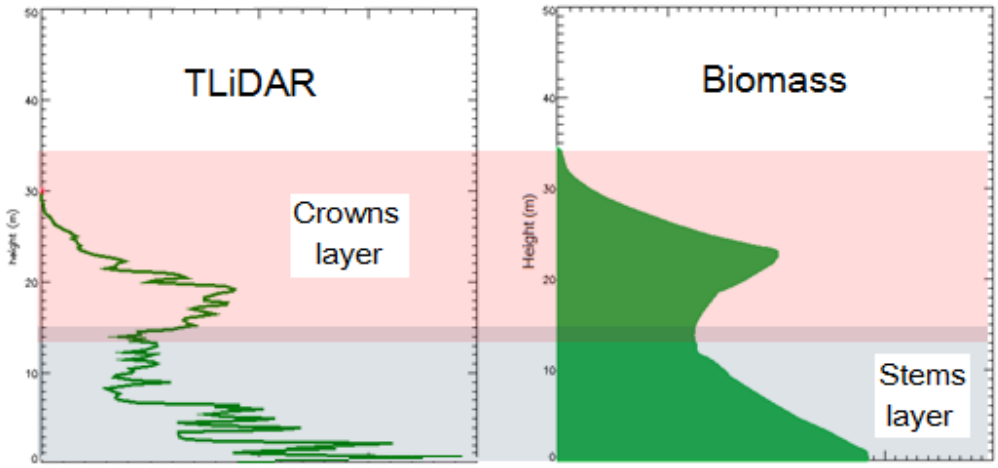

Figure 14 – TLIDAR based comparisons. Vertical biomass profiles are compared with the TLIDAR profiles to check for similarities in the profile shape. Generally, the crowns layer and the stems layer are detected and can be analyzed individually.

At forest level the results obtained from the different models can be represented in regression plots of biomass (total biomass per plot) against height (plot top height). The correlations that can be calculated for the different tree models can be evaluated within the models and compared. At the same time, they are compared with previous allometric relations derived for the Traunstein test site, (Mette, 2007), see Ch. 3.1.1.1.

After both analyses, a biomass model is selected considering the combination of tree compartment models that best fit with the available TLIDAR profiles.

2.4 Structure measurements

Vertical biomass profiles contain information about the vertical biomass structure. However, it is a problem to determine a method that can provide structural parameters with only once characteristic. This parameter has to be comparable and reproducible in order to compare different profiles and models and to validate further results.

Some methods found in literature have been tested with different results. The main ones are explained in this section. The tested parameters will be compared analyzing each of the correlations with the corresponding biomass. Therefore, the method that is able to provide the

parameter that best explains the biomass from vertical structure will be selected for the development of an allometric relation.

2.4.1 Metrics

To compare different field derived vertical profiles first, parameters investigated are quantile metrics of the biomass profiles and the total biomass obtained from the model. A quantile metric represents the height (dependent variable) at which a certain fraction of the area covered by the profile is achieved, e.g. the 75 quantile represents the height at which the 75% of the biomass is achieved (Sun, et al., 2008). For each metric the correlation of biomass available is examined using the values of all plots.

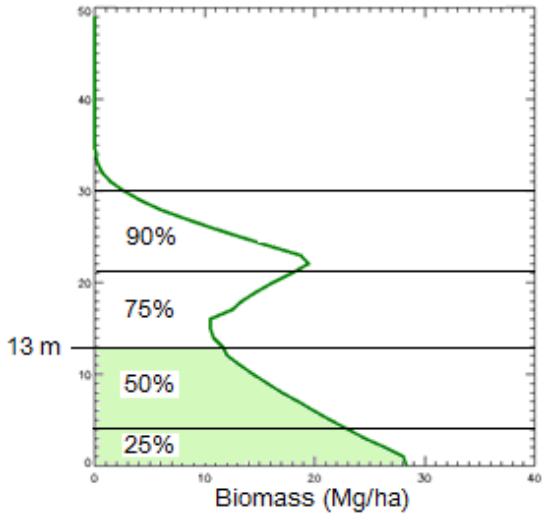

Figure 15 – Profile percentiles calculation. Each line represents the height where each percentage of biomass (profile area) is achieved.

2.4.2 Centre of Gravity

The next parameter investigated is the centre of gravity. The centre of gravity in a biomass profile is the point at which the system's whole mass is balanced. The center of gravity is a function only of the positions and masses that compose this system (biomass and height).

It is defined by two coordinates; one corresponds to the biomass (C_B) and other to the height (C_H) according to the equations:

$$C_B = \frac{\sum_{i=0}^{H} B_i \cdot h_i}{\sum_{i=0}^{H} B_i} \tag{2.4.1}$$

$$C_H = \frac{\sum_{i=0}^{H} B_i \cdot h_i}{\sum_{i=0}^{H} h_i} \tag{2.4.2}$$

where *B* is the biomass in Mg and *h* the height in 1 m samples and *H* the top height.

2.4.3 Decomposition

The form of the vertical biomass profiles can also be accounted decomposing them by several characteristic functions. Here a decomposition using Fourier and Legendre series is used. Thus, it is possible to calculate reproducible and comparable parameters from complex vertical profiles. These parameters are the decomposition factors.

2.4.3.1 Fourier analysis

Fourier analysis decomposes a function *f(x)* into a sum of sines and cosines functions, i.e. a composition into different frequencies. Then, complicated periodic functions are written as the sum of simple waves mathematically represented by sines and cosines.

The Fourier series is defined assuming a period of 2π:

$$f(x) = \frac{a_0}{2} - \sum_{n=1}^{\infty} a_n \cos(nx) + \sum_{n=1}^{\infty} b_n \sin(nx) \tag{2.4.3}$$

where a_0,a_n, b_n are defined as:

$$a_0 = \frac{1}{\pi} \int_{-\pi}^{\pi} f(x)dx \tag{2.4.4}$$

$$a_n = \int_{-\pi}^{\pi} f(x) \cdot \cos(nx)dx \tag{2.4.5}$$

$$b_n = \int_{-\pi}^{\pi} f(x) \cdot \sin(nx) dx \tag{2.4.6}$$

The impact of each frequency n is determined by the coefficients a_n and b_n. The coefficient a_0 is the integral (in our case the total biomass) of the measurement (offset) – constant line along height and is modified by the single frequencies according to their weightening a_n , b_n. All estimated a_n and b_n are called the Amplitude spectrum A(ω) for a_n and B(ω) for b_n. In case f(x) is a series of measurements (A(ω), B(ω)) is estimated using a discrete Fourier Transformation as provided by the programming language IDL 6.2 (Interactive Data Language):

$$A(\omega) = \frac{1}{N} \sum_{x=0}^{N-1} f(x) \cos(\omega x / N)$$
$$B(\omega) = \frac{1}{N} \sum_{x=\delta}^{N-1} f(x) \sin(\omega x / N) \tag{2.4.7}$$

where $\omega = 2\pi u$ and u is the frequency.

2.4.3.2 Legendre

The Legendre transform is analogue to the Fourier, but it is defined as the operation that transforms one real valued function of a real variable into another.

After the analysis of the first decomposition results it was observed that the Legendre polynomials offer the best performance for forest structure measurement so this method has been selected as the main structure measurement. Thus, the Legendre decomposition procedure for structure characterization is explained in detail in the next chapter.

2.5 Theory of decomposition: The Legendre decomposition

2.5.1.1 Legendre polynomials derivation

Legendre polynomials $P_n(z)$ are solutions of the Legendre's differential equation and can be defined as the coefficients in a Taylor series expansion (Arfken, et al., 2005):

$$\sum_{n=0}^{\infty} P_n(z)t^n = \frac{1}{\sqrt{1-2zt+t^2}} \tag{2.5.1}$$

Expanding the Taylor series for the first two terms gives:

$$P_0(z) = 1 \tag{2.5.2}$$

$$P_1(z) = z \tag{2.5.3}$$

for the first two Legendre polynomials. To obtain further terms without resorting to direct expansion of the Taylor series, the eq.(2.5.1) is differentiated with respect to t on both sides and rearranged to obtain:

$$(1-2zt+t^2)\sum_{n=0}^{\infty} nP_n(z)t^{n-1} = \frac{z-t}{\sqrt{1-2zt+t^2}} \tag{2.5.4}$$

Replacing the quotient of the square root with its definition in eq.(2.5.4), and equating the coefficients of powers of t in the resulting expansion gives Bonnet's recursion formula:

$$(n+1)P_{n+1}(z) = (2n+1)zP_n(z) - nP_{n-1}(z) \tag{2.5.5}$$

This relation, along with the first two polynomials P_0 and P_1 allows the Legendre Polynomials to be generated recursively.

Equations of Legendre Polynomials $P_2(z)$ to $P_{10}(z)$ are shown in Figure 16:

$$P_2(z)=\frac{1}{2}(3z^2-1)$$

$$P_3(z)=\frac{1}{2}(5z^2-3z)$$

$$P_4(z)=\frac{1}{8}(35z^5-30z^3+3)$$

$$P_5(z)=\frac{1}{8}(63z^5-70z^3+15z)$$

$$P_6(z)=\frac{1}{16}(231z^6-315z^4+105z^2-5) \qquad (2.5.6)$$

$$P_7(z)=\frac{1}{16}(429z^7-693z^5+315z^3-35z)$$

$$P_8(z)=\frac{1}{128}(6435z^8-12012z^6+6930z^4-1260z^2+35)$$

$$P_9(z)=\frac{1}{128}(12155z^9-25740z^7+18018z^5-4620z^3+315z)$$

$$P_{10}(z)=\frac{1}{256}(46189z^{10}-109385z^8+90090z^6-30030z^4+3465z^2-63)$$

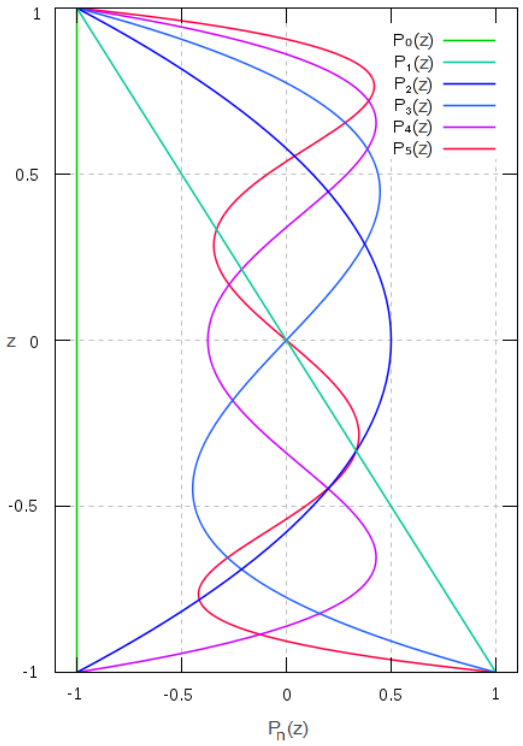

Figure 16 – Vertical representation of the Legendre polynomials until order 6 (P_0- P_5 (z)).

2.5.2 Interpretation of the Legendre decompostion

A biomass profile can, therefore, be decomposed in *n* Legendre polynomials using a least square fit for every polynomial. The first order polynomial $P_0(z)$ will define a "box" with the same height as the maximum height of the profile whereas the area equal to the integral of the biomass profile (total biomass). The rest of the polynomials will modify this box adding and subtracting the covered area until achieving, with *n* number of polynomials, the original profile (Figure 17).

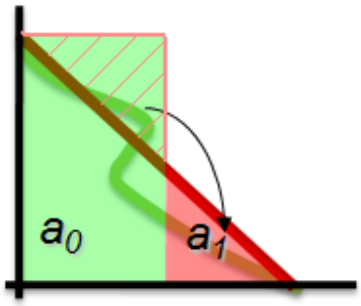

Figure 17 – Schematic representation of the Legendre decomposition for the two first polynomials. The green area corresponds with the integral of the profile represented by the coefficient a_0. The red triangle is the area corrected by the coefficient a_1 from a_0.

Each of the Legendre coefficients represents the degree of adjustment of the polynomial with the original curve (biomass profile). Thus the product $a_n \cdot P_n$ (Legendre component) represents the total biomass that a certain polynomial must add and subtract to adjust it to the original curve.

If B is the total biomass represented by one or several polynomials (excluding P_0), this can be reconstructed using the following expression:

$$B_n = \sum_{i=0}^{H} \sum_{j=1}^{n} a_j \cdot P_j \qquad (2.5.7)$$

where P is the Legendre polynomial, a the Legendre coefficient, H the maximum height of the vertical biomass profile and n the order of the Legendre polynomial.

2.6 Remote sensing systems: LIDAR and radar

2.6.1 LIDAR background theory

Airborne laser scanning (ALS) is an active remote sensing technique providing direct distance measurements between the laser scanner and the Earth's topography. The altimertic accuracy of a topographic LIDAR measurement is <0.1 and hence of high quality (Mallet, et al., 2009). Depending on the characteristics of the illuminated areas, several backscattered echoes can be recorded for a single pulse emission. This happens in particular on forested areas. LIDAR systems are able to penetrate into vegetation; hence they can measure both the canopy height and the terrain elevation underneath at once. Forest distance measurements are recorded as 3D point clouds. Moreover, LIDAR data are known to be useful in many specific applications such as 3D city modeling, bridge and power line detection or Digital Terrain Model generation and forest parameters estimations.

Since 2004, new ALS commercial systems called full waveform LIDAR have appeared with the ability to record the complete waveform of the backscattered signal echo. Thus, in addition to distance measurements, further physical properties of imaged objects included in the diffraction cone may be derived with an analysis of the backscattered waveforms.

The first active sensors carried by airborne satellite platforms were designed at the beginning of the 1970s. They provided 1D profiles along the sensor track (nadir view) by sequences of single pulses. Modern sensors acquire many parallel strips of 150-600m swath width, which may overlap, due to specific scan patterns. Such technology provides denser point clouds with more than 100 pts/m^2 in some specific applications, e.g. river monitoring (Baltasatias, 1999b).

Topographic LIDAR is now fully operational for many specific applications such as meteorology, forest parameters estimation, target or power line detection, coastal or opencast mapping.

2.6.1.1 Physical principles

The ALS used in this study is a LIDAR pulsed system. Pulsed systems measure the round tips time of a short light pulse from laser to the target and back to the receiver. Continuous wave systems carry out ranging by measuring the phase difference between the transmitted and received signal. This study will focused on pulsed systems.

ALS physical principles consist of the emission of laser pulses from an airborne platform at a high repetition frequency. The two-way run time of the laser signal from the sensor to the Earth surface is measured so it enables the distance from the LIDAR system to the surface (Baltasatias, 1999b).

Depending on the wavelength, the emitted electromagnetic wave interacts with atmospheric particles (absorption or scattering, known to have negligible influence if rain is excluded), but is mainly scattered by natural or man-made objects from the Earth surface.

The PRF depends on the acquisition mode and on the flying altitude. A pulse release is done when the previous pulse recording is closed. However, the latest systems have even the ability to fire a second laser pulse before the recording of the previous pulse (Roth, et al., 2008)

For georeferencing processes a system using both GPS (differential measurements with a ground station located near the survey area) and inertial measurements (IMU) are used to optimally calculate supporting vector attitudes and the absolute orientation of the laser sensor (Heipke, et al., 2002)

Basic airborne LIDAR systems consist of a laser transmitter and a receiver (rangefinder unit which receives the reflected pulses and measures the distance), a mechanical scanner, a hybrid positioning system, a storage medium, and an operating system for signal digitization and on-line data acquisition for monitoring and synchronizing points (Baltasavias, 1999a)

2.6.1.2 LIDAR measurement formulas

The standard LIDAR equation is derived from the radar equation. It describes the process by taking the detector and target characteristics into account. It also relates the power of the transmitted and return signals. In case of targets distributed in space, the reflected signal is the superposition echoes at different distances (Wagner, et al., 2006).

It can be expressed as an integral:

$$P_r(t) = \frac{D^2}{4\pi\lambda^2} \int_0^H \frac{\eta_{sys}\eta_{ant}}{R^4} P_t\left(t - \frac{2R}{v_g}\right)\sigma(R)dR \qquad (2.6.1)$$

where t is the time, D the aperture diameter of the receiver optics, P_r the received power, P_t the emitted power, λ the wavelength, H the flying height, R the distance from the system to the target, η_{ant} and η_{sys} respectively the atmospheric and system transmission factors, v_g the group velocity of the laser pulse, and $\sigma(R)dR$ the apparent effective differential cross section (Wagner, et al., 2006). The cross section is called "apparent" since an object reflecting the signal at a given distance can occlude and object further away.

2.6.1.3 Tomographic LIDAR technology: Multiple pulse systems

The first commercially available airborne laser scanners provided only one backscattered echo per emitted pulse. The recording of a single echo is sufficient if there is only one target within the diffraction cone. However, even for small laser footprints (0.2-2 m), there may be many objects within the travel path of the laser pulse: individual scattering contributions are generated for each encountered object. Multi-echo or multiple pulse laser scanning systems are designed to record more than one echo. They typically collect first and last pulses. Some are able to discriminate up to six individual returns from a single pulse. The two first echoes contain about 90% of the total reflected signal power. Real-time detection of more than five pulses requires thus the detection of low signal intensity within noise (Mallet, et al., 2009).

Multiple reflections occur on vegetated areas. When the vegetation is not very dense, it is often assumed that the first echo belongs to the canopy top and the last pulse to the ground. In reality this is not always the case. At a particular viewing angle, when the laser beam hits a building edge, two echoes can be generated. The first pulse corresponds to the roof while the second one to the ground.

2.6.1.4 Geometric quality of the laser scanning

Laser altimetry is a technique known to provide elevation data with reliability and high altimertic accuracy (<0.1 m) as well as good planimetric accuracy (<0.4 cm). Compared with

multi-stereo resolution photogrammetric products, LIDAR points are certainly more accurate but less dense so irregular sampling is one of the main problems.

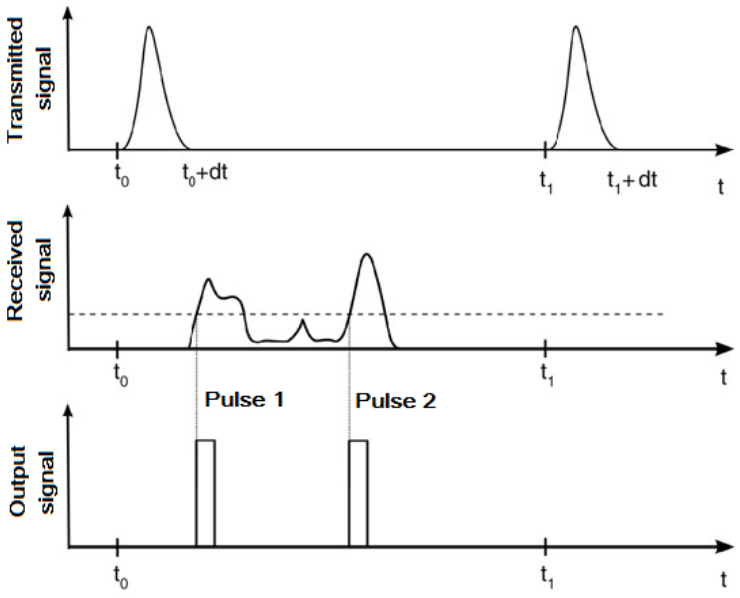

Figure 18 – Simplified pulse emission (above) and the corresponding received signal (middle). Two significant peaks are detected with the threshold method (middle and bottom). Two echoes will be generated for this pulse instead of four (Mallet, et al., 2009).

Pulse detection problem

For multi-echo systems, pulse detection is performed in real-time on the backscattered signal. The hardware system detector samples a continuous incoming waveform to several system pulses, giving the position of individual targets. The number of timing of the recorded pulses is critically dependant on the detection method. Figure 18 presents an example of wrong pulse detection with the threshold method. An erroneous detection could lead to a misinterpretation of the survey area, whereas a shift between the real time detected pulse position and the real location leads to an inaccurate position of the object. Moreover, in presence of low ground vegetation in woodlands the detection method would not be able to find two echoes if the range between two targets is less than 1.5 m. LIDAR waveform processing permits to cope with the most of these issues.

The advent of full-waveform LIDAR systems

Waveform analysis is an advanced processing method which increase pulse detection reliability, accuracy and resolution. Furthermore, the new technology of full waveform LIDAR systems allows a more detailed interpretation process of the physical measurement. It provides additional information about the structure and the physical backscattering properties of the illuminated surface (reflectance and number of scatterers).

The interpretation of full waveforms requires a pre-processing step. On one hand, waveforms can be decomposed into a sum of echoes to generate a 3D point cloud. Resulting data can be used in classical LIDAR algorithms. On the other hand, new approaches are also conceivable.

Recording full-waveform data

To record the waveform, i.e. the laser backscattered energy as a function of time, a digitization terminal has been added to the systems and hard disks with high storage capacity. Waveforms are usually digitized on 8 bits. The volume of data is bound to be five times superior to the 3D point cloud over the same area. The main limitation of surveying areas with a full-waveform LIDAR system is subsequently the storage capacity. The present issue with full-waveform data deals with data handling and management since much larger data volume are now recorded.

2.6.1.5 Typology of full waveform LIDAR systems

The first full waveform systems were designed in the 1980s for bathymetric purposes. Topographic devices appeared in the mid- 1990s with experimental systems. Full waveform topographic LIDAR systems mainly differ in footprint size, pulse energy and PRF. Small footprint and large footprint systems do not collect the same information over the same areas. Therefore, applications and data interpretation differ from each other.

Most commercial systems are small footprint (0.2-3 m diameter, depending on flying height and beam divergence) with higher PRF. They provide a high point density and an accurate altimetric description within the diffraction cone (Figure 19 left). Nevertheless, mapping large

areas requires extensive surveys. Besides, small-footprint systems often miss tree tops. It is difficult to determine whether the ground has been reached under dense vegetation. Consequently, ground and tree heights can be systematically biased (Dubayah, et al., 2000).

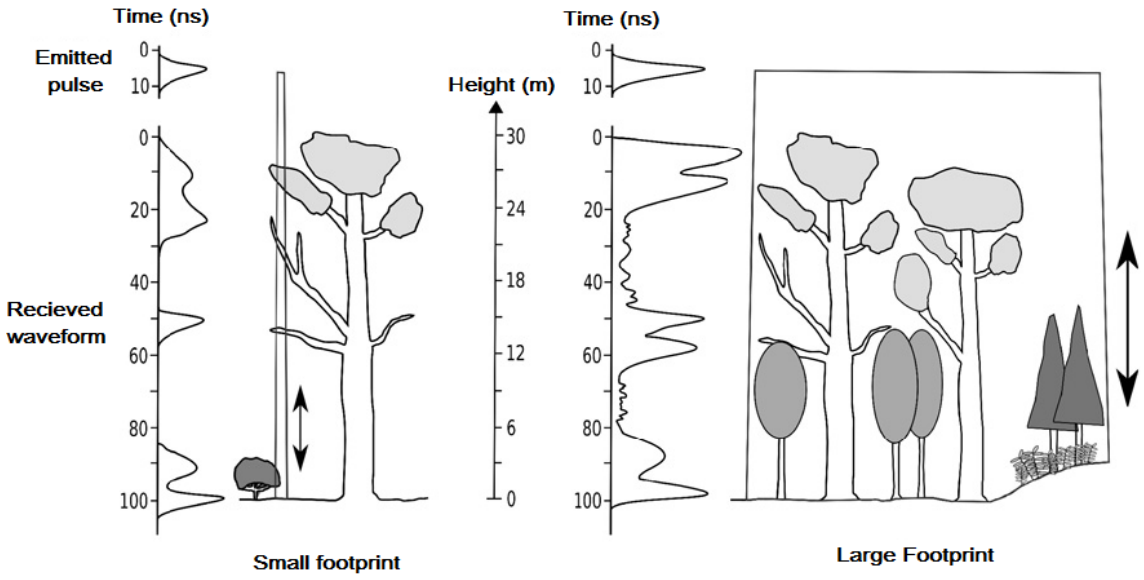

Figure 19 – Transmitted and received signals in a wooded area with a small footprint LIDAR (left) and a large footprint LIDAR (right). With a small-sized footprint, all targets strongly contribute to the waveform shape but the laser beam has highly probability of missing the ground. When considering large footprints, the last pulse is bound to be the ground but each echo is the integration of several targets at different locations and with different properties (Mallet, et al., 2009).

Large-footprint systems (10-70 m diameter) increase the probability to both hit the ground and the canopy top. They avoid the biases of small-footprint systems. Thus, the return waveform gives a record of the vertical distribution of intercepted surface within a wider area (Figure 19 right). The first experimental full-waveform topographic systems were large-footprint and LIDAR systems operated from satellite platforms. With a higher flying altitude, pulses must be fired at a lower frequency with a higher energy.

Experimental LIDAR systems

The following prototypes developed by NASA have been designed to assess the characteristics of woodlands or land cover. They aim at mapping large areas to provide data at a resolution of several meters and a swath width up to 1-2 km.:

- Scanning LIDAR Imager of Canopies by Echo Recovery (SLICER): the precursor of the topographic systems described below (LVIS and GLAS) was designed to characterize the vertical structure of the canopy. With a medium size footprint dimension the airborne device demonstrated that full-waveform systems could be used to assess the characteristics of woodlands, and allow to distinguish tree ages and species, and characterize vegetation structure of extensive areas (Lefsky, et al., 1999).
- Laser Vegetation Imaging Sensor (LVIS): this improved version of SLICER was used to test and provide data for developing algorithms, calibration instruments and evaluating the performance of measurements to asses the future Vegetation Canopy LIDAR (VCL) mission. It also demonstrated the potential of full-waveform data to characterize woodland areas and measure the Earth's topography, even below canopy (Sun, et al., 2008). It was mainly used to develop a real-time algorithm for classifying ground points by analyzing the return waveform.
- Geoscience Laser Altimeter System (GLAS): the five year ISCESat satellite mission, carrying the GLAS sensor, was launched in January 2003 to study the evolution of land and sea glacial masses in the Antarctic and Greenland, the roughness and thickness of sea ice and the vertical structure of clouds and aerosols. It has also been applied to above-ground biomass estimations or canopy height (Lefsky, et al., 2005)

Commercial LIDAR systems

Operational versions of commercial full-waveform systems have been available since 2004. These small footprint systems have considerable potential but do not have any dedicated application. The manufacturing companies are Riegl (Austria), Toposys (Germany), TopoEye/Blom (Sweden) , Optech (Canda) and Leica (Switzerland-Germany).

2.6.1.6 Processing the backscattered waveform

Two approaches are conceivable for processing the vertical profiles recorded by the new generation of airborne LIDAR sensors. On one hand, the waveform is decomposed into a sum of

components or echoes, allowing the detection of the different targets along the path of the laser beam. The aim of this approach is to maximize the detection rate of relevant peaks, to generate a denser 3D point cloud and, finally, to extend waveform processing capabilities by fostering information extraction from the raw signal. Increasing the number of 3D points is of interest for forestry applications. Extracting more information can be useful for segmentation and classification, also in forest environments.

On the other hand, the whole 1D signal is preserved. A spatio-temporal analysis is applied to find features within a 3D waveform space. However this approach is specially used for urban environments where the geometry is more regular.

The latter approach has barely been investigated. Most research on full-waveform analysis has been focused on the enhanced 3D point cloud.

Modeling and fitting waveforms

When modeling the echoes within a waveform, a parametric approach is chosen, for each detected peak is the signal. These parameters provide additional information about the target characteristics (shape and reflectance) and extend waveform processing capabilities. Statistical elements extracted by signal processing techniques are the number of significant peaks, their range to the sensor and the parameters of the model. A single function is always used to model all echoes of the waveforms.

One wishes to decompose a waveform $y = f(x_i)$ into a sum of n components:

$$y = \sum_{k=1}^{n} \phi_k(x_i) + b_i \tag{2.6.2}$$

where f is the waveform model, ϕ the echo model with a set of parameters and b the noise. A relevant echo model is particularly suitable so that related parameters could be used for segmentation the 3D point cloud. A large body of literature addresses the issue of fitting waveforms with a given parametric model (Mallet, et al., 2009).

A waveform is a convolution between a laser transmitted pulse (assumed to be a Gaussian shape with a a calibrated width) and a “surface” scattering function, often considered as a

Gaussian function (Wagner, et al., 2006). The received signal is then assumed to be a mixture of Gaussian distributions. Such modeling is the most frequently used method to process full waveform data. The analytical expression of the Gaussian function is:

$$\phi_k(x) = A_k \, e^{\left(-\frac{(x-\mu_k)^2}{2\sigma_k^2}\right)} \tag{2.6.3}$$

where A_k is the pulse amplitude, σ_k the pulse width, μ_k the pulse range.

The Gaussian model is sufficient for most applications, especially for large footprint LIDAR data. However, for small and medium-sized footprints, this model is not always justified.

The advantages of waveform processing are threefold:

- First, the new algorithms no longer limit the number of peaks that can be detected.
- Second, waveform processing improves object range detection, even over complex surfaces. For instance, in forested areas, both canopy and ground height estimates can be improved but this result depends on the survey specifications and the landscape.
- Third, modeling the echoes provide additional parameters that can be useful for classification purposes.

The Gaussian approximation is shown to be satisfactory and sufficient for most of the mapping applications in forest areas, for large and small footprint LIDAR data shows that fitting Gaussians to the echoes is however less satisfactory for high amplitudes. Furthermore, for low amplitude pulses the estimation of the echo parameters is less accurate. Other models, such as the generalized Gaussian function, may be of interest (Mallet, et al., 2009).

2.6.1.7 Calibration of laser intensity data

Intensity is not yet a clearly defined term. The echo amplitude is most commonly referred to as intensity. However, the intensity should be associated with the total energy of the echo (i.e. $I = \sqrt{2\pi}A\sigma$ for a pulse of Gaussian shape, where A is the amplitude and σ is the width). The echo amplitude depends on main factors, target characteristics, LIDAR system, scan geometry,

etc. Fluctuations can be noticed on large data sets between surveys, for instance due to different atmospheric conditions, and even between flight strips. The intensity/amplitude values provided by commercial LIDAR systems as well as those extracted from waveforms processing are neither calibrated nor corrected. They aim at converting intensity to a relative but comparable measurement for different epochs with different conditions, e.g., for multi-temporal analysis classification.

Results from the Finnish Geodetic Institute (FGI) show that reflectance plays a predominant role on the amplitude and width of the peak. The influence of the albedo cannot be separated from other target properties. However, the calibration protocol makes it possible to use intensity as data in its own right.

Calibration can be done using the LIDAR equation (Wagner, et al., 2006) and external reference targets of known cross-sections. For that purpose, the echo amplitude and width are needed. Therefore, only full-waveform sensors allow an accurate calibration for all target classes. No hypothesis is required.

2.6.1.8 Application of full-waveform LIDAR data

Full-waveform LIDAR data have been widely used for forest analysis. The waveforms are decomposed to produce dense 3D point clouds in the canopy which are then used to estimate forest parameters at the scale of the stand. Most of the literature on full-waveform systems deals with this topic. On one hand, one tries to benefit from a denser point cloud to improve forest parameter estimation. On the other hand, modeling is performed to understand the influence of forest parameters on the waveform shape.

Many studies have already been carried out to estimate forest parameters using multi-echo LIDAR data; high point density can be used to extract trees in small areas, their height and crown diameter, and their volume, to classify them according to species, to estimate their particular characteristics and even to measure the growth of the forest and detect trees that have been felled. Woodland parameters can be estimated at large scale: density of population, coverage or even biomass.

Full-waveform LIDAR metrics are used to estimate the following woodland parameters:

- Canopy height: modeled from the measurement of the difference between the height of the first and last echoes, for different types of forest (temperate, boreal and tropical), at the tree or the stand levels. It is generally underestimated by a least one meter.
- Vertical distribution of canopy material: essential to determine other canopy features such as the above-ground biomass, predicting the state of the forest and determining the age of a plantation.
- Canopy height profile: This is the fraction of the signal reflected by the target corrected by the estimated ground reflectance.
- Canopy volume profile: obtained by modeling. It can show the qualitative and quantitative differences between different ages of a given species. It can also provide information on vertical leaf profiles.
- Above-ground biomass: modeled from the tree height measurements. This correlation was demonstrated in even aged stands, especially in coniferous species.
- Basal area: cross sectional area of the trunk, at diameter at breast height.
- Mean stem diameter: tree height is strongly correlated to the stem diameter. Allometric equations allow one to derive the stem diameter according to the canopy height and the tree species.
- Crown and stem volume: these features are inferred. The crown volume (tree parameter) is computed knowing the canopy volume (stand parameter), the tree density and species. The stem volume is inferred according to the mean stem diameter and the tree height.

Certain variables are obtained using allometric equations and vary according to the type of forest and their main characteristics (Hyde, et al., 2005). It is therefore difficult to obtain from LIDAR data a comprehensive estimation of forest parameters (even for main parameters such as tree height and crown diameter), and consequently parameters inferred as well as general relationships between structural forest variables for a given type of biome. Metrics derived from full-waveform data are not always significantly correlated with forest structural characteristics at the tree level, even if it works well for some forest types (Anderson, et al., 2006)

Finally, forest parameter retrieval on sloped terrain has to be mentioned. Here forest height depends on the position where the laser penetrates down to the ground. If this is far from the mentioned position, tree height will be biased. In case of erroneous DTM, several forest parameters, such as the canopy height, crucial for modeling and inferring other features, will be incorrect. It would be consequently of interest to introduce waveforms features, such as pulse amplitude and width, to improve ground/of-ground segmentation algorithms and derive more reliable DTMs.

Modeling forested areas is particularly difficult due to the strong complexity structure of the trees. Several studies have been carried out on this topic, mainly with large footprint LIDAR data. Waveforms are generated over large areas (footprint around 10 m) in order not to take small tree elements into account. Tree models with a high level of details (leaves) are therefore not necessary.

Blair and Hofton (1999) developed a model for forest scenes by simulating full-waveform LIDAR data. They simulate waveforms by breaking down the surface hit into small surfaces with their own backscattering characteristics but with the same reflectivity (typical for dense forest). A strong correlation between this data and that form the LVIS sensor is obtained. They show that the unmodeled effects, such as multiple backscattering, do not make a significant contribution to the shape of the return waveform.

2.6.2 LIDAR profiles generation

The generation of the vertical LIDAR profiles is analogue to the generation of the field-based vertical biomass profiles in Ch. 2.3.3. The vertical LIDAR profiles are generated by summing amplitude/intensity, in 1m bins along the height.

However, transmitted laser energy per unit area decreases with penetration depth through the canopy due reflection and absorption (Harding, et al., 2001). In addition, because the spatial distribution of laser energy is not constant across the laser footprint, the horizontal distribution of the reflecting surfaces with respect to the spatial distribution of the laser energy affects the intensity of the return. Energy decreases from the beam center to the beam boundary (Blair, et al., 1999). The main purpose of this study is the derivation of biomass information, which is mainly

accumulated in the woody surfaces of the lower layers of the canopy and the stems. It is therefore needed to correct the attenuation of the response due to the canopy attenuation. For this purpose the canopy height profile is a helpful tool.

2.6.2.1 Canopy height profile

The canopy height profile (CHP) is a modification of the foliage height profile of FHP (MacArthur, et al., 1969). The FHP quantifies the distribution of foliage surface area as a function of height. Because airborne LIDAR systems cannot distinguish woody surface from foliage surface area, the CHP is used to define the distribution of both foliar and woody surface as a function of height.

The main method to estimate FHP is the cross site comparisons developed by MacArthur and Horn (1969) (Lefsky, et al., 1999). Using this method, optical point quadrats, using a camera with telephoto lens, are established and multiple observations of vertical distance to first leaf intersection are made. This distribution is used to estimate the cumulative percent cover of foliage as a function of height. These estimates of cover are transformed into the vertical distribution of the foliage using a method that assumes that leaf angle remains constant with height and the horizontal distribution of leaves is random. Given these assumptions, an equation derived from the Possion distribution can be used to relate the percent cover to the amount of foliage:

$$FHP_c(h) = -\ln\left(1 - cover(h)\right) \tag{2.6.4}$$

where FHP_c is the cumulative one-sided leaf surface area (or LAI) expressed as fraction of projected ground area above height h, and $cover(h)$ is the fraction of sky obscured by foliage above height h.

For LIDAR applications the CHP is characterized according to Lefsky (1999). It is hypothesized that the power of the backscattered laser illumination is subject to the same process of occlusion observed in the field measurements of height to first intersection, and modifies the FHP method, in the way that this approach can be applied to the ALS return energy waveforms. After removing background noise created by the sensor's digitizer, the critical step in the process of modification is the separation of the portion of the waveform returned from the ground surface

(the ground "return") from the balance of the waveform. The power ratio of the ground return to the total signal power is inversely proportional to the total canopy cover, but, to estimate canopy cover. The total horizontal canopy cover at each height increment can be calculated, allowing the use of the MacArthur equation (eq.(2.6.4)).

There are two measurements recommended by Lefsky (1999) weightening the height of the CHPs calculation, the mean canopy height and the quadratic canopy height. The mean canopy height is measured as the mean of the canopy height profile weighted by the height of each element. The quadratic canopy height is measured as the mean of the canopy height profile weighted by squared height of each element. In this study, the mean canopy height is selected because of simplicity reasons. Aerial cover of each field is calculated with the equation:

$$Cover = 1 - \frac{K \cdot GroundReturn}{CanopyReturn + K \cdot GroundReturn} \tag{2.6.5}$$

where the ground and canopy returns are the total power reflected from the ground and canopy, respectively. The ground return power of the waveform is multiplied by K to account for difference in the albedo of ground and foliage (about a twofold difference) so K is set to 2.0. (Lefsky, et al., 1999)

2.7 Short introduction to radar profiles

Radar (Radio Detection and Ranging) is an active remote sensing techniques that operates in the microwave region. This fact improves the penetration, especially trough the atmosphere, and reduce drastically the impact of clouds, fog of rain. Radar is also is able to penetrate vegetation depending on the wavelength used.

Radar imaging systems are characterized through their side looking geometry. In general, a monostatic radar system consists of a pulsed microwave transmitter, an antenna which can be used for transmission and reception, and a receiver (Figure 20).

Radar is a "ranging" system, which measures the distances (phase) to objects and the received signal power (amplitude). With the combination of two images acquired from different

perspectives radar systems are able to use interferometry to measure distances with higher precision.

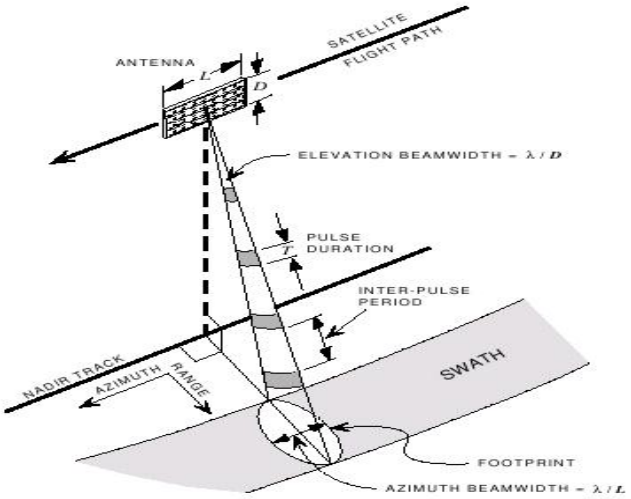

Figure 20 – SAR imaging geometry (Curlander, et al., 1991).

The backscattered signal of one radar resolution unit (RU) is composed of scattering processes of all the scatterers received from this RU. Thanks to POLinSAR (Papathanassiou, 1999); interferometry radar is capable to measure volume along the height. In the case of volumes the measured signal is composed of scattering processes along the volume (Figure 21).

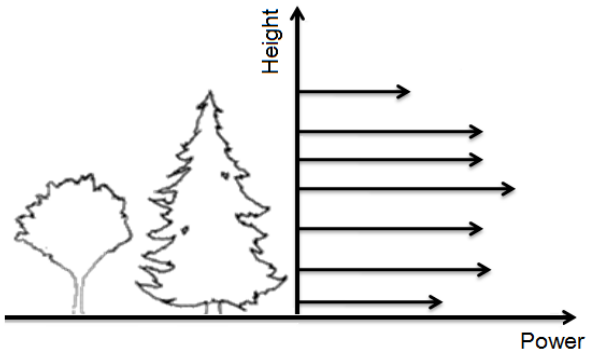

Figure 21 – Visual content of one resolution unit (RU)

There are two techniques capable of solving the vertical backscattering profile: tomography and PCT (Polarization Coherence Tomography). The acquisitions configurations are different for the two techniques:

- Tomography: Needs many acquisitions (20-30) but it is able to reconstruct the real backscattering profile. An example for just 4 tracks (low vertical resolution) is displayed in Figure 22.
- PCT: Only needs a small number of acquisitions (even 4 (Cloude, 2007)). It uses the Legendre polynomials to approximate the vertical backscattering profile.

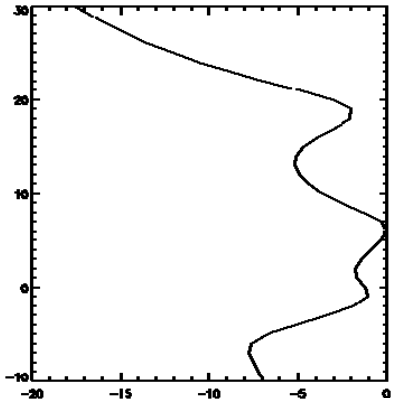

Figure 22 – Tomography profile for the Traunstein test site made for L-band with four tracks.

2.8 General validation

2.8.1 Validation of biomass model: the Monte Carlo simulation

Monte Carlo methods are a class of computational algorithms that rely on random sampling to compute their results. Monte Carlo methods are often used in simulations of physical and mathematical systems, although they can be applied to natural systems. Because of their reliance on repeated computation of random or pseudo-random numbers, these methods are particularly useful when it is infeasible or impossible to compute exact result with a deterministic algorithm.

Natural systems as forests are affected by a significant uncertainty in the inputs and these systems have an important number of degrees of freedom. A Monte Carlo simulation can test the effects of random errors over the mean of results. For this purpose a random error is simulated using 1000 repetitions, following a Gaussian function for each of the variables that participate in the final allometric equation.

Results were evaluated using a histogram of results. By introducing errors on the single parameters the robustness of the final equation was tested. Introduced errors go from 10 to 40% in 10% steps.

2.8.2 LIDAR vertical profiles for biomass estimation

In the following three chapters the three main steps for going from LIDAR vertical profiles to biomass are described. First, it is mandatory to check the spatial position of the available data, especially regarding the correct overlap of LIDAR and inventory data. Second, the calculation of a transfer function that can connect the LIDAR profiles to the vertical biomass profile needs to be calculated and finally, the decomposition and correlation of the LIDAR with the biomass is done.

2.8.2.1 Geo-coding

The overlap between the positions of the field measured plots with the coordinates in the LIDAR image is of great importance for the validation of the results. Small displacements can introduce big biases, especially in the height measurements (plot top height) because LIDAR measurements also include adjacent trees not covered by ground measurements. Moreover, the size of the inventory plots is relatively small (12.62 m) so there is not surface enough to compensate the errors introduced with these displacements due to averaging.

The inventory data provides exact measurements of the tree height and the relative positions of the inventoried trees with respect to the centre of the plot. Then the relative displacement error is only contributed by the biased centre coordinates of the plot introduced by GPS measurements. By comparing positions of measured tree heights with the positions of the measured LIDAR heights mismatches could be manually corrected. Two examples of these corrections are displayed in Figure 23.

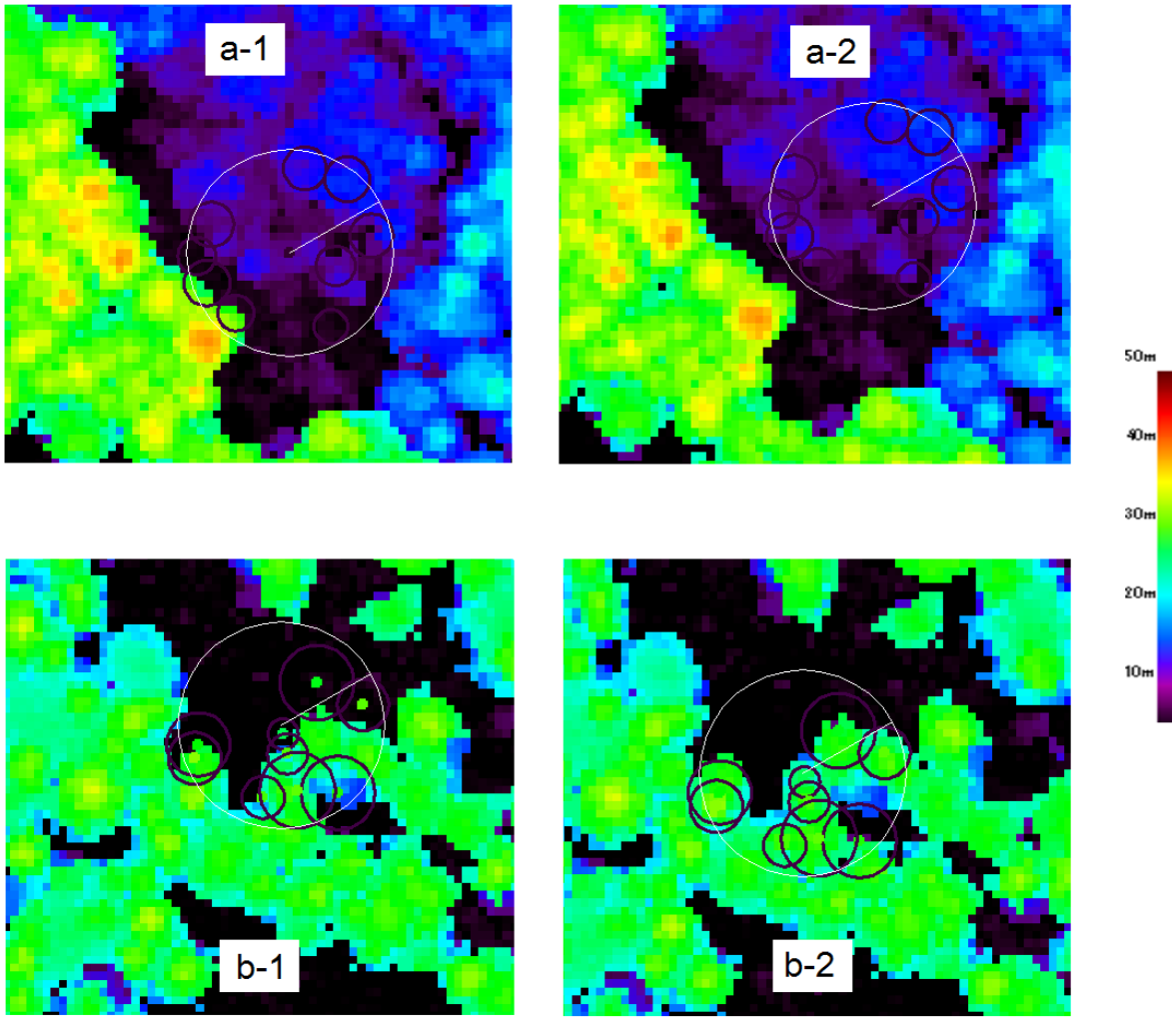

Figure 23 – Displacement of the inventory plots centre coordinates. The background image is the LIDAR height map and over plotted the measured trees from ground survey. Each tree is surrounded by a circle representing the maximum crown radius. The color bar represents the tree height from 0 to 50 m. The images displayed on the left (a-1, b-1) before correction and on the left (a-2, b-2) after correction.

2.8.2.2 Transfer function

Field and LIDAR based vertical profiles represent different features along height. LIDAR profiles depend on attenuation, density and geometric orientation of biomass components (stems, branches and leaves). This makes it difficult to establish a direct correlation between both systems, even after the CHP correction. However, it is possible to see some general tendencies by comparing biomass and LIDAR, considering all plot profiles. This allows us to develop a transfer

function going from LIDAR to biomass profiles. The transfer function is then used to correct the LIDAR profiles.

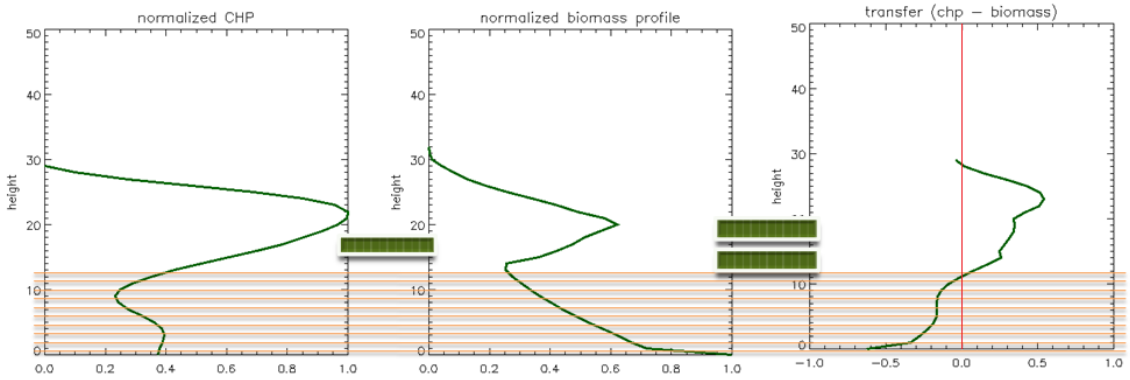

Figure 24 – Calculation of the transfer function. For each plot the normalized values of the vertical biomass profile are subtracted from the CHP in 1 meter units, to obtain a "differences profile". The sum of all the "difference profiles" used to generate the transfer function.

Both CHP and field based vertical profiles are calculated in 1 m. sample units so that it is possible to calculate the difference on a meter level for all the profiles pairs. However, as units differ from LIDAR (intensity) to field (biomass), both profiles are normalized by the maximum to establish a comparable basis (Figure 24). Then, all the different profiles for all the pairs are combined in a two dimensional histogram in which a function is fitted:

- Fitting a polynomial function.
- Following point by point the maximum of the histogram.
- Following point by point the mean of the histogram.

2.8.2.3 Legendre decompositions

The CHPs from LIDAR have been corrected using the transfer functions as derived in the previous chapter. In this stage, the obtained profiles are comparable to the vertical biomass profiles. After correction, LIDAR profiles are decomposed using Legendre polynomials.

The results of the decomposition for the CHPs are directly correlated with the same results for the biomass profiles (see Ch. 3.2.4.2). Therefore, the biomass structural components

(represented in the Legendre components) can be derived from the LIDAR Legendre components, closing the circle to get biomass form LIDAR measurements.

However, depending on the transfer function used for the CHPs correction and the number of Legendre components, different correlations can be found. Therefore the cases that offer the best correlation will be the ones used for the final biomass inversion equation.

3 Results

3.1 Vertical biomass profiles

3.1.1 Model selection: Terrestrial LIDAR based comparisons at plot level

In the following different models for the tree compartments, stem and crown, are evaluated. As mentioned in Ch. 2.3.4.1, TLIDAR is used as a reference for the motel, representing vertical biomass distribution. A biomass model for the stems is represented first, then one for the crowns (without stems) and then, one for the combination of both.

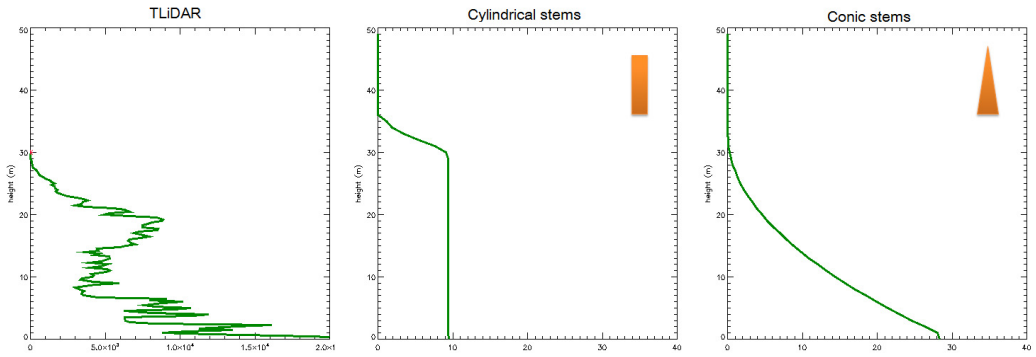

Figure 25 – Comparison of a TLIDAR profile against stem compartments model for plot 3011017: cylindrical model (middle) and conic model (right).

For the stem compartment model two forms are considered: cylinder and cone. The cylinder does not follow the trend of biomass distribution seen by the TLIDAR (Figure 25). In the LIDAR profiles the biomass, especially considering the lower parts (stem contribution), decreases evenly with height, while in a cylindrical representation the biomass as a function of height is represented by a box (Figure 25- middle). However, when stems are modeled as cones this trend given by the TLIDAR plots (Figure 25- right) is much better achieved. Thus, this

comparison already advises the selection of the cone as the stem form that better represents the vertical biomass distribution in the stems.

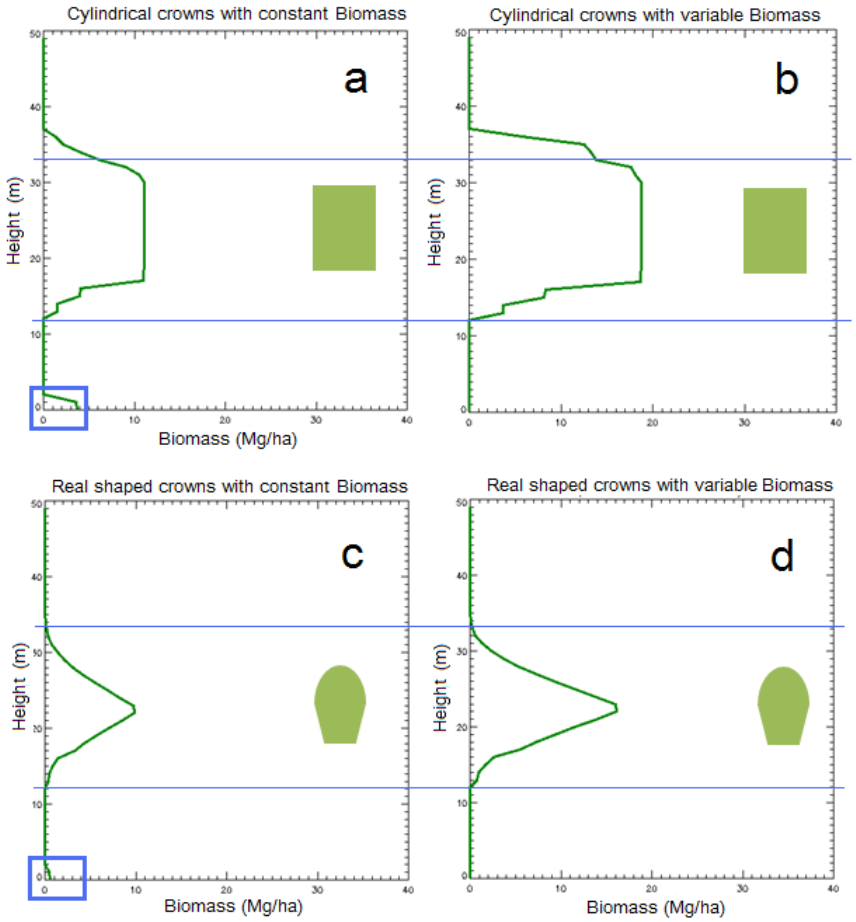

Figure 26 – Crown models comparison for plot 3011017. The following models are displayed cylindrical crowns with constant biomass (a), cylindrical crowns with allometrically derived biomass (b), modeled crowns with constant (0.002 Mg/ha) biomass (c), and modeled crowns with allometrically derived (variable) biomass (d). The blue lines help to appreciate the adjustment of the crown layer and the errors of the top height estimation.

The crown representation is more complex due to the complex form and variety of structures between tree sizes and species. Modeling crowns with allometrically derived biomass or with constant density have important effects in the biomass distribution. Figure 26 represents the differences for crown models, without stem contribution. They are the following:

- Cylindrical crowns with constant biomass (0.002 Mg/ha).
- Cylindrical crowns with allometrically derived (variable) biomass

- Modeled shape crowns with constant biomass (0.002 Mg/ha).
- Modeled shape crowns with allometric (variable) biomass.

When using constant density, especially in the case of cylindrical crowns, the biomass contribution from the understory crowns tends to be overestimated (Figure 26 –a and c). However, in the case of modeled crowns this effect is not clear (Figure 26 –b and d).

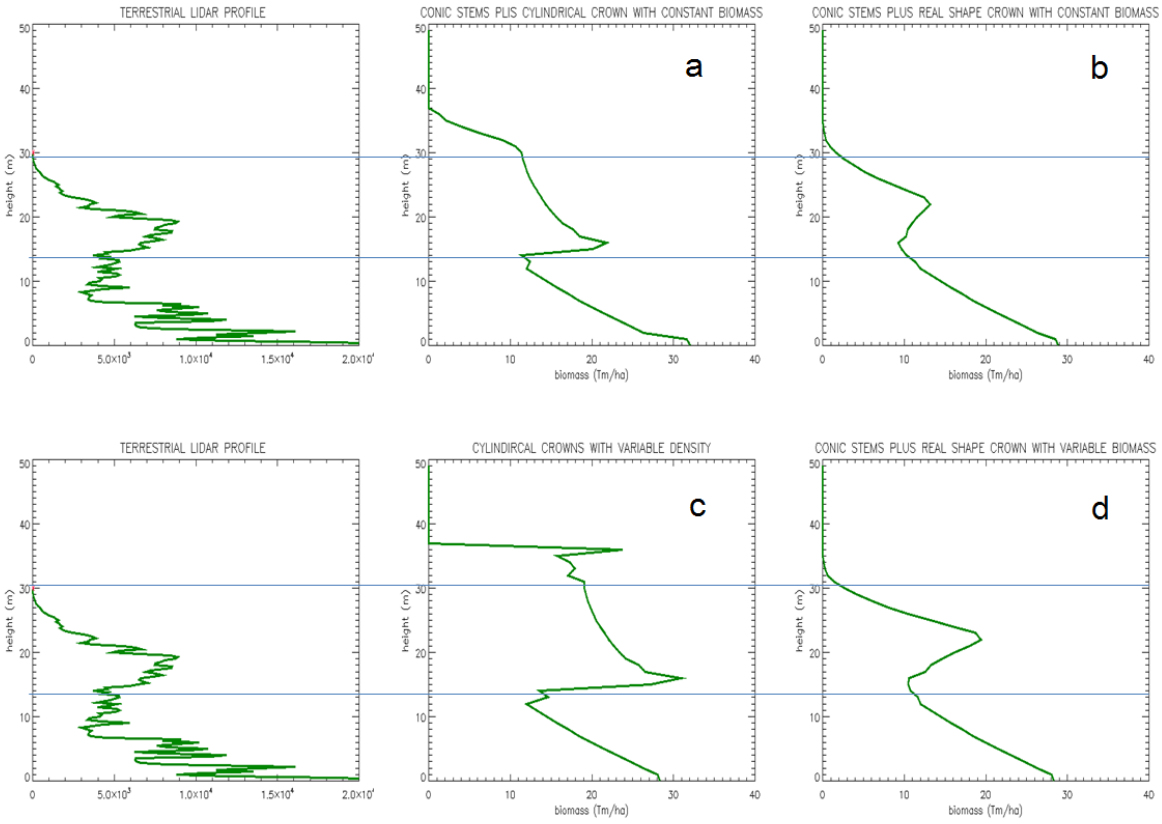

Figure 27 – Biomass model test against a TLIDAR profile for plot 3011017. From left to right it is shown: a TLIDAR profile and the vertical biomass profiles, conic stem + cylindrical crowns with constant biomass, conic stem + modeled crowns with constant density, and conic stem + modeled crowns with allometrically derived biomass. The blue lines help to appreciate the adjustment of the crown layer and the errors of the top height estimation.

In all the crown cases the crown base is always equally represented; however between cylinders, with and without modeled shapes, the biomass of the top is always higher than the modeled crown case. On the other hand, the height of the maximum biomass is also equal between cylinders and modeled shapes if considering the same system of biomass derivation (e.g. allometrically derived biomass).

Figure 27 displays the comparison between TLIDAR and the four different total biomass models (see Figure 10). In this figure it is possible to see the difference between modeling the crown as cylinder (a and b) or with a modeled shape and biomass calculated according to allometric relations (c and d).

Two analyses are done with this comparison:

1. Top biomass representation: The cylindrical crown (Figure 27– a and b) tends to give an overestimation of the biomass in the top part of the crown and the shape does not correspond to the majority of the TLIDAR profiles. However, when using modeled crowns the shape of the crown layer tends to follow the TLIDAR and the estimation of the top crown biomass is more accurate (Figure 27 c and d).
2. Influence of biomass estimation model: there are significant effects of the usage of allometrically derived biomass, especially in the amplitude of the crown layer. In the case of using a constant biomass the relative differences in the amplitude of the crown with respect to the stem part is small (Figure 27 – a and c), while in the allometric case (Figure 27 – b and d) it is higher and the relation between stem and crowns maxima has a similar amplitude to the TLIDAR- profile.

After this analysis the biomass model "modeled crown with allometrically derived biomass and conic stems" is, a priori, selected as the best biomass model (Figure 28).

The previous comparisons for the eight TLIDAR plots show that the shape of the profiles matches extensively with the LIDAR. However, it is necessary to say that a constant underestimation of top height, as seen in Figure 27, exists for the TLIDAR profiles and two of them offer a poor representation of the stand (Figure 29). The 8 TLIDAR vertical profiles can be seen in Annex 1 and the entire set of vertical biomass profiles for the selected model in Annex 2.

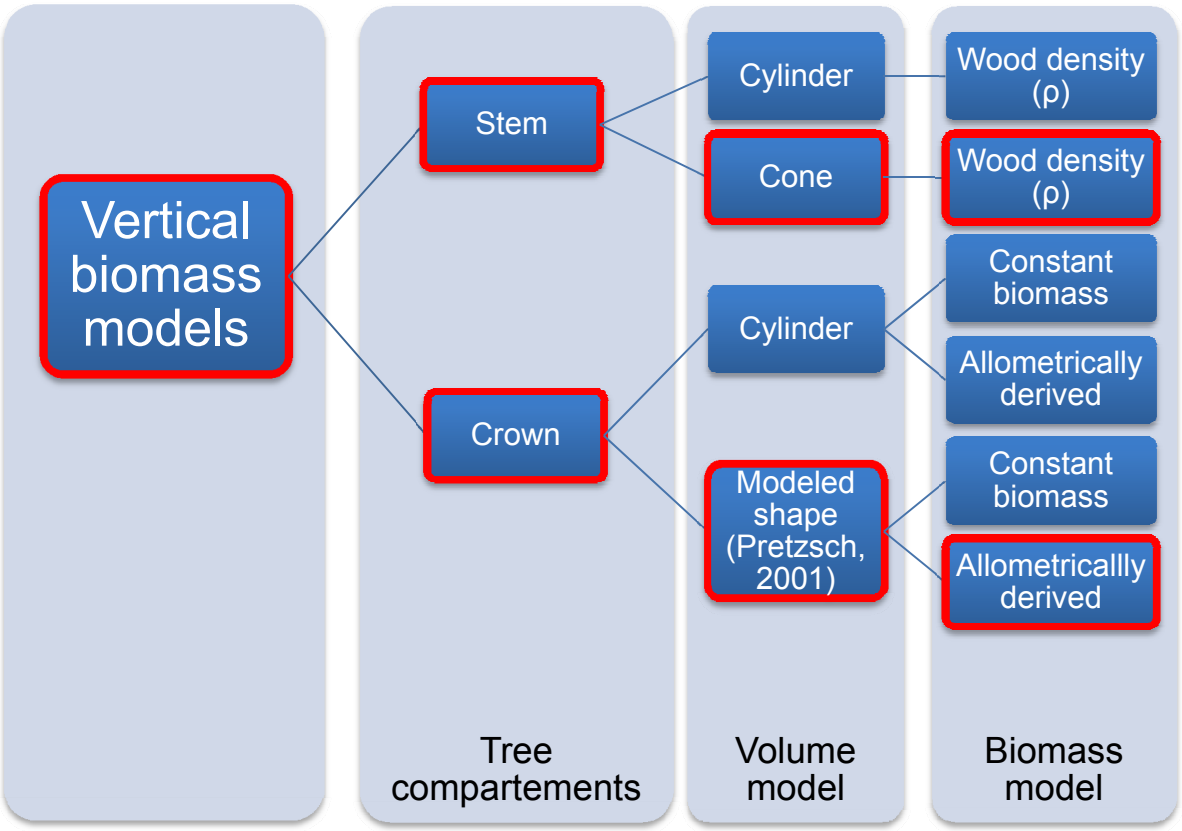

Figure 28 – Path for vertical biomass selected model. The selected models are highlighted in red.

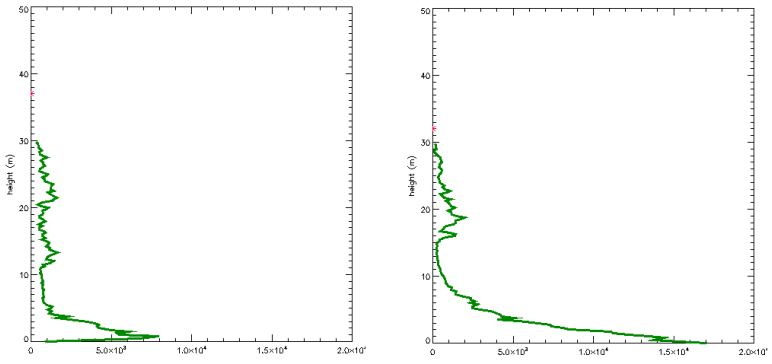

Figure 29 – Example of TLIDAR profiles that are not representative for the vertical biomass profiles validation. The terrestrial scanner is situated too close to an open area so the representation of the crown layer is underestimated.

3.1.1.1 Forest level: Height to biomass allometry

The previous analyses are done on a plot level; however, for a further validation of the selected biomass model it is needed to move to a higher level by looking at all plots at the same time. At this level we can see the main tendencies of the obtained results for the models. The height to biomass allometric equation from Mette (2007) is compared with the results obtained from the current modeled biomass (Ch. 2.2.4).

In Figure 30 we can see the differences between the original formulas developed in Traunstein for the "stem height to biomass allometry" with the analogue relations for the "combined crown and stem height to biomass allometry". The first result points the decrease of the allometric level value from the conditions of Mette (2007) to the conditions of this study (Figure 30- a). The red line represents the allometric level la as obtained by the yield tables (0.925) and the blue line is the allometric level adapted to the Traunstein site (0.625). This proves the important reduction of the biomass stock as a consequence of the management plan between 1998 and 2008 (see Ch. 2.1.3).

When analyzing the case of cylindrical crowns a significant correlation is not observed for allometrically derived or constant biomass (Figure 30- b and c). Both show a correlation coefficient of 0.39 although the allometrically derived case shows a lower dispersion (Figure 30- c).

If the relation evaluated in the "stem height to biomass allometry" (Figure 30- a) is applied in the modeled crown, for the constant biomass case (Figure 30- d) the correlation is low (R^2= 0.46); however for the allometrically derived case (Figure 30- e), the same correlation coefficient is obtained (0.56) with an allometric level *la* of 1.025. For both cases the inclusion of crowns in the model increases the average biomass by ca. 40%.

In conclusion, this analysis supports the selected case: "modeled crown with allometrically derived biomass and conic stems" (Figure 28).

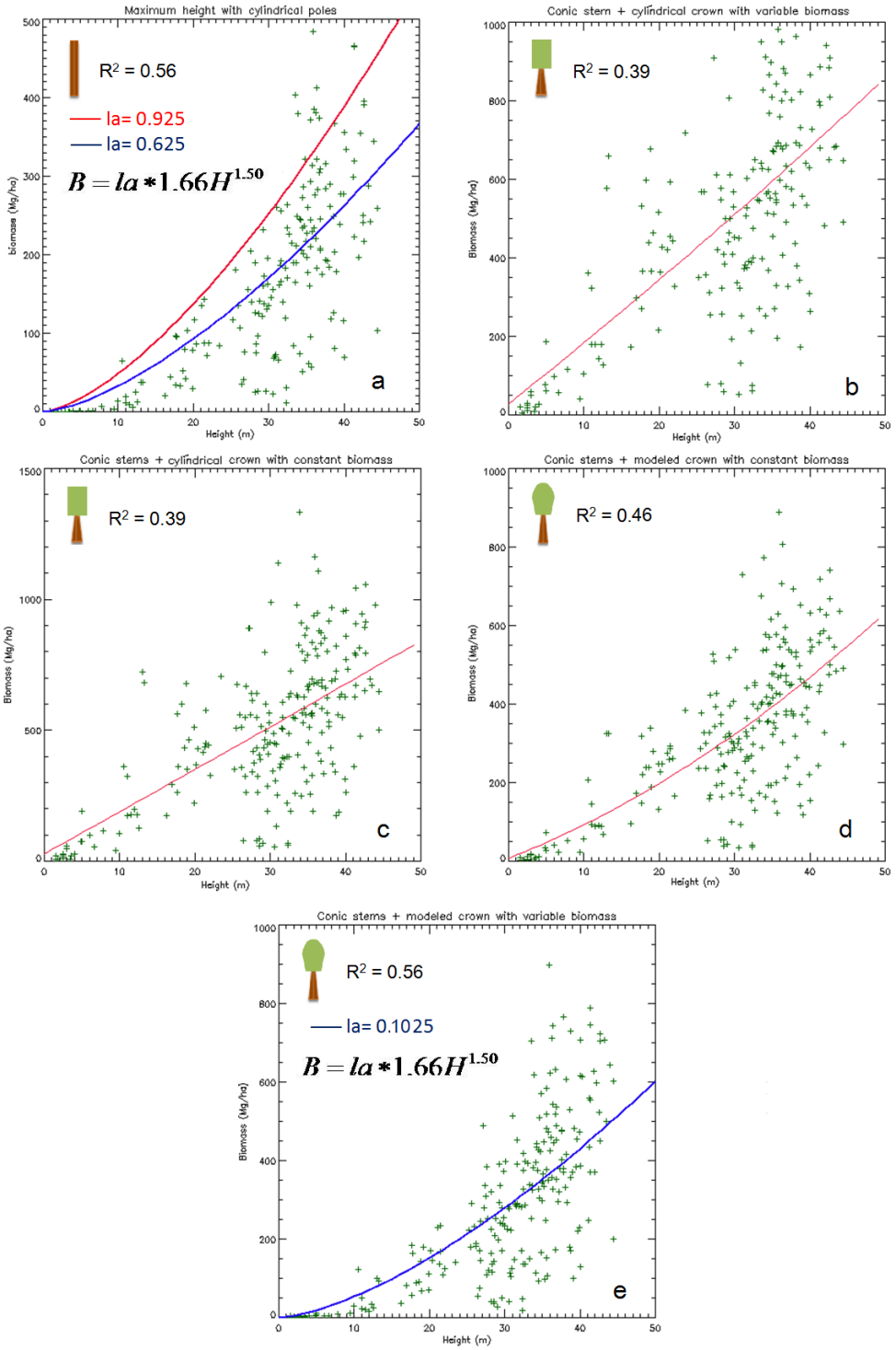

Figure 30 – Comparison between the allometric relations at forest level for three biomass model types. "Stem height to biomass allometry (upper left plot); "combined crown and stem height to biomass allometry" for the cylindrical crown (upper right plot) and "combined crown and stem height to biomass allometry" for modeled crown (bottom plot).

3.1.2 General features of a vertical biomass profile

In a characteristic profile it is possible to recognize the contribution of the different tree compartments to the total biomass of a stand. The most commonly observed case corresponds to a two layers stand where the maximum biomass contribut ion is given by the lower part of the stems (the maximum is always at the bottom, i.e. height 0), decreasing with height until finding a second maximum given by the crowns of the overstory. The relative amplitude difference between these two maxima gives information related with the crown-stem proportion.

A priori, the observation of the profile shape contains also information about the tree species that are in a stand. Especially when considering the difference between coniferous and broadleaves it is possible to see the influence of the characteristic crown shapes (Figure 31). Conifers tend to have a sharper crown with a clear maximum while broadleaves produce a smoother profile where the biomass is evenly distributed along height.

3.1.2.1 Profiles diversity

The 8 plots that were used for the TLIDAR based comparisons correspond to homogenous areas and they do not differ much from each other. However, at the test site of Traunstein there is a much higher diversity of stands that can be represented by the vertical biomass profiles.

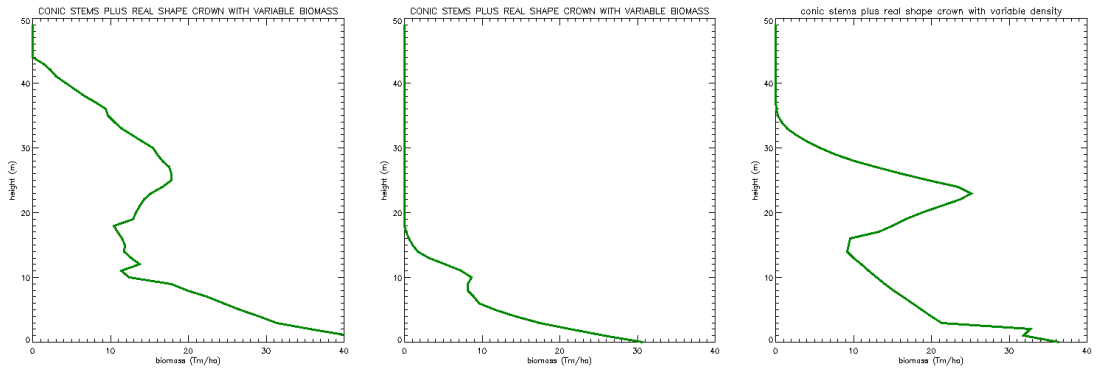

Figure 31 – Biomass profiles from three extreme cases. The profile on the left corresponds with a high biomass content broadleaves stand with high structural diversity. The profile in the middle corresponds with a stand in a growing stage and on the right there is a profile that corresponds with a strong layered coniferous stand with a mature overstory and a regeneration stage.

In Figure 31 three profiles that correspond to very different conditions are shown. The plot on the left corresponds with a high content biomass plot and dominance of broadleaves. The profile shape is not very sharp and the differentiation of overstory and understory is not clear. Therefore, it is seen how the characteristic conic stem contribution is very influenced by the crown biomass in the lower canopy layers. The profile in the middle is a typical profile of a stand in a growing stage where the crown layer is not strongly differentiated to produce a strong second biomass maximum. In contrast, the profile on the right corresponds to a coniferous stand with a high content of biomass. It represents a clear two layers stand with a highly dominant of the overstory (strong maximum in at the height of 25 m.) but with a big contribution of lower vegetation, corresponding to a bush and regeneration layer that is able to modify the typical stem conic profile shape.

These are just three representative profiles of different extreme conditions. Hence, all over the test site many different intermediate cases can be found (ANNEX 2).

3.2 Forest structure measurements

3.2.1 Stand Density Index (SDI)

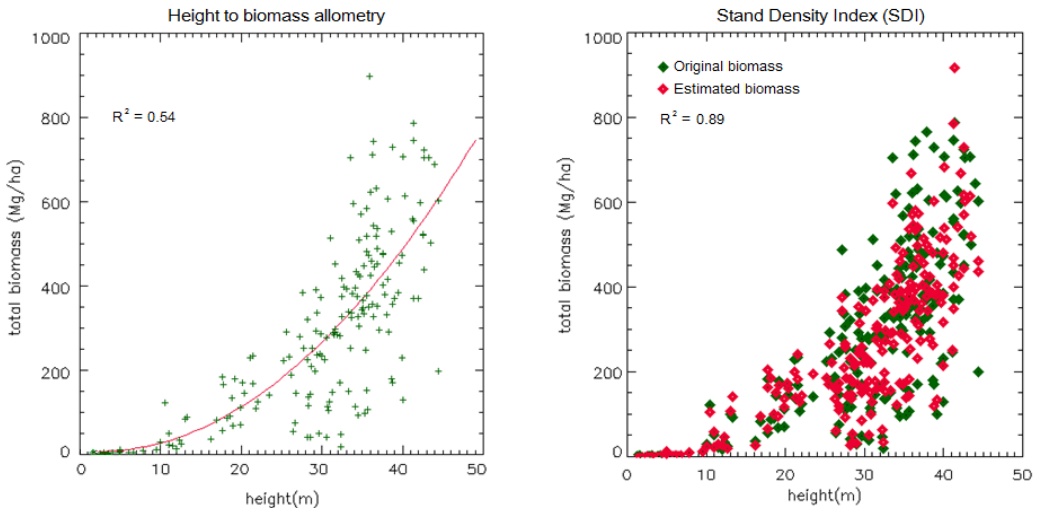

Figure 32 – Stand Density Index estimation. On the left side the figure shows the height to biomass plot and on the right side the Stand Density Index (SDI) plot. The red dots correspond to the estimated biomass with the SDI and the green to the original (real) biomass. The correlation coefficient R^2 for the height to biomass allometry is 0.54,with the usage of the SDI it increases until 0.89

The SDI is not a vertical but a horizontal structure measurement. However, it is placed here because it is a possible improvement in the allometric relation of height to biomass. Moreover, the results obtained will give interesting conclusions and will be helpful for further analyses.

The correlation coefficient R^2 for the height to biomass allometry is 0.56. After applying the SDI following the eq. (2.2.13) in Ch. 2.2.2.2, the correlation coefficient increases to a value of 0.89. In Figure 32 it is possible to see the height to biomass allometry in the plot on the left and in the plot on the right, the correspondence between the real biomass obtained from the model in green and the estimated biomass using the allometric relation with height and SDI in red. Additional structure information improves the height to biomass relation.

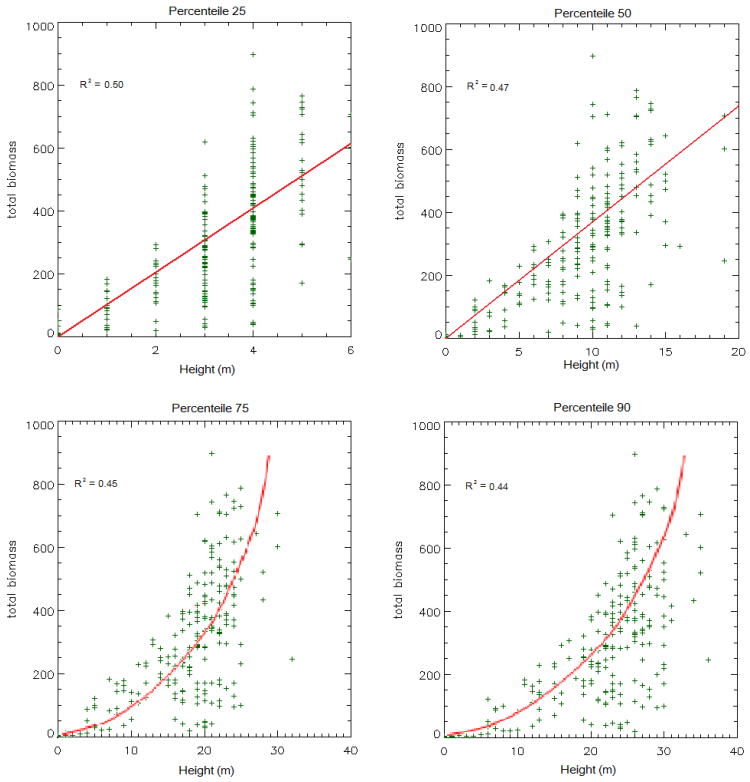

Figure 33 – Metrics diagram. Four regressions for the percentile heights and the total biomass are performed without getting any correlation coefficient higher than 0.5. For percentiles 25 and 50 the regression tends towards linearity, while for 75 and 90 it is a polynomial, similar to the height to biomass allometry.

3.2.2 Metrics

Hence biomass sensitivity for the height metrics is tested according to Ch. 2.4.1. The usage of metrics to characterize vertical biomass structure has not shown any significant result for the percentiles that have been tested. All the values of correlation between the height percentiles and the total biomass are below 0.5 (Figure 33). In the percentiles 25 and 50 the relation tends to be linear but the variance is too high to be considered a conclusive result. The same happens with the percentiles 75 and 90 where the correlation is even lower but more similar to the original height to biomass allometry.

3.2.3 Centre of gravity

Centre of gravity is calculated according to Ch. 2.4.2. The two coordinates that define the centre of gravity are plotted against the total biomass at plot level. The results differ significantly from the biomass coordinate to the height coordinate. In the first case the correlation coefficient has a value of 0.93 while in the case of height this correlation is just 0.49. Moreover, the relation for the biomass coordinate is linear while for the height it is a polynomial.

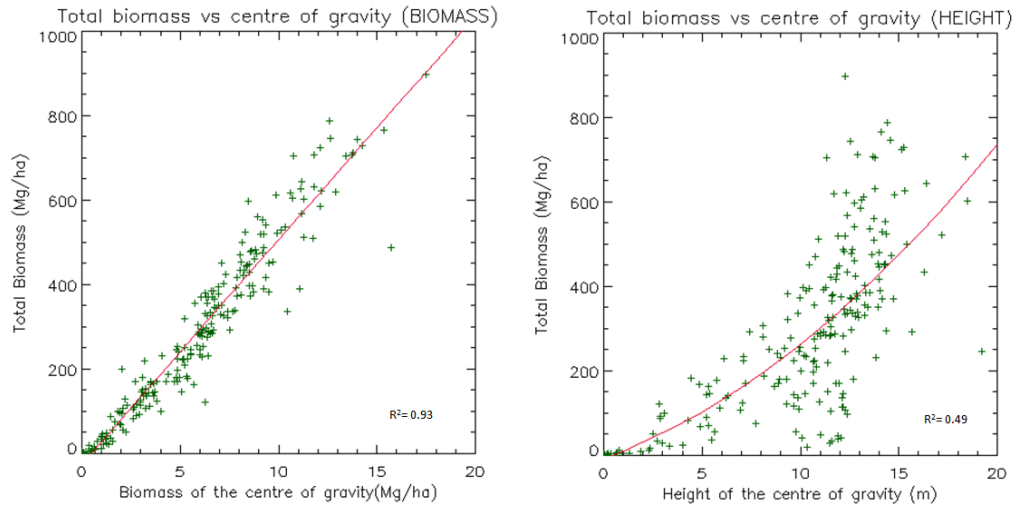

Figure 34 – Regression of the two components of the centre of gravity against total biomass. The biomass component is placed on the left and the height on the right.

In the case of the biomass it could be assumed that this correlation can be used for structure parameterization, however, as it will be outlined in the CH. 4.2.2 this relation does not provide any extra information. The correlation coefficient from the centre of gravity height

coordinate and the total biomass is very similar to the one obtained from the height to biomass allometry.

3.2.4 Decomposition

In Figure 35 three examples from the profile reconstruction are shown. The green lines corresponds to the Legendre profile reconstruction, the red line to the Fourier profile reconstruction and the black line to the original biomass profile (the yellow dot represents the position of the centre of gravity).

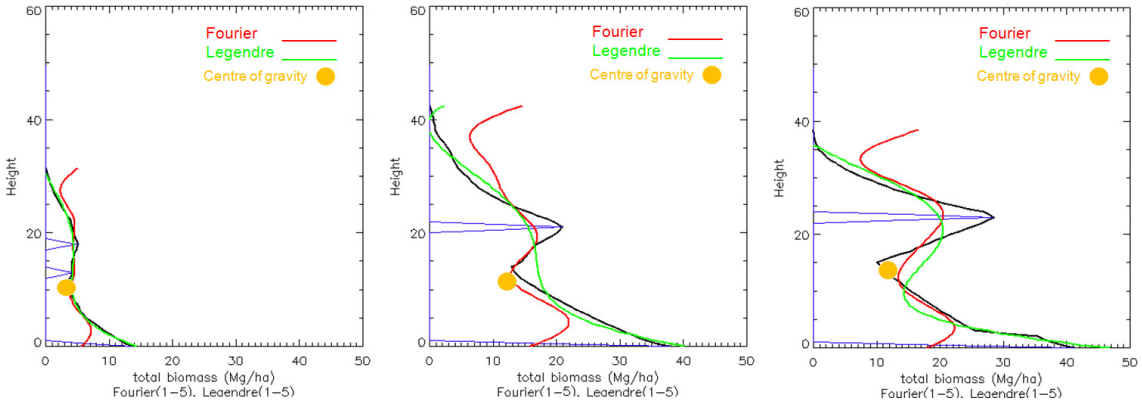

Figure 35 – Reconstruction of biomass profiles with 5 Legendre (green) and 5 Fourier coefficients (red). The yellow dot represents the position of the centre of gravity.

For Figure 35 first the original profile was decomposed and then reconstructed using the single components from Fourier and Legendre. the capacity of decomposition methodologies to reconstruct the profile with just the usage of low frequency components, i.e., the components from 1 to 5 are shown. Both methods can reconstruct the total biomass with a high accuracy for these components, although the performance between Fourier and Legendre is very different. The Legendre method tends to reconstruct the original shape of the profile with fewer components than the Fourier. As it is seen in Figure 35 the Fourier reconstructed profile (red line) tends to overestimate the biomass content in the higher parts of the profile while it underestimates it in the lower parts (basic Fourier rule: starting point = end value). In contrast, the Legendre reconstructed profile (green line) represents the main features of the profile very well, also in the lower and upper parts. Only in some cases, like in the profile placed in the middle, it does not fit

with the biomass of the top of the profile. Nevertheless the reconstruction accuracy achieved with Legendre is always higher than with Fourier.

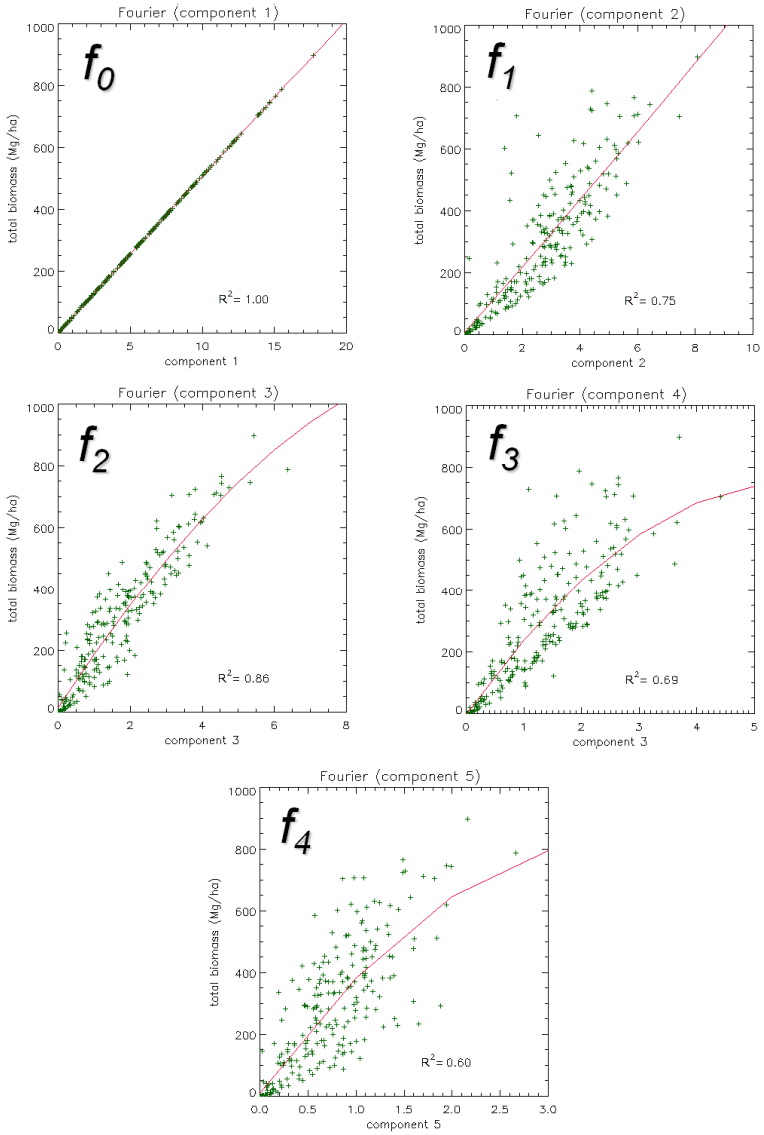

Figure 36 – Regression analysis, total biomass vs. the Fourier coefficients (1-5). the value of the coefficient is represented On the x-axis it and the total biomass (Mg/ha) on the y-axis.

The most important characteristic for forest vertical structure parameterization is not the total biomass of a profile but the characteristic shape features, like the position of the layers, relative sizes of the lobes with respect to each other, etc. Therefore, after this analysis, the

Legendre decomposition is then established as the optimal method for structure parameterization. The results from the Legendre decomposition will be explained in more detail in the following sections.

3.2.4.1 Fourier decomposition

The results from the Fourier regressions are displayed in Figure 36 . The first coefficient *f0* presents a value of correlation equal to 1, as this coefficient represents the integral of the profile (total biomass). The rest of the coefficients present a correlation coefficient over 0.60 what indicates acceptable values for these relations. What is more, f_1 and f_2 present correlation values of 0.75 and 0. 86 respectively; f_3 has a correlation of 0.69 and f_4 0.60. This indicates that the structure represented for these coefficients has a good correlation with total biomass. No more coefficients are considered because the agreement with the vertical biomass profiles is too low.

However, as it is explained in Ch. 4.2.3 in this study is the exact relation between these coefficients and the vertical structure is not clear (in contrast with the Legendre coefficients).

3.2.4.2 Legendre decomposition

Legendre regressions

Regressions of Legendre polynomials were investigated in two levels: the first set (Figure 38) corresponds to the regression of the direct correlation between the total biomass and the value of the Legendre coefficients, whilst the second set is the total biomass and the biomass contribution obtained from each of the polynomials (Figure 37). Different conclusions will be obtained from the results of these two comparisons.

Individual Legendre coefficients (Figure 37): The results from the correlations are very different depending of the characteristic polynomial that is used in each regression. Only the first five correlations are taken into account as the rest of the values do not offer significant agreements (~0.00). The coefficient a_0 has a correlation to the total biomass of 0.93; however, this coefficient does not represent vertical structure (see Ch. 2.5.2). The coefficient a_1 and a_3 present the highest correlation coefficients, 0.67 and 0.78. The regression of a_2, instead, has a

correlation coefficient of 0.02 and a_4 one of 0.03. In the cases where the correlation is significant (a_1, a_0 and a_3) the regression is clearly linear.

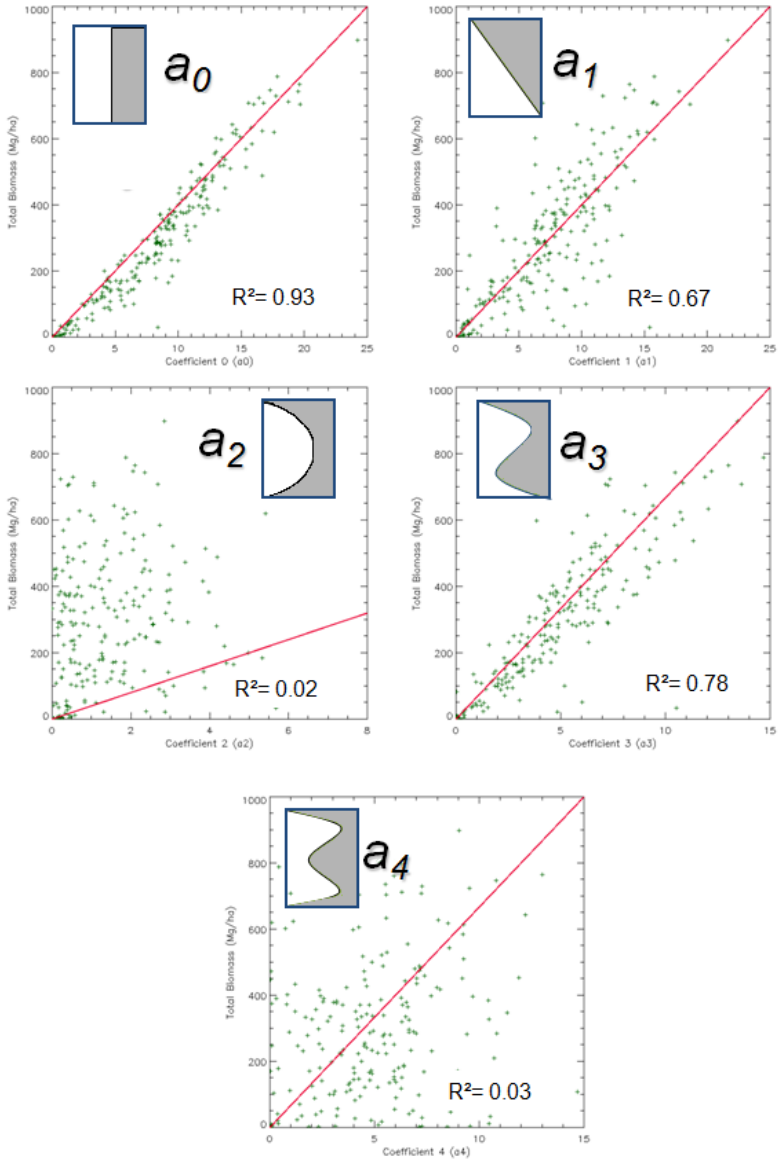

Figure 37 – Regression plots between the total biomass and the individual Legendre coefficients for the five first cases. On the x-axis the value of each coefficient (no dimension) is represented and on the y-axis the total biomass (Mg/ha).

Biomass components contribution (Figure 38): in this case the height is included in the calculation (see Ch. 2.5.2). Still, the results are very similar to the Legendre coefficients contribution, although the values of the correlations increase for all cases. The correlation for the

first component (a_oP_o) is equal to 1 and with a 1:1 relation (in this case it represents the profile integral). Moreover, the correlation a_1P_1 is higher than the correlation for a_3P_3 and both are higher than the previous results (0.88 abs 0.81, instead of 0.67 and 0.78). The value for a_4P_4 is higher than for a_4 (0.40).

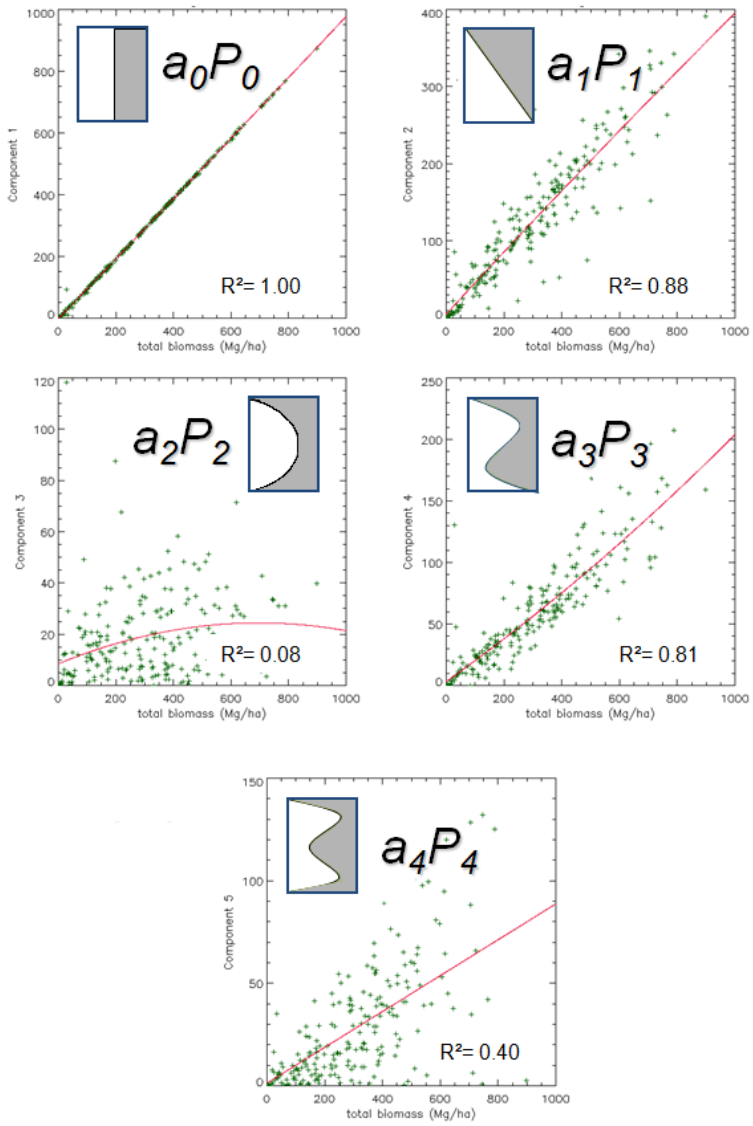

Figure 38 – Regression plots between the total biomass and the proportion of biomass contributed by the Legendre components, for the first five cases. On the x-axis it is represented the total biomass (Mg/ha) and on the y-axis the proportion of biomass (Mg/ha)

The allometric relation

In the previous analyses it was observed that the second and the fourth Legendre components are the ones that can explain the total biomass best (if the first component is excluded it does not content structure information). The second component is kept, in order to cover the range of characteristic shapes and to keep the sequence of low frequency components (see Ch. 4.2.3.1).

Combining the individual Legendre components strengthens the relation between biomass and amount of biomass is explained by structure (see 4.2.3.3 in the Discussion). This yields a linear relation (Figure 39). A correlation coefficient R^2 of 0.92 and a slope of 2.88 are obtained. Thus, it can be concluded that the fraction of biomass from components 1 to 3 is able to explain the total biomass by a 92%.

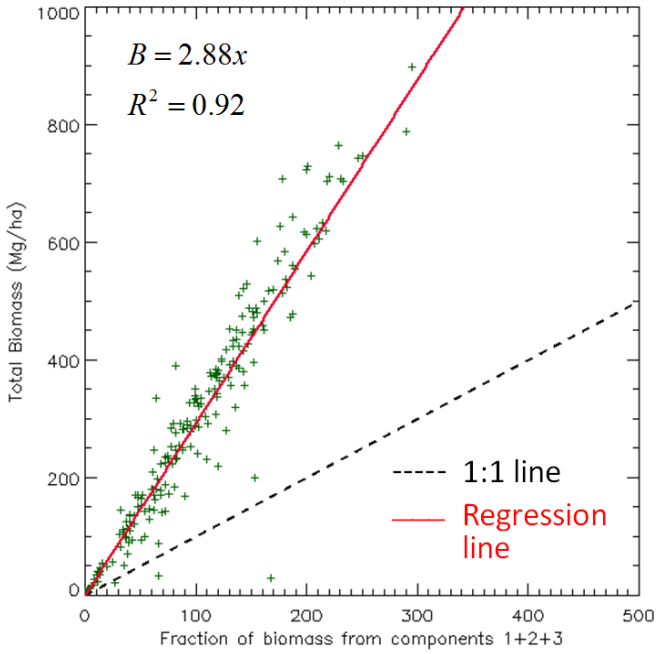

Figure 39 – The allometric relation. The fraction of biomass from the components 1, 2 and 3 is on the x-axis (Mg/ha) and the total biomass (Mg/ha) on the y-axis. The regression line is represented in red (B=2.88x), where B is the total biomass and x the fraction of biomass from Legendre components. The dashed black line indicates the 1:1 line for equivalent values of biomass (fraction and total biomass).

Then the structure to biomass allometry can be formulated using eq. (2.5.7) as:

$$B = 2.88 * \sum_{i=0}^{H} \sum_{j=1}^{3} a_j \cdot P_j \qquad (3.2.1)$$

Monte Carlo simulation

Figure 40 is an example of output results obtained from the Monte Carlo simulation for a 10% deviation in the case of the combination of Legendre components 1+2+3. This procedure has been performed for the combination of the three selected Legendre components and for only one of the components. Therefore, the set of results is too extensive to be shown in this section. A summary of the results can be seen in Table 5 while the graphs are collected in ANNEX 5.

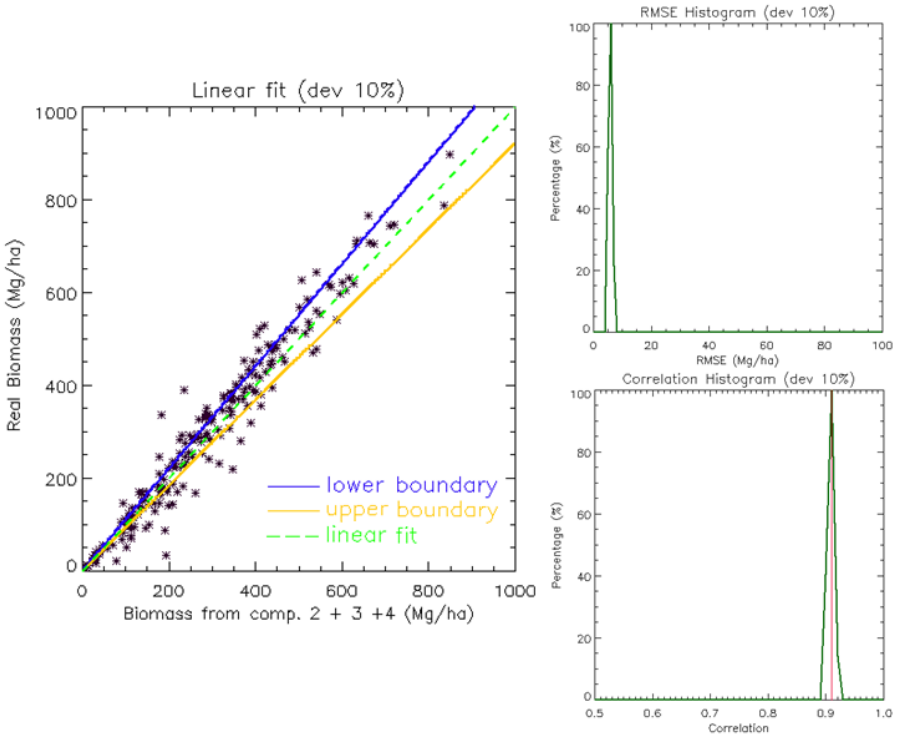

Figure 40 – Example of the Monte Carlo analysis for the Eq. (3.2.1) and an error of 10%. The plot on the left hand side represents the correlation of the real biomass against the estimated biomass from the allometric relation of eq. (3.2.1). The dashed green line represents the linear fit (degree of correlation), the yellow line the linear fit for the maximum additive deviation (lower boundary) and the blue line the maximum subtractive deviation (upper boundary). The plot on the upper right side is the histogram of Root Mean Square Error (RMSE) and the lower right side plot the histogram of the correlation coefficient.

Table 5 – Monte Carlo test results.

		RMSE (Mg/ha)			R^2		
Legendre component	**Deviation**	**Min.**	**Max.**	**Mean**	**Min.**	**Max.**	**Mean**
1+2+3	10%	4	6	5	0.89	0.`93	0.91
	20%	3	10	6	0.87	0.94	0.90
	30%	2	11	6	0.85	0.92	0.89
	40%	1	13	7	0.68	0.81	0.88
1	10%	1	5	3	0.74	0.81	0.76
	20%	4	10	6	0.72	0.83	0.80
	30%	1	6	3	0.68	0.85	0.79
	40%	1	7	3	0.63	0.86	0.79
2	10%	2	8	5	0.00	0.10	0.02
3	10%	3	8	5	0.30	0.45	0.38
	20%	30	50	43	0.25	0.35	0.32
	30%	30	46	43	0.22	0.55	0.34
	40%	29	57	43	0.18	0.60	0.25

The Monte Carlo simulation of eq. (3.2.1) shows high values of the correlation coefficient (~0.91) with low variances until an error of 30%, where the correlation coefficient starts to have a second maximum in 0.7 (Figure 41Figure 27). The values of RMSE remain low (~5 Mg/ha) with a low variance even with the introduction of an error of 40% (see Table 5).

In Table 5 is also seen that the behavior of individual Legendre components the results are more variable:

- Component 1 presents initially higher values of correlation and lower RMSE than the combined case (3 Mg/ha). When errors are higher than 20% the variance of the correlation becomes very noisy and the mean decreases until values of ca. 0.70. The variance of the RMSE remains stable.

- Component 2 in the Monte Carlo simulation does not show any significant result (the correlation did originally not exist).
- Component 3 initially has low values of RMSE (5 Mg/ha), however after a 10% deviation the value increases drastically (up to 43 Mg/ha). The correlation coefficient becomes noisy and low from the 10% deviation (from 0.38 to 0.25 at 40%).

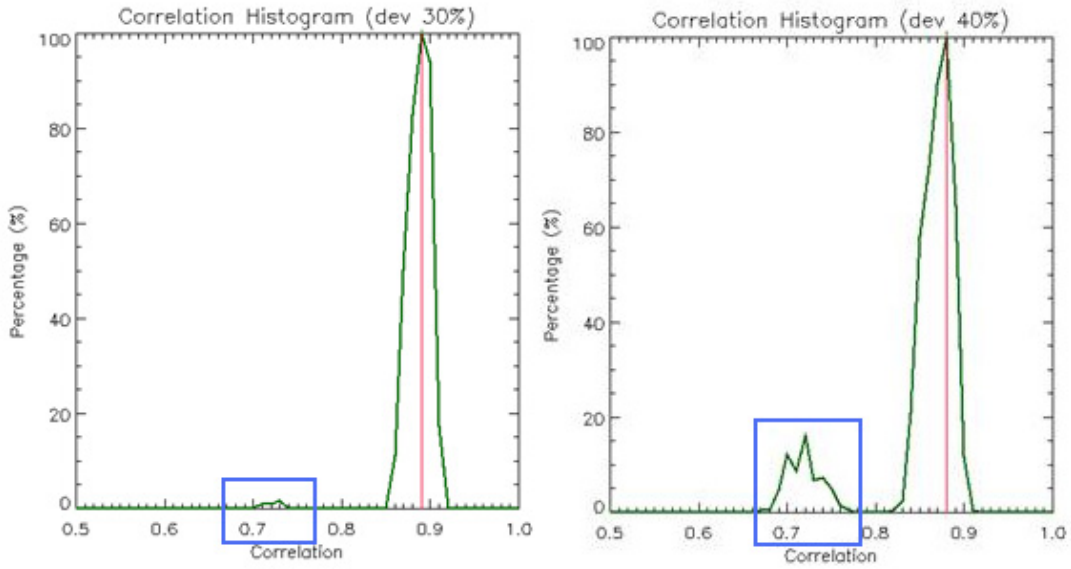

Figure 41 – Monte Carlo correlation histograms for the Legendre components 1+2+3, for a deviation of 30% (left) and 40% (right). The blue squares highlight the second maxima that are observed in these histograms.

3.3 Application to LIDAR data

3.3.1 LIDAR height map

Figure 42 shows a zoom of the LIDAR height map. This map is able to represent with a high accuracy the height of the trees over the DTM. The color ramp characterizes the height of the trees, starting from black at 0 meters (height from the DTM) to a maximum of 50 m in dark red. It is possible to observe how well the tree crowns are distinguished and it is even possible to delineate different stands or even to appreciate different structures.

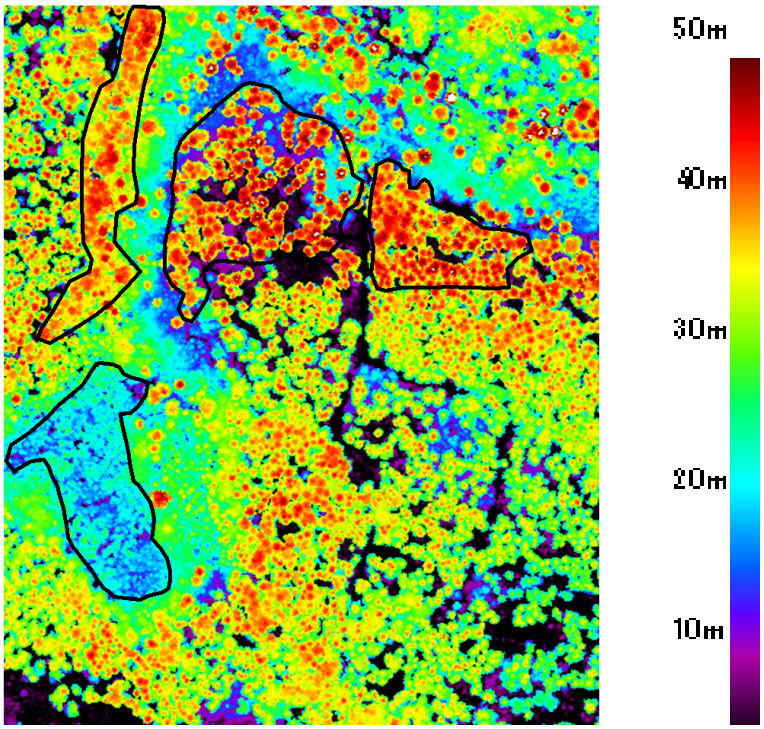

Figure 42 – Sample of the LIDAR height map. The color ramp (on the right side) moves from purple to dark red indicating the height of each pixel. The minimum height is 0m (black) and the maximum 50 m. Four examples of structural stands are deliniated in black.

3.3.2 LIDAR vs. ground measurements

Figure 43 is a plot of the comparison, after the location correction (see Ch.2.8.2.1), between the maximum heights obtained from the LIDAR plots against the top height – H100 (dominant height according to Assman) of each of the corresponding field measured plots. The correlation factor R^2 is 0.90 and RMSE 3.46 m.

It can be observed that even after the geo-location correction there are still several plots when height deviates strongly in both measurements from each other. The general trend shows that LIDAR heights overestimate to field measured heights (considered as real height). The deviation in height is higher for plots with shorter trees, which are in general overestimated, while in plots with high trees both over and underestimation could be detected.

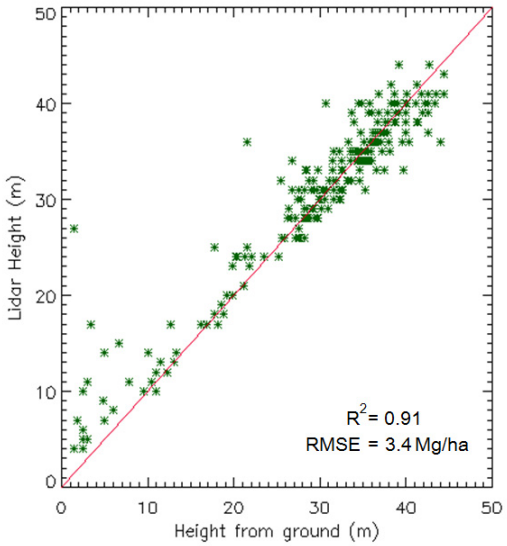

Figure 43- Height measured with LIDAR against height measured from the ground. The red line represents the 1:1 line where both heights have the same value.

3.3.3 LIDAR profiles

The LIDAR profiles are done in an analogous way, like are the biomass profiles. Tree height (m) is in the y-axis but in the x-axis instead of biomass it is represented the backscattered total intensity or amplitude is plotted in1m bins along height (Figure 44 - left). The collection of all the intensity airborne lidar profiles can be found in Annex 3.

Hence, the characteristic features of the LIDAR profiles are similar to the biomass profiles and therefore both profiles can be easily compared. Going from top to bottom it is first observed a maximum in the crown layer, later a characteristic minimum and, finally, and increase for the lower part of the stems. However, due to the characteristics of the airborne LIDAR systems some differences to biomass profiles can be observed. The most common difference is the dominance of the crown components in these profiles. In the most of the cases, LIDAR profiles present a clear maximum in the canopy upper layers, especially for the plots located in mature dense stands (typical example in Figure 44 - left).

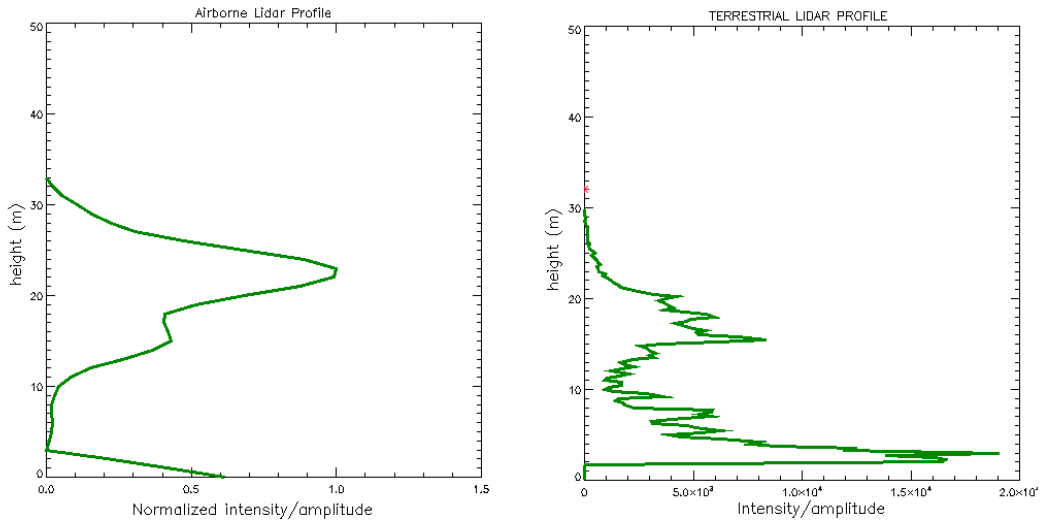

Figure 44 – LIDAR profiles. Right: airborne LIDAR profile, Left: Terrestrial Lidar (TLiDAR) profile.

Considering the ground backscattering two different types of LIDAR profiles can be created: with or without ground backscattering. In Figure 45 two of these profiles can be seen: on the left there is a plot where the intensity from all the hits over 0m have been summed (ground contribution); and on the right a profile where the hits that are under 30 cm. are removed from the profile generation (without ground). It is observed that the relative amplitude of the canopy lobes is smaller in the case were the ground hits are not removed. In Figure 45 it is also seen the strong ground contribution: only the first 30 cm can strongly influence the shape of the profile.

For the eight profiles which TLIDAR profiles are available it is possible to examine the difference in the detection with ALS. Differences between these profiles could also be derived from the comparison between ALS and the vertical biomass profiles. In the 8 profiles TLIDAR always offers a better representation in the lower parts of the profiles, which corresponds with the stems and lower vegetation. However ALS gives a better characterization of the canopy layers and a more precise estimation of tree height peaks (maximum heights) (Figure 44).

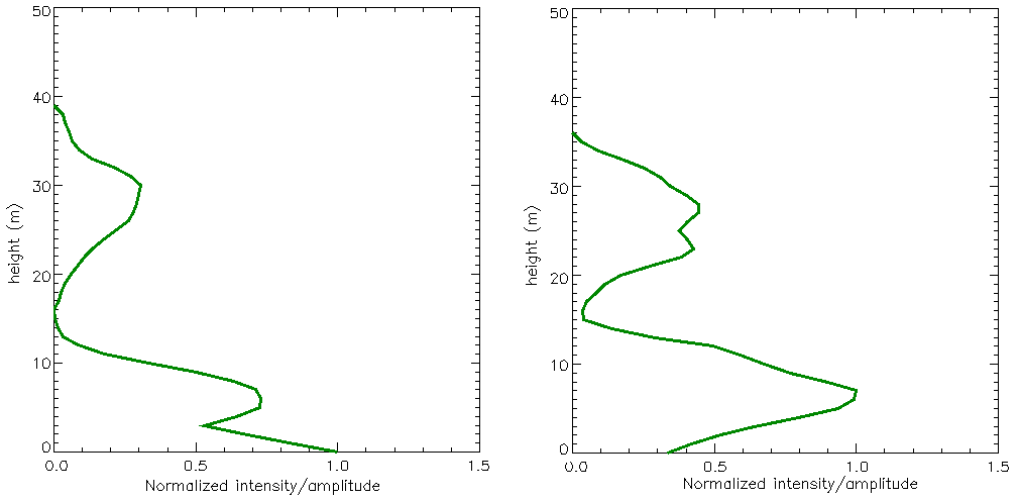

Figure 45 – Test of ground hits removal. In the plot at left hand side the profile is calculated in a normalized basis with the total amount of returns. The plot at the right hand side is calculated without the returns encountered in the first 30 cm (the x-axis represents the sum of the intensity of all returns in 1m.)

3.3.4 LIDAR backscattering

LIDAR backscattering including LIDAR profiles depends on several factors in the acquisition and in the forest conditions. Figure 46 displays the 3D of the backscattering. The first returns from the laser beam are represented in green, the second in red and the third in green. The returns from the ground are represented in black.

Figure 47 it represents on a 2D basis the projection on the plane ZX of the cloud of hits. The observation of these plots confirms the results obtained from the LIDAR profiles. In case of a close dense canopy the number of hits that are detected in the intermediate layers is strongly reduced (Figure 47- plot 3007018). In the contrary when the crowns are sparse (Figure 47- plot 3008009) or the overstory is not present the number of returns in the lower layers increases. The entire set of plots can be found in Annex 4.

The relative position of the plots with respect to plane position is another important factor in the interpretation of the profile. Profiles located under the nadir (in the orthogonal direction from the sensor) the detection under the canopy, especially when they are very dense, is much lower than if the plot is located in a position with higher view angle. As wider is the looking

angle as better is the detection of lower vegetation and stems under dense canopies (see Figure 47- plot 3008013).

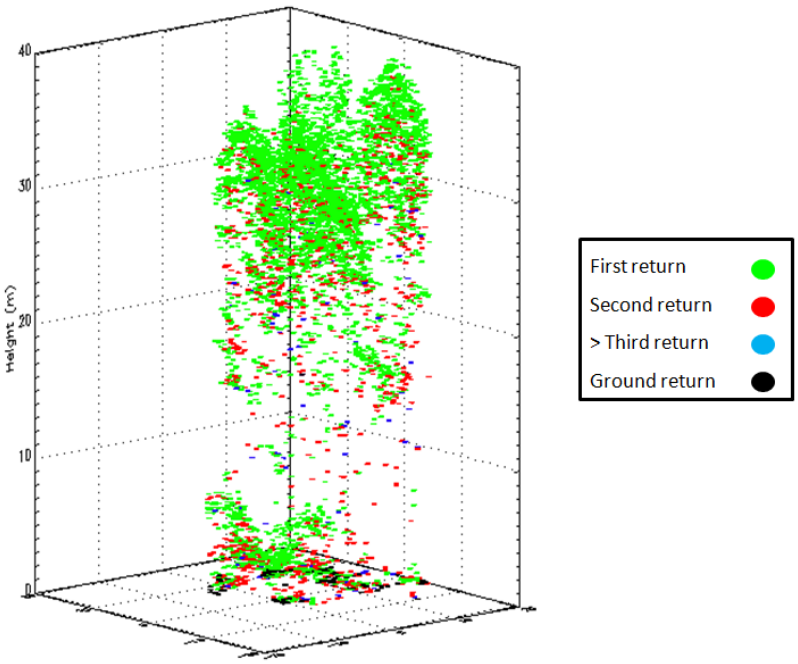

Figure 46 – Three dimensional representations of the LIDAR pulses (hits) positions. First returns are represented in green, second in red, third in blue and the ground returns in black. The height is situated on the z-axis while the x- and y axes corresponds to the X and Y pulses coordinates.

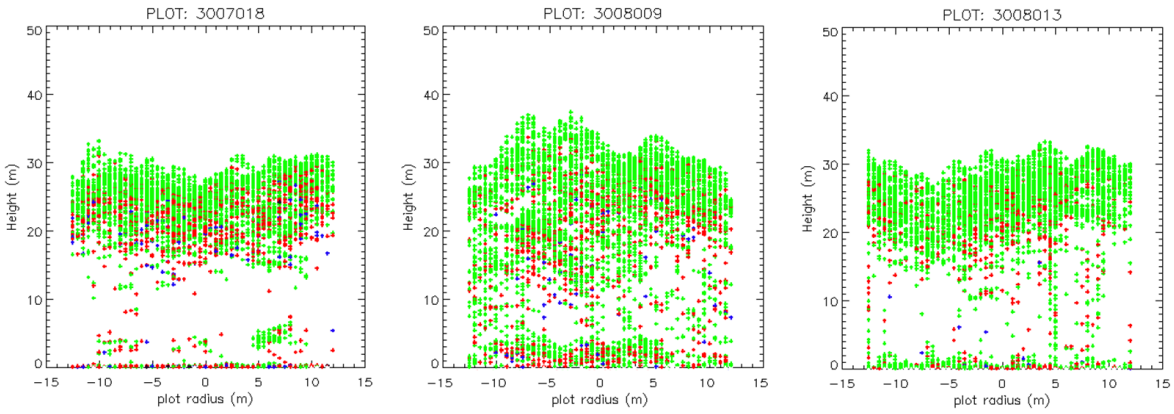

Figure 47 – Vertical projection of the 3d pulse plot on the YZ axis. First returns are represented in green, second in red, third in blue (ground returns are not included here). In the x-axis it is plotted the distance of the pulses to the centre of the plot in m. Left: dense canopy plot under the nadir; middle: sparse canopy, right: dense canopy under a high looking

3.3.5 Canopy Height Profiles

In Figure 48 two CHP examples with the original LIDAR profile are shown. The profiles on the left correspond to the LIDAR profiles and on the right to the CHPs. The upper case shows a good CHP derivation as the LIDAR profile as been correctly modified. In the lower case the CHP has not been able to correct the strong gap that the LIDAR profile presents between the canopy layer and the ground.

In order to see how well the CHPs can adapt the LIDAR profiles to the vertical biomass profiles they have been over plotted together (Figure 49). First, both profiles (biomass and CHP) are normalized in the x-axis by the maximum with the same unit basis. In Figure 49 the original profile is represented in blue while the CHP is represented in green.

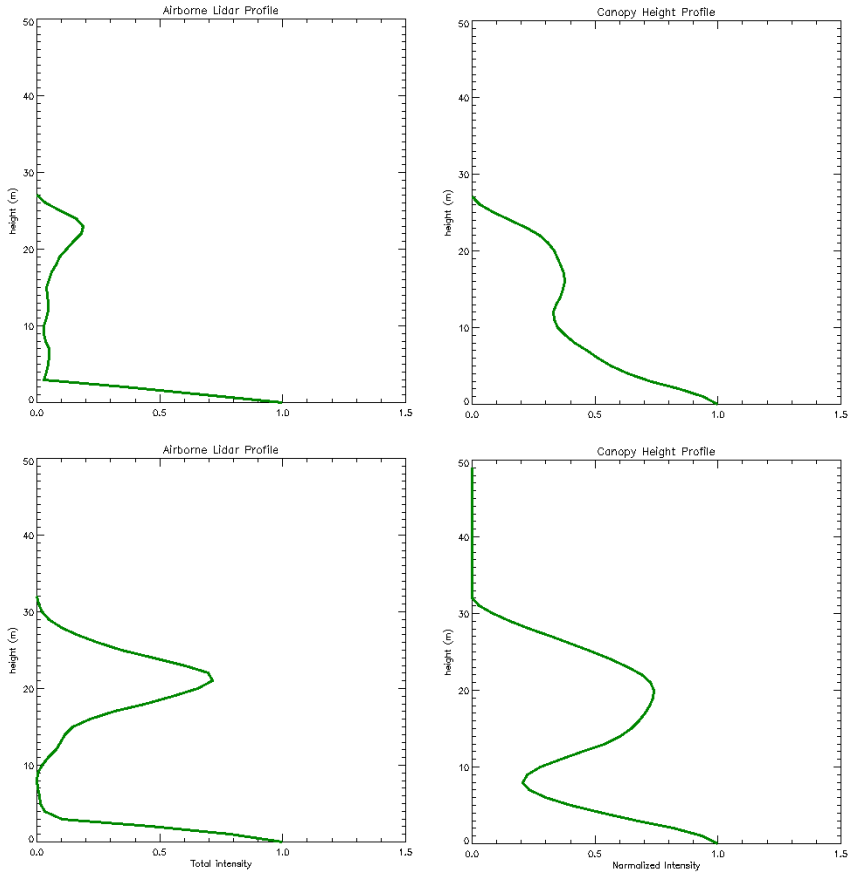

Figure 48 – Airborne Lidar Profile (left) vs. Canopy Height Profile (right) for a optimum case (top) and a bad case (bottom)

For the majority of the profiles a major improvement can be observed, especially in the adjustment between the profiles in the mentioned lower parts of the profile. On the other hand there is a relevant group of profiles where the CHP is not well adjusted to the vertical biomass profile but they follow, generally, the same trend (Figure 49 - left). In these profiles, the CHP gets a maximum at the height 0, as the vertical biomass profile does, but then it presents a gap before the canopy maximum (Figure 49 - right). Another important group of profiles are profiles with the lower heights, where the CHP significantly improves the adjustment.

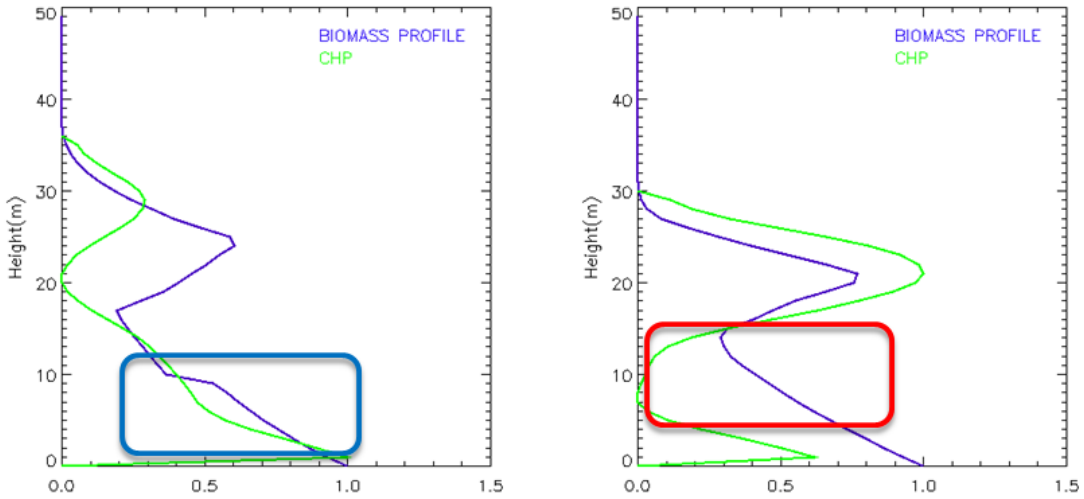

Figure 49 – Canopy Height Profile (CHP) test. The CHP (green) is plotted on top (blue) on a vertical biomass profile to test the adjustment between the two profiles. Rectangles: are of special interest; blue for a good adjustment and red for a poor adjustment..

3.3.6 Biomass inversion

3.3.6.1 Transfer function

The first step to get biomass from lidar of the inversion is to calculate the transfer function. For each of the profiles available for the ALS detection a profile of differences has been calculated (see Ch. 2.8.2.2). This was done using the difference in normalized profiles whereas for LIDAR the CHP was used. Differences profiles of follow a characteristic curves and can be grouped in two big clusters:

- Mature forest plots: in this group the profiles achieve high altitudes, and the differences tends to be negative in the lower part due a high biomass content of the vertical biomass

profile and positive in the top due to the stronger crown representation of the LIDAR. However, for many profiles the differences at the bottom are very low, so they contribute to increase the occurrence of the histogram in this area (see Figure 50).

- Young forest plots: In this case the difference in profiles (biomass, CHP) is very low, compared to the previous group.

The differences profiles are summarized in a 2D histogram (Figure 50). In this case the height is represented on x-axis while the normalized difference between the profiles is represented on the y-axis. Two main trends can be observed. The highest concentration of points is located between 0 and 5 m, while for the rest of the range of heights the variance is much higher. The largest differences are located between at heights from 15 to 17 m, where the mean difference between the CHP and the vertical biomass profiles becomes 0.40 (40%). Another higher concentration of points is observed in a height of 25 m; although this one is not as representative as the one located between 0 and 5 m. Here LIDAR measurements are coincident with the Biomass profiles.

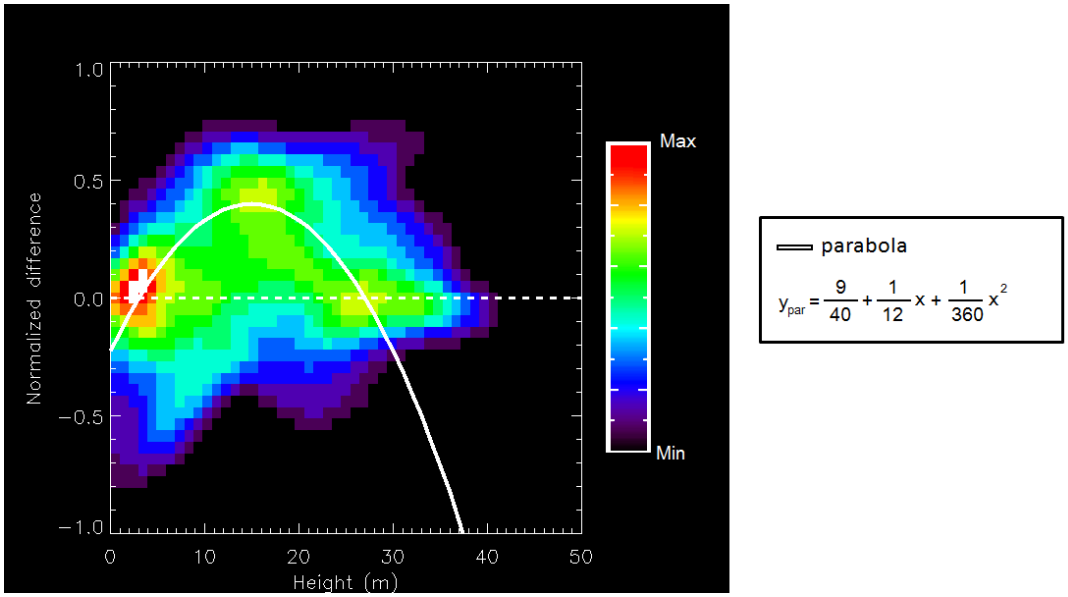

Figure 50 – 2D histogram of occurrence (CHP profiles – biomass profiles). See legend on the left for frequency.

The maxima in the 2D histograms can be approximated best by a polynomial of second order (parabola):

$$y = -\frac{9}{40} + \frac{1}{12}x - \frac{1}{360}x^2 \qquad (3.3.1)$$

where y is the difference between profiles and x the height. This parabola has the maximum at 16m. Parabola is superimposed in Figure 50.

3.3.6.2 Decomposition and biomass inversion

The process to derive Biomass from the LIDAR (CHP) can be summarized with the following steps:

1. Decomposition of the CHP with Legendre polynomials.
2. Normalization of the vertical biomass profiles and decomposition.
3. Estimation of the contribution from the Legendre components for CHPs and vertical biomass.
4. Regression between both contributions obtaining Eq.(3.3.2)
5. Evaluation of the equation with the correlation coefficient and RMSE.

In Figure 51 it is displayed the final regression between the Legendre components 1+2+3 from the corrected CHPs and the same components from the vertical biomass profiles The normalized LIDAR information is represented in the x-axis while the normalized biomass is represented in the y-axis. This is the relation that will allow the derivation of biomass from the LIDAR intensity/amplitude information. A logarithmic Function has given the best adjustments achieving a correlation coefficient of 0.76:

$$y = \log\left(x^{5.8} + 1\right) \qquad (3.3.3)$$

In order to invert biomass it is necessary to account for the absolute fraction of biomass necessary for the "structure to biomass allometric equation (Eq.(3.3.4))". However, as it will be extended in Ch. 4.3.3, the relation between the normalized biomass contributions from the

Legendre components and the absolute ones needs to be further investigated, because it is observed a lack of precision in the correlation.

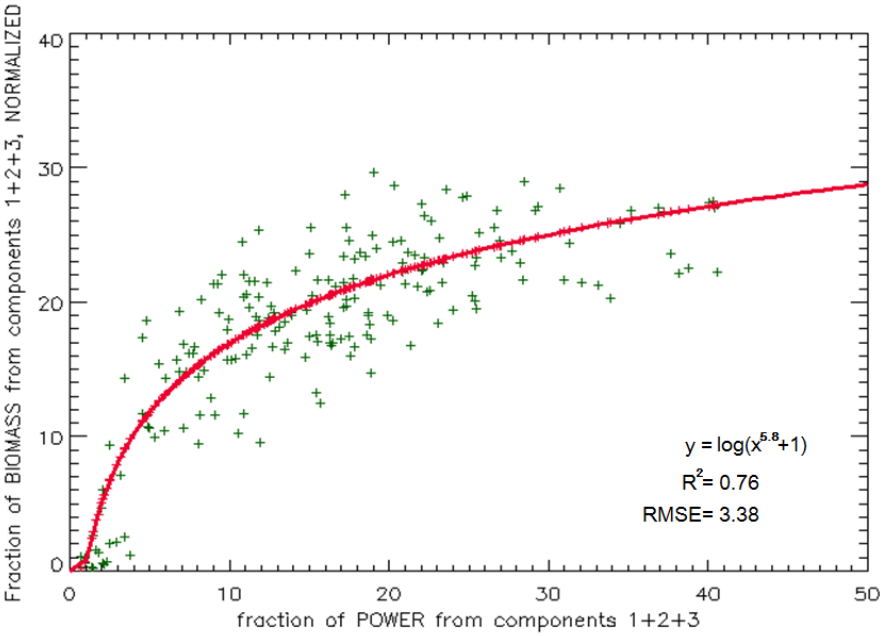

Figure 51 – Biomass inversion plot from CHP Legendre components. The red line represents the logarithmic equation that offers the best fit for this regression: $y = \log(x^{5.8} + 1)$. The fraction of power from the first 3 Legendre components is represented on the x-axis and the fraction of biomass from the same components on the y-axis.

4 Discussion

4.1 The forest vertical biomass profiles

4.1.1 Biomass model selection

The selected model had to fulfill two main factors: first, to represent volume and second, to derive biomass as accurately as possible, for each tree compartment (crown and stems). The complexity of this process depends on the considered tree compartment: in the case of the stems, the form model is much simpler and better studied in literature. The crown case however is more complex, as many different variables affect the crown shape and its density, e.g. it is necessary to derive the biomass.

A cone was selected as the best volume form to represent the tree stem. It is an easy figure to model and compute, it is more complex than a cylinder and better represents the general stem form, especially for conifers. As biomass is directly derived from the volume using dry wood density, it is trivial to say that the considered stem form is the main variable to evaluate the biomass distribution. The use of stem form equations would have been an improvement in the stem model. On the other hand, the availability of stem form equations in literature is much reduced for the most of the species. Moreover, the cone model has shown to be capable of modeling the biomass distribution with sufficient accuracy. Two tests can support this assumption:

- First, in the comparisons with the TLIDAR profiles, the distribution of the biomass along height, excluding the crowns, follows the same tendency as the one observed in the biomass profiles.

- Second, the height to biomass relation (using the cone as stem form) and the height to biomass relation obtained using the volume with form factor (provided by the inventory data) are very similar.

The test for the crowns is more complicated but also offers stronger results, especially when comparing the results of the model with the TLIDAR. As it was shown in Ch. 3.1.1 the combined models stem + crown have pointed out that that "conic stem + allometrically derived biomass for the shaped modeled crown" as the best fitting model. The maximum amplitude of the crown layers with respect to the stems is a key characteristic of the profiles in order to characterize structure.

On the other hand, the parameters used in the crown shape model haven been derived from an extensive collection of data with similar growth and species composition (Pretzsch, 2001). For crown biomass estimation, those equations that could best describe the conditions of the test site Traunstein were selected (Ch. 2.3.2.2).

4.1.1.1 Limitations of TLIDAR

TLIDAR cannot measure biomass directly from the vegetation; however, it can offer a very detailed representation of the vegetation distribution visible to it. Thus, it is assumed that the biomass is directly related to the presence of vegetated surfaces (leaves, twigs, branches and stems).

The first problem noticed is the systematic underestimation of the height by the TLIDAR. Regarding the vertical biomass profiles, the height measurements in the field are considered very accurate. Height underestimation arises because of attenuation and insufficient penetration that the TLIDAR has, especially with dense vegetation condition. Sometimes the laser is already reflected by the dense crowns, before achieving the crown tops. Thus, information from the upper parts of the forest canopy is missing. Even if the maximum canopy height is measured, this effect also impacts he amplitude of the crown lobes in the LIDAR profiles, under-representing the upper parts of the canopy.

Another problem is the low quantity of TLIDAR profiles that were available for this study. Moreover, the available profiles are very similar among themselves so they represent the

same types of stands, i.e. very similar structural characteristics. This is coniferous forest in a medium-high advanced stage of development and with a dominant overstory (canopy layer) with, more or less a regeneration layer. The test site of Traunstein is composed by a high diversity of stands with a mixture of species in several stages of development. Thus, a larger collection of TLIDAR measurements would improve the validation of the models used for the vertical biomass profiles.

4.1.1.2 Traunstein test site for vertical biomass structure modeling

It has been mentioned that the test site of Traunstein is an optimum location for analyzing forest structure in central European conditions and, especially, in southern Germany. After analyzing the results from this study, this premise has been proved. The collection of vertical biomass profiles, from all the inventory plots, shows a big variety of cases (see Ch. 3.1.2.1 and Annex 2): from young to mature stands, even to uneven structures and single to mixed species. Also this variety is observed, when the results at forest level are analyzed. The biomass stocks are evenly represented from the lower quantities (5 to 10 Mg/ha) to high quantities (up 880 Mg/ha). This extensive range of different forest structures has allowed us to extract, with a high confidence, conclusions that can be extrapolated to other forests under the same conditions. It is even possible to consider that these results can be applied to different conditions, as the range of profiles could represent many different structure types.

4.1.2 Impact of the tree crown in the vertical biomass structure: biomass profiles and the allometric relations

It has been shown that crown modeling is essential for the total biomass stock estimation and also for the study of vertical structure. Figure 52 shows the difference between profiles considering only stems and profiles with stems and crowns biomass. Thus, an increase of information about vertical structure going from stem profiles (Figure 52-left) to total biomass profiles can be observed (Figure 52- right).

When modeling only stems the biomass decreases from the forest bottom to the top, although sometimes, when the contribution from the understory is very strong, also this can be observed (Figure 52- upper left). However, in most of the cases stem biomass of the overstory is very dominant in comparison with the understory; it is thus very difficult to distinguish other

contributions. Nevertheless, the stems which belong to the overstory trees introduce such high biomass values in the stem profiles, that they hide any other contribution. This fact is important to characterize structure at an individual profile, but it is even more relevant to analyze the differences between different profiles (plots) (Figure 52).

In Figure 52 it can be observed that the differences between the stem profiles (Figure 52 – top left vs. bottom left) are lower than in the case of the total profiles (Figure 52 - right). For example, in the case of the total biomass profiles it is possible to distinguish between different species, just from observing the shape of the profile. The upper one is formed by coniferous species, while in the case of the bottom profile there are species mixtures, probably with broadleaves, which produce a smoother shape.

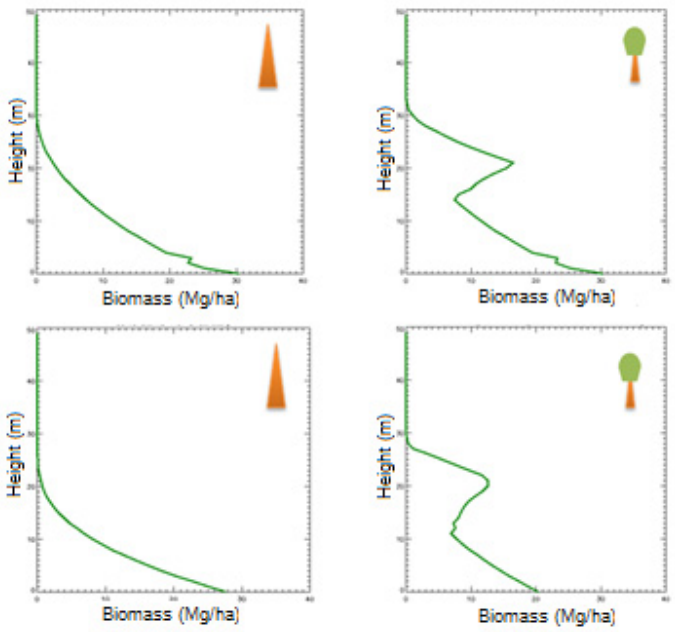

Figure 52 – Impact of the crowns in forest vertical structure characterization. The two graphs on the left correspond with a model from conic stems (without crown) and on the right the selected model: "conic stems + model crowns with allometric biomass".

For above-ground biomass calculations crowns are essential, as they represent, in mature stands in central European conditions, 20 to 40% of the total biomass (Pretzsch, 2009) . On forest level, the allometric relations remain constant when adding crowns, compared with the "only

stem" case and, moreover, the biomass stock calculation increases in almost a 40% (Figure 30). This result leads to the conclusion that including crowns in biomass calculations does not decrease the potential of the allometric relations as found for height and biomass.

4.2 Improvement of the height to biomass allometry: The structure measurement methods

As shown in Figure 30 pure height to biomass allometry is not ecnough to get sufficient accuracy in biomass estimations. Therefore, a second parameter is needed. Here the potential of forest structure was investigated to improve biomass estimates. Several methods capable of detecting forest vertical structure, available in literature or new ones have been tested with different results. This chapter is intended to summarize the capacity of these methods to characterize the vertical structure and their applicability.

As a first step, impact of the SDI as a horizontal structure parameter on biomass estimation was tested to prove the impact of structure on biomass estimations. This correlation is already confirmed in literature. (Pretzsch, et al., 2005)

4.2.1 The Stand Density Index (SDI)

In Figure 32 it was observed that including the SDI increases the accuracy/relation of the height to biomass allometry from 54 to 89 % for the Traunstein case. This result would recommend the SDI as a valuable parameter for biomass estimations. However, as it has been mentioned in Ch. 2.2.2.2, this index depends on density measurements (horizontal structure), which the available remote sensing systems (LIDAR and Radar) cannot resolve. Consequently, as the purpose of this study is the application of biomass estimations to a remote sensing system, the SDI is of minor importance for this study.

In conclusion, the SDI outlined the importance of structure to improve the height to biomass allometric relations.

In forests, as found in the test site Traunstein, the height to biomass allometry does reach its limits, although with the usage of SDI it is possible to achieve better results. Thus, the vertical biomass structure, which can be measured by Remote Sensing systems, becomes an interesting

parameter to improve the height to biomass allometry for forests with complex structure. The inclusion of horizontal structure improves height to biomass allometry, and then also forest structure could also improve this allometric relation.

4.2.2 Metrics and the centre of gravity

Height metrics have been used in several studies as a feasible method to describe vertical forest structure parameters (Sun, et al., 2008). However in this study the obtained results have not given good results for any of the percentiles (Figure 33). It can be assumed that the high diversity of the Traunstein forest introduces too much variety.

The centre of gravity method is based in a similar concept as the metrics. The centre of gravity does not consider beside biomass amplitudes in addition to the heights, expressed in a pair of biomass-height coordinate (see Ch. 2.4.2). At this respect it can be considered that this method is more strongly related with the profile shapes.

A priori the results shown in Figure 34 point to an excellent relation, however when making a closer analysis it is observed that these results do not provide with extra information, i.e. they does not provide with reproducible variables. In the case of the height coordinate the regression analysis is analogue to the height to biomass allometry but using ca. the half of the height. For the biomass component, the regression achieves 93%; however this just means that the biomass of the plots is highly correlated with a proportion of it.

Perhaps a further investigation of the centre of gravity method could lead to better results; however because of the predicted context of this study and the good performance of the decomposition methods this method has not been further developed and followed.

4.2.3 Decomposition: Fourier and Legendre

Decomposition methods arise to be very powerful for the parameterization of forest vertical structure. They are able to reconstruct the vertical biomass profiles with a high accuracy using low frequency components and they provide stable and easily reproducible parameters. There is a big collection of decomposition methods, although in this study only the Fourier and the Legendre transforms have been used. The main reason for this selection is that both methods are already weekly established in Remote Sensing techniques..

The selection of one method is based on the ability to represent the total biomass stock with low frequency components and therefore the capacity to explain the biomass with vertical structure parameters. In principle both methods seem similar as the correlation coefficients give similar results. However, because of the need of characterizing structure rather than total biomass values (Figure 35 and Ch. 3.2.4), the Legendre decomposition suits the purpose of this study better.

In comparison to the Fourier decomposition, which uses sines and cosines, defined polynomials are used in the Legendre decomposition. Moreover, some of these polynomials have a good adjustment to the vertical biomass profiles, as component 3 in shown in Figure 53.

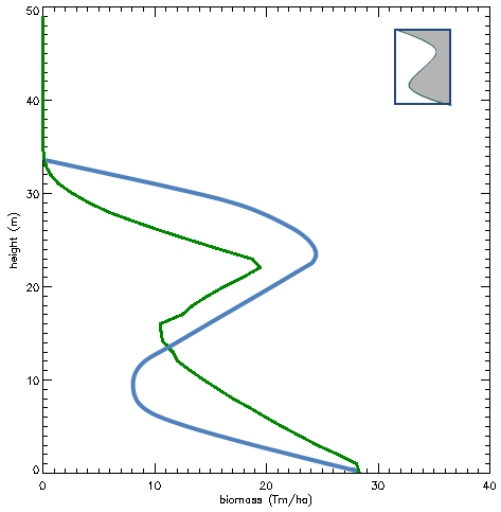

Figure 53 – Example of the similarity between a vertical biomass profile and the polynomial P_3. The green line represents a characteristic profile and the blue line the shape of the Legendre Polynomial P_3.

4.2.3.1 The Legendre polynomials: the structure to biomass allometry

Three of the Legendre components, explained as the fraction of biomass that each of the polynomials modifies from the biomass profile, are used to derive the structure to biomass allometric relation. From the regressions displayed in Figure 38 it can be observed that the components that get the highest correlation coefficients are the ones whose shape form is more similar to the general biomass profile's shapes (see also Figure 53). First, the polynomial P_1 is a line that explains the main tendency of the profiles and the polynomial P_3 is very similar to the majority of the profiles, especially the one layer coniferous plots, which are the most represented

in Traunstein (Figure 53). P_3 is a polynomial especially capable of explaining the biomass profiles shape, particularly when close to the ground, where other polynomials, or the sins and cosines tend to underestimate the biomass and, also, in the top height, where the opposite tends to occur. Over the fourth component the frequency of the polynomials is too high and therefore they are no longer capable of explaining the biomass profiles.

Component 0 of Legendre series represents the integral of the biomass in from of a plot. It is useless for the extraction of any structural information.

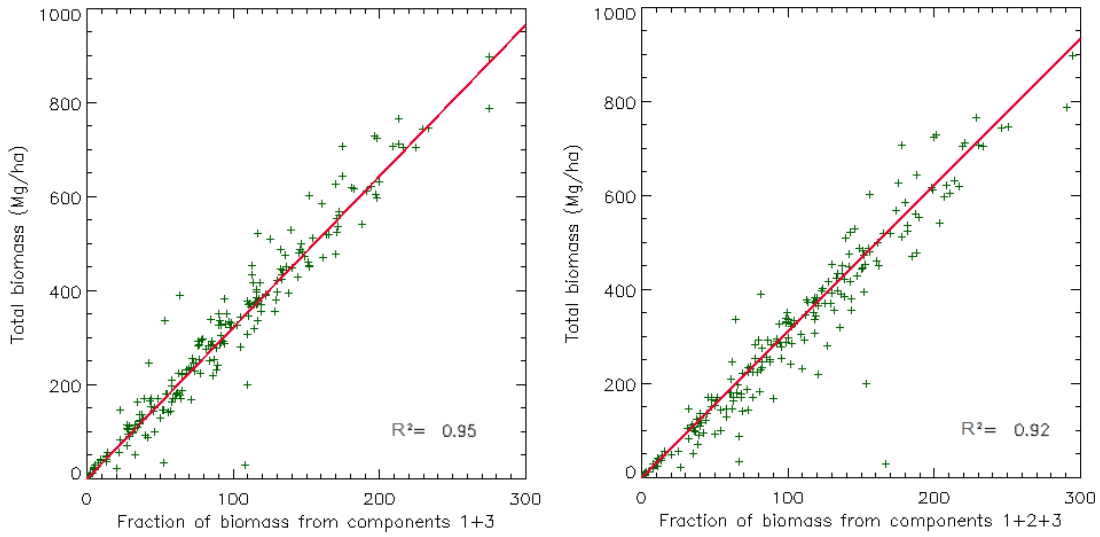

Figure 54 – Total biomass regression plots for the combination of components 2+4 (left) and components 2+3+4 (right). The total biomass components is represented against the proportion of biomass from. The correlation coefficient for 2+4 is 0.95 while for 2+3+4 is 0.92

The structure to biomass allometry has been developed with the usage of three Legendre components (1+2+3). However, only two of the components (1 and 3) are highly correlated to biomass (Figure 54). Component 2 (parabola) introduces only noise in the relation. Yet, component 2 has been used for different reasons:

- The shape of this polynomial can be important for other forest conditions differing strongly from Traunstein, where these kinds of biomass distributions can be dominant. The aim of the study is to create an allometric relation that can be extrapolated to as many conditions as possible.

- To keep the relation between the structure of vertical biomass profiles and radar (tomography - PCT) profiles. Polynomial P_2 represents a step in scale of complexity that helps to explain of certain frequency components.

Finally, a regression of the total biomass against the combination of components 1+2+3 is done. Figure 39 displays this regression and the linear equation derived from it (eq.(3.2.1)). Some aspects of this equation are of special relevance:

- With the usage of this equation the relation obtained from the height to biomass allometry is improved from a correlation of 52 to 92%.
- This equation is linear, in contrast with the exponential height to biomass allometry.
- Only a small fraction of biomass is able to explain 92% of the total biomass stock.

A maximum of 300 Mg/ha explains a biomass level up to 850 Mg/ha of the total biomass (Figure 54). Consequently, only the small proportion of biomass forming the structural components (represented by the Legendre components) is capable of explaining the total of the biomass. This relation can be explained as follows: the dependence of the above-ground biomass stock of a stand from its vertical structure is very strong, especially in diverse forests. In conclusion, in this case study it has been shown that the relation of the total biomass stock to vertical structure is higher than to forest height.

4.2.3.2 The evolution of structure: The role of height in the structure to biomass allometric relation

In the height to biomass relation, as described in the previous chapter, height information is also included.

The stand structure does not remain constant during the stand development, i.e. when a young stand evolves due to the ecological relations between trees, the vertical biomass distribution also changes (Ch. 2.2.5.2). In order to test this evolution, the Legendre coefficients alone (without the height contribution) turn out to be very useful.

Figure 55 – Diagram of forest evolution. The forest development over time results in an evolution of the structural arrangements. The black lines represent the possible evolution of the vertical biomass profiles and the green arrow the change of the dominant height.

The Legendre coefficients correct the adjustment of the corresponding polynomial to the original profile. Hence, it can be interpreted that they can directly measure how similar a certain type of structure (represented by the polynomial) is to the profile, without the influence of height information.

In Figure 37 the regression between the values of the coefficients and the polynomials is shown. In this scenario coefficient 1 and 3 reach high correlation coefficients (0.67, 0.78 respectively). Especially coefficient 3 is directly related to the total biomass content and independently from the height. Each of the coefficient values can be related to a biomass value, following a linear tendency. Thus it is seen how the contribution of the structure changes for each stage of the biomass evolution (represented by the total above-ground biomass stock).

The role of height can be seen by comparing the values of the correlations for the coefficients 1 and 3 with the values of the components 1 and 3. The correlation for coefficient 3 (R^2=0.81) is higher than the correlation for component 3 (R^2=0.78) while for coefficient 1 (R^2=0.88) is lower than for component 3 (R^2=0.93). The main conclusions are the following:

- The polynomial P_1 is the diagonal whose shape does not have a big adjustment with the profile shapes, but represents very well the general tendency of the

vertical biomass distribution for the majority of profiles (decreasing from the bottom to the top), which better appears including alsog the height (+0.05).

- For the polynomial P_3 the opposite happens. This polynomial fits already very well with the shape of the majority of the profiles, however when including forest height the improvement of correlation is lower (+ 0.03).

Therefore, it can be conclude that the height is able to adjust the structural coefficients to general tendency. This fact can be clearly observed in the case of the 0 coefficient. If using only the coefficient the correlation coefficient is R^2=0.93 but when adding the height component it increases until 1.00. It can therefore be concluded that the structural coefficients can explain the total biomass with a very high correlation, but in order to explain the total biomass contribution the height information is necessary.

Finally, the correlation coefficients for the Legendre components (when including height) is higher than when just using coefficients: the height contributes with a higher stability to derive the total biomass and makes the allometric equation more stable.

4.2.3.3 Performance analysis: the Monte Carlo simulation

With the Monte Carlo simulation the robustness of the method is tested for random errors, by modifying all the parameters of the structure to biomass allometric equation (errors are distributed normally). This methodology has been very useful to test how the equation behaves against random errors and the maximum and minimum boundaries between the estimated results can be reliable.

The combination of three components gives a stable equation that can be used without biasing the estimated biomass results until errors over 30%. The single components 1 and 3, which initially give better correlations when used alone, are not stable and the estimations quickly become noisy against random errors (larger than 10%).

The combination of the different structural elements that are contained in the Legendre components can compensate the errors in opposite directions; therefore, they remain more stable against deviations or disturbances. Moreover, it is again proved that only the combination of low frequency components is enough to estimate the biomass with a high accuracy and/or stability.

4.3 Biomass inversion from a Airborne LIDAR System (ALS)

During this study it was shown how an airborne LIDAR system is a remote sensing technique with a very high potential for the estimation of forest biomass (Drake, et al., 2002). The ALS systems are capable not only to accurately estimate the canopy height but to detect forest vertical structure in a highly diverse forest type. With a high precision (Figure 42) the LIDAR instrument reliably provides important forest characteristics that can then be used to estimate biomass in forests.

During the process of biomass derivation the possibility to empirically relate the LIDAR intensity/amplitude to biomass was shown. However, this process was not exempt of problems because of the differences between biomass and LIDAR measurements. In contrast to the field biomass estimations which relate changes in the height distributions of individual measured trees to the changes in biomass; in an ALS the relationship is between LIDAR-backscattering and total biomass, but for all the detected vegetated surfaces within the area of interest. This aspect is of special importance and the rest of the study is focused on achieving a comparable relation between LIDAR backscattering and biomass.

4.3.1 Accuracy of measurements

The first accuracy problem is the reliability of the relative positioning between the LIDAR and the inventory data. The area of interest that is selected is relatively small. For the inventory purposes it is optimal, and the precision of the location does not need to be as high as for LIDAR comparisons. However, small displacements between the two sources of information can lead to big biases in the final results, as the surface is not big enough to rely on compensations due to averaging. It is such that in the distance of 1 meter a high tree that was not accounted for in the inventory, is introduced in the measured LIDAR plot and so, the vertical LIDAR structure profile changes drastically.

The problem of geo-location has been carefully analyzed and manually corrected, so the majority of the discrepancies between the two measurements have been minimized. On the other hand, some cases, like the interception of electric wires or birds, can be corrected by applying a smoothing in the processing; but other cases, like the effects of bending trees, are extremely difficult to detect, especially in a study like this. However, due to the LIDAR geometry and

system limitations, some of these discrepancies do not depend on the geo-location and thus can neither be detected nor corrected in this process. However, this last point is not considered of particular relevance.

In Figure 43 it is shown that the LIDAR tends to overestimate the height, especially for lower trees. In this case the deviation of heights is understood as follows: the plots that have a low dominant height are more sensitive to very small deviations, e.g. in an extreme case, only one meter of displacement can introduce a branch of a high tree inside of the LIDAR plot and the maximum computed height will therefore be erroneous. Still, these high deviations only affect to a small proportion of plots. The cases of plots with higher trees are more resistant to these deviations, as the maximum height is not usually modified and this kind of structure is more stable. For example, the inclusions of external branches that are lower than the main canopy layer in a plot will not affect neither the maximum height neither nor the main structure type.

4.3.2 LIDAR profiles and applicability of the Canopy Height Profiles (CHPs)

CHP has proved to be as a good tool to solve some of the limitations of the ALS measurements. However, due to the high variability of profiles used in this study the CHP performance is not the same for all the profiles. The CHP methodology described here connects the ALS profiles and adapts them more to the shapes given by the biomass profiles. According with Harding (2001) CHP reproduces the overall stature and the height of the principal models in the distribution of plant area. Yet, even if not all the CHPs look exactly like the biomass distribution a clearer tendency can be observed. CHPs are later used to generate a transfer function going from LIDAR to biomass.

CHPs have more information than the LIDAR intensity profiles (Lefsky, et al., 1999). The CHP method attempts to relate the power of the waveform to the total density of the foliage at each height. CHP assumes even distribution of foliage within the stand. Conditions in Traunstein probably do not fit this assumption because the forest structure is very heterogeneous. This implies that the density of canopy surfaces should be the same within and between individual crowns. Some of the problems found in the applicability of the CHP may suggest that the method should be adjusted depending on the diversity of conditions.

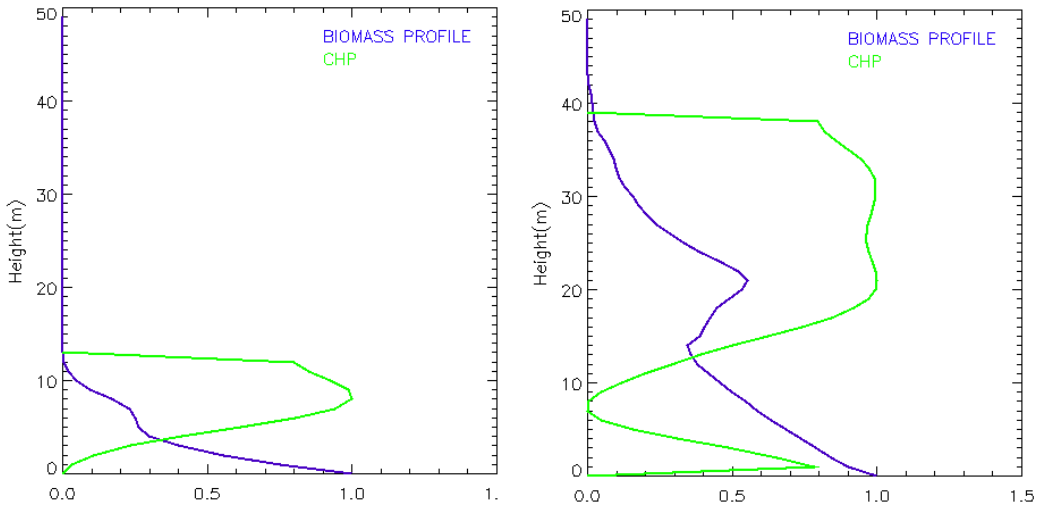

Figure 56 – Examples for bad performances of the Canopy Height Profile. On the left it is shown an example for a low height profile, where the canopy is over represented and on the right the same problem for a very tall profile.

4.3.3 The problem of normalization in the LIDAR to biomass relation

One of the main problems of comparing profiles (LIDAR and biomass) is that they measure two different variables: biomass and intensity/amplitude. Therefore, even if the vertical biomass profiles have similar shapes as the LIDAR (CHP) profiles the units are not comparable, especially in scale. Whilst the values of biomass are in the order of 100s the intensity/amplitude is two to three orders larger.

In literature the method most extensively applied to solve this problem is normalization. Profiles are usually normalized by the maximum amplitude, either biomass or intensity. The height-axis, which is equal for both profiles, is kept unchanged. It is very difficult to quantify the information lost in the normalization process. Figure 57 shows the relation between the proportion of the biomass from the normalized Legendre components and the total biomass. Eq. (3.3.5) changed from a linear function with a correlation coefficient of 0.92 to an exponential function with a correlation coefficient of 0.66.

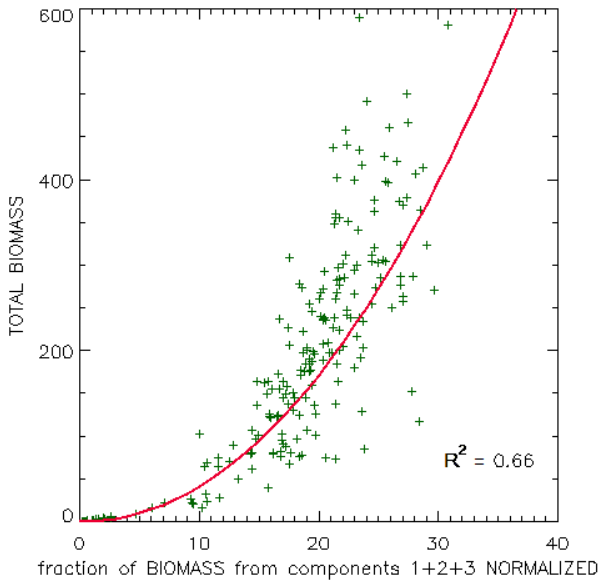

Figure 57 – Regression between the fractions of biomass from the normalized Legendre components and the Total Biomass. The correlation coefficient is 0.66

4.3.3.1 Transfer function

For the calculation of a transfer function normalization is mandatory. This function is created from the direct subtraction of the values of one profile from the other (CHP minus vertical biomass). If both profiles are not on the same scale this operation is not feasible.

4.3.3.2 The LIDAR to biomass relation

In Figure 51 the Legendre components from both profiles (vertical biomass and CHPs) are correlated. A correlation coefficient R^2 of 0.76 can be found with a logarithmic function. However, biomass cannot be directly estimated by means of Eq.(3.3.6). This equation shows the similarity of correction from Legendre components derived from LIDAR to components derived from biomass measurements. Trough the normalization process, biomass information is changed. Thus, the Legendre components do not really mean a portion of biomass but they are related to the shape and height of the profile. When only the biomass-axis is normalized the value of the integral (component 0) is equal to the maximum height, and therefore the rest of the components express a proportion from the height value, instead of biomass.

Before and after the normalization the structural information should remain. Still, when attempting to return from the normalized state of the vertical biomass profiles to the not normalized ones, the values of correlation decrease.

It is also seen that in order to achieve a good correlation between LIDAR and biomass some plots needed to be filtered before the analysis. The discordance between this plots and the rest was too big to be considered. Moreover after the subtraction of these profiles the increase in correlation was significant. Still, the proportion of eliminated plots is small compared with the total (11 out of 221).

This point needs to be further investigated, especially to find a more stable method being able to relate the intensity/amplitude information directly with the. Nevertheless the results showed in Figure 51 point to a clear relation and they represent a promising basis for further research.

4.3.4 The inversion path

Summarizing the last chapters and also as main result of this study a clear path to follow in the process biomass inversion has been defined. The aim of this path is to clarify the possible steps needed to derive biomass from LIDAR data based on vertical biomass profiles. As mentioned previously, LIDAR is not able to directly estimate forest density and therefore the structural parameters arise to be a possible solution to invert biomass from structure. In the previous section it was shown how the above-ground biomass depends on the vertical forest structure.

The low frequency components can be detected by the LIDAR. In order to arrive at comparable parameters to relate the LIDAR data and biomass several steps are needed (Figure 58):

1. In a first step LIDAR profiles are weighted using CHP to calibrate vegetation backscattering by ground backscattering (Lefsky, et al., 1999). The Canopy Height Profiles have proven to be a useful algorithm that can modify the LIDAR profiles weightening the intensity per meter according to the proportion of returns between canopy and ground.

2. The CHPs are then corrected by a transfer function. This function corrects the relation between real biomass distribution and forest backscattering as seen by LIDAR.
3. The corrected CHPs are now comparable to the vertical biomass profiles and so can be decomposed to extract the LIDAR structural components and, from them, the vertical biomass structural components.
4. Finally, with the usage of the structure components from the step 3, in the structure to biomass allometry the above-ground biomass can be estimated.

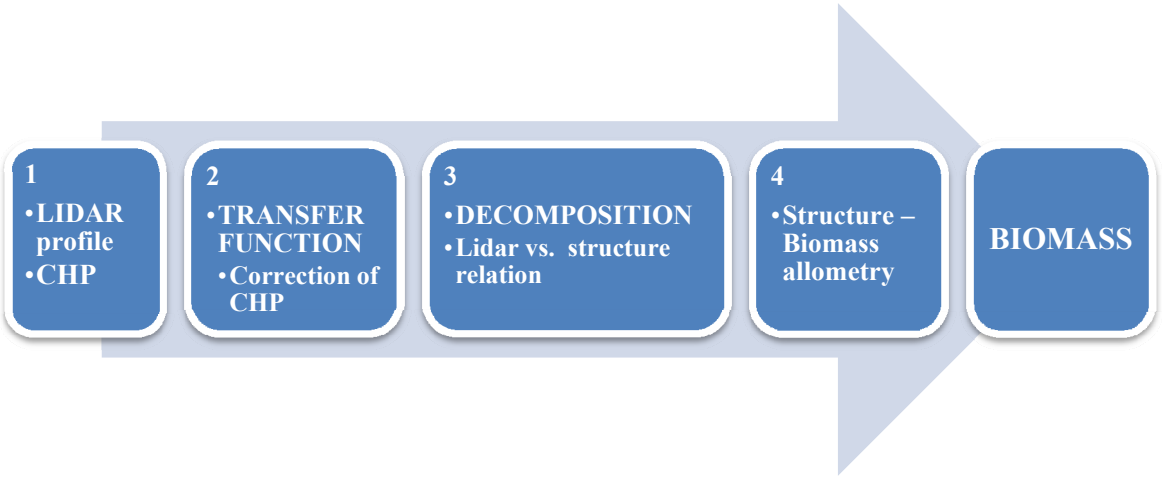

Figure 58 – Biomass inversion path. This figure shows the necessary steps to obtain forest biomass from LIDAR data.

5 Conclusions and outlook

5.1 Structure to biomass allometry

A direct relation between forest vertical biomass structure and forest biomass has been verified. The vertical biomass profiles developed in this study are shown to be a powerful tool to describe forest vertical biomass structure. These profiles can contain much information about the forest. They can not only quantify the total biomass stock but also provide characteristic forest features information, like stratification, maturity or tree species (coniferous or broadleaves). Moreover, forest vertical biomass profiles can be a variable for analyzing changes of biomass distribution during time.

Traunstein forest has been presented as a very suitable environment to study forest structure because of the high range of different conditions that can be found. The variability in the profiles in terms of height and structure proves this fact. Moreover, the diversity of Traunstein allows extrapolating the obtained results to other environments.

Legendre polynomials have appeared to be a valuable tool to describe forest vertical biomass structure. They have been able to represent forest vertical biomass structure better than the rest of methodologies tested in this study. Hence, this method arises to be more stable and reproducible, at the same time it offers a very good adjustment for complex forest conditions.

The combination of forest height with low frequency Legendre components (1-3) yields to an allometric relation within a correlation coefficient of 92% for biomass estimations in complex forest ecosystems (Traunstein test site). With only three components, which represent just a small proportion of biomass, it is possible to explain the total biomass stock. This relation has proved that the structure represented by the components can explain most of the biomass, including height as a factor that improves this correlation.

The structure to biomass relation has been defined in an allometric equation that can be tested in different forest systems. The equation has been developed trying to cover a high range of structures types. For the Legendre component 2 correlation with biomass for this test site is low. However it was kept because it could be a valuable contribution in other ecosystems and it does not introduce a significant addition of noise.

Finally, the strength and stability of the structure to biomass allometric equation is tested with the Monte Carlo analysis. The structure to biomass allometric equation is capable of producing stable results even for high deviations (30%) with low standard deviations.

5.2 Remote sensing application

It has been shown that full waveform airborne LIDAR is able to reconstruct the forest vertical structure. Better adjustment to vertical biomass structure could be obtained using CHP (Canopy Height Profiles) (Lefsky, et al., 2002).

In this study forest inventory data from a large set of plots were compared to LIDAR data. The small area that is the basis of comparison between field and LIDAR data has caused problems because of the need for a very high precision in the geo-location. However these problems could partly be corrected, significantly increasing the results.

In order to derive an allometric relation as found for the structure to biomass a transfer function is needed, adapting Lidar backscattering to vertical biomass profiles.

For a direct comparison between LIDAR and biomass, normalization is necessary (different reference systems). Normalization biases biomass information. This problem is not clarified at the end of the study; but a relation between vertical biomass structure and LIDAR profiles is shown.

5.3 Outlook

The transfer from remote sensing data to biomass needs to be further investigated and improved. Especially the problem of normalization needs a deeper investigation and other methods need to be tested in order to find a better way to relate LIDAR intensity/amplitude to biomass.

This study is placed in the context of large scale investigations. Thus, even if structural diversity in the Traunstein test site allows for the extrapolation of the results to a more general context, other test sites need to be investigated (boreal, tropical, temperate, etc.) in order to prove the general validity of the structure to biomass allometry. Structural characteristics between forest ecosystems can vary extremely between the major biomes, so inventory data from them should be investigated

Finally, this study shows the potential of future remote sensing missions like DESDynI and Tandem-L for forest monitoring. The algorithms developed here and tested in the context of this study, show the potential of deriving biomass from remote sensing systems able to resolve the vertical structure as is the case in DESDynI and Tandem-L missions.

6 References

Anderson J. [et al.] “The use of waveform lidar to measure northern temperature mixed conifer and deciduous forest structure in New Hampshire”. *Remote Sensing and Enviroment*. - 2006. - pp. 105(3):248-261.

Arfken George B and Weber Hans J. “Mathematical Methods for Physicists”. - London : *Elsevier Academic Press*, 2005.

Baltasatias E.P. “Airborne Laser scanning: basic relations and formulas”. *ISPRS Journal of Photogramtery and & Remote Sensing*. - 1999b. - pp. 53(2-3):199-214.

Baltasavias E.P. “Airborne laser scanning: Existing systems and firms and other ressources”. *ISPRS Journal of Photogrametry & Remote Sensing* : ISPRS, 1999a. - pp. 54 (2-3):164-198.

Balzter H., Rowland C. S. and Saich P. “Forest canopy height and carbon estimation at Monks Wood National Nature Reserve, using dual-wavelenght SAR interferometry”. *Remote Sensing for Enviroment*. - 2007. - pp. 108:224-239.

Bertalanffy L.V. “Theoretische Biologie; Zweiter Band: Stoffwechsel und Wachstum”. - Berlin : *Borntraeger*, 1942.

Blair J.B. and Hofton M.A. “Modeling lase altimeter return waveforms over complex vegetation using high-resolution elevation data”. *Geophysical research letters*. - 1999. - pp. 26: 2509-2512.

Brown Sandra. “Estimationg biomass and biomass change of tropical forests”. - Rome : *FAO*, 1997.

Burschel P and Huss J. “Grundriss des Waldbaus”. - Berlin : *Pareys Studientexte*, 1997.

Cloude Shane R. “Dual Baseline Coherence Tomography*”. IEEE Geoscience and Remote Sensing Letters*. - 2007. - pp. 4: 124-131.

Cloude Shane R. “Polarization coherence tomgraphy”. *Radio Science*. - 2005. - p. 41: RS4017.

Cote Jean-Francois [et al.]. “The strucutural and radiative consistency of three-dimensional tree reconstructions from terrestrial lidar”. *Remote Sensing of Enviroment*. - 2009. - pp. 113, 1067-1081.

Curlander J. C. and McDonough R. N. “Synthetic Aperture Radar, Systems and Signal Processing”. - New York : *John Wiley & Sons*, 1991.

Drake Jason B. [et al.] “Sensitivity of large-footprint lidar to canopy structure and biomass in a neotropical rainforest”. *Remote Sensing of Enviroment*. - 2002. - pp. 81: 378-392.

Dubayah A. and Blair J. “Lidar remote sensing for forestry applications”. *Journal of Forestry*. - 2000. - pp. 98(6):211-217.

FAO. “Food and Agricultural Organization of the UN Forest Resource Assement”. *FAO forestry paper* No140. - Rome : www.fao.org/forestry, 2001. - pp. 0258-6150.

Freeman Anthony [et al.] “Deformation, Ecosystem Structure, and Dynamics of Ice (DESDyni)”. *EUSAR*. - Friedrichsgafen, 2008.

Harding D.J. [et al.]. “Laser altimeter canopy height profiles. Methods and validation for closed-canopy, brodaleaves forest”. *Remote Sensing of Enviroment*. - 2001. - pp. 76:283-297.

Heipke C., Jacobsen K. and Wegmann H. “Analysis of the results of the OEEPE test 'Integrated sensor orientation"”: Thecnical report. *OEEPE Official Publications*, 2002.

Hopkinson C. [et al.]. “Assessing forest metrics with a ground based scanning lidar”. *Canadian journal of Forest Research*. - 2004. - pp. 34, 573-583.

Houghton R. A., Hall Forrest and Goetz Scott J. “Importance of biomass in the global carbon cycle”. *Journal of Geophsycal Research*. - 2009. - p. 114: G00E03.

Hyde P. [et al.]. “Mapping forest strucuture for wildlife habitat analysis using waveform lidar: Validation of montane ecosystems”. *Remote Sensing of Enviorment*. - 2005. - pp. 96(3-4): 427-437.

Koetz B. “Inversion of Lidar Waveform Model for Forest Biophysical Parameter Estiamtion”. *IEEE Geoscience and Remote Sensing Letters*. - 2006. - p. 3: no1.

Köhler Peter and Huth Andreas. “Towards ground-truthing of satellite-based estimates of above-ground biomass and leaf area index in tropical rain forests”. *Manuscript - Biogeosciences* . - January 13, 2010.

Krieger G. [et al.] “The Tandem-L Mission Proposal: Monitoring Earth's Dynamics with High Resolution SAR Interferometry”. *Radarcon*. - Pasadena: IEEE, 2009. - p. 6.

Kugler Florian. “Temporäre Dekorrelation von Radarfernerkungunsdaten über einem temperaten Micshwald”. - Munich: *Dimploma thesis at Deutsches Zentrum für Luft und Raumfahrt*, 2004.

Lathan Penelope A., Zuuring Hans R. and Coble Dean W. “A method quantifiying vertical forest structure”. *Forest Ecology and Management.* - 1998. - pp. 104: 157-170.

Lefsky A. Michael [et al.] “Estimates of forest canopy height and above ground biomass using ICEsat”. *Geophysical research letters,* 2005. - L22SS02 : Vol. 32.

Lefsky M. A. [et al.]. “Lidar Remote Sensing of Forest Canopy Structure and Byophysical Properties of Douglas-Fir Wstern Hemlock Forests”. *Remote Sensing and Enviroment*. - 1999. - pp. 70:339-361.

Lefsky Michael A. [et al.]. “Lidar Remote Sensing for Ecosystem Studies”. *BioScience*. - 2002. - pp. 52: 19-30.

MacArthur R.H. and Horn H.S. “Foliage profile by vertical measurments”. *Ecology*. - 1969. - pp. 50:802-804.

Mallet C. and Bretar F. “Full-waveform topographic lidar: State-of-the-art”. *ISPRS Journal of Photogrametry and Remote Sensing*. - 2009. - pp. 64: 1-16.

Mette T. “Forest Biomass Estimation from polarimetric SAR interferometry”. Munich : *Deutsches Zentrum fuer Luft un Raumfahr*, 2007.

Mette T. [et al.]. “Forest BIomass Estimation using Polarimetric SAR Interferometry”. *POLinSAR*. - Frascati : IEEE, 2003. - pp. 1-7.

Moshammer Ralf. “Management PLan for the Municipal Forest Traunstein”, *in Press*, 2010.

Niklas K.J. “Plant allometry:the scaling of form and process.” Chicago: *Univ. Chicago Press*, 1994.

Pajtík Jozef, Konopka Bohdan and Lukac Martin. “Biomass function and expansion factors in young Norway Spruce trees”. *Forest Ecology and Management*. - 2008. - pp. 256: 1096-1103.

Papathanassiou K. *Polarimetric SAR Interferometry*. *DLR-Forschungsbericht*.1999-2007, 1999.

Pretzsch H. “A unified low spatial allometry for woody and herbaceous plants”. *Plant Biology*. 2002. - pp. 4, 159-166.

Pretzsch H. *Modellierung des Waldwachstums*. - Berlin: *Parey*, 2001.

Pretzsch H. “Species-specific allometric scaling under self-thinning: evidence form long-term plots in forest stands”. *Oecologia*. - 2006. - pp. 146: 572-583.

Pretzsch H., Biber P. and Durský J. “The single tree-based stand simulator SILVA: construction, application and evaluation”. *Forest ecology and management*. - 2002. - pp. 162:3-21.

Pretzsch Hans and Biber Peter. “A Re-Evaluation of Reineke's Rule and Stand Density Index”. *Forest Scienc*e. - 2005. - pp. 51(4):304-320.

Pretzsch Hans. “From total biomass to the carbon pool. Forest Dynamics, Growth and Yield”. - Berlin-Heidelberg: *Springer*, 2009.

Reigber A. [et al.]. “SAR Tomography and Interferometry for the Remote Sensing of Forested Terrain”. *EUSAR*. - Munich : VDE Verlag, 2000. - Vols. 23-25.

Reineke L.H. “Perfecting a stand density index for even-aged forests”. *Journal of Agricultural Research*. - 1933. - pp. 46:627-638.

Roth R.B. and Thompson J. “Practical application of multple-pulse in the air (MPiA) lidar in large area surveys”. *International Archives of Photogrametry, Remote Sensing and Spatial Information Sciences*. - 2008. - pp. 37 (Part 1): 183-188.

Sun G. [et al.]. “Forest vertical structure from GLAS: An evaluation using LVIS and SRTM data”. *Remote Sensing of Enviroment*. - 2008. - pp. 112: 107-117.

Tebaldini S., Rocca F. and Monti Guarneri A. “Model Based SAR Tomography of forested areas”. *IGARSS*. - Naples : IEEE, 2008. - pp. 593-596.

Wagner W. [et al.]. “Gaussian decomposition and calibration of a novel small-footprint full-waveform digitising airborne laser scanner”. *ISPRS Journal of Photogramery & Remote Sensing*. - 2006. - pp. 60(2): 100-112.

Wood density data base. - July 8, 2009. - *www.worldagroforestrycentre.org*.

Yoda, K.; Kira, T.; Ogawa, H; Hozummi, K. “Self-thinning in overcrowded pure stands under cultivated and natural conditions (Intraspecific competition among higher plants XI)”. *Journal of the institute of polythecnics*, Osaka city University. - 1963. - pp. Series D. 14:107-129.

Zianis Dimitris [et al.]. “Biomass and Stem Volume Equations for tree Species in Europe”. *The Finish Society of Forest Science*, 2005.